UNIVERSIDAD AUTÓNOMA DE MADRID

FACULTAD DE CIENCIAS

DEPARTAMENTO DE BIOLOGÍA MOLECULAR

ROLE OF UPF1 AND CSX1 IN POSTTRANSCRIPTIONAL REGULATION OF GENE EXPRESSION IN *SCHIZOSACCHAROMYCES POMBE*

Memoria presentada para optar al grado de Doctor por:

Dña. Ana María Matia González

Director:

Miguel Ángel Rodríguez Gabriel

Esta Tesis Doctoral ha sido posible gracias a las siguientes ayudas:

- Beca de formación de personal investigador (FPI) del Ministerio de Educación y Ciencia. BES-2007-16324. Junio 2007-Junio 2011.
- Ayuda para estancia breve asociada a la beca FPI del Ministerio de Educación y Ciencia en el laboratorio del Dr. Juan Mata, University of Cambridge, Cambridge, United Kingdom. Septiembre-Diciembre 2008.
- Ayuda para estancia breve asociada a la beca FPI del Ministerio de Educación y Ciencia en el laboratorio del Dr. Jürg Bähler, Department of Genetics, Evolution & Environment and UCL Cancer Institute, University College of London, London, United Kingdom. Junio-Septiembre 2009.
- Ayuda para estancia breve asociada a la beca FPI del Ministerio de Educación y Ciencia en el laboratorio del Dr. Lynne E. Maquat, Department of Biochemistry & Biophysics, School of Medicine and Dentistry, University of Rochester Medical Centre, Rochester, New York, United States of America. Marzo-Agosto 2010.

El trabajo descrito ha sido financiado por los siguientes proyectos:

- "Especificidad de señalización en *Schizosaccharomyces pombe*: MAP quinasas y proteínas de unión a RNA". BFU 2006-01767. Ministerio de Educación y Ciencia.
- "Especificidad de señalización en células eucarióticas: MAP quinasas y proteínas de unión a RNA en *Schizosaccharomyces pombe*". BFU 2009-09116. Ministerio de Ciencia e Innovación.

ABBREVIATIONS

ADAR	Adenosine deaminase-RNA specific
AMP	Adenosine monophosphate
ATP	Adenosine triphosphate
BiFC	Bimolecular fluorescence complementation
bp	Base pairs
cAMP	Cyclic adenosine monophosphate
CBC	Cap binding complex
cDNA	Complementary deoxyribonucleic acid
CPF	Cleavage and polyadenylation factor
CRE	cAMP element response
CTD	Carboxyl-terminal domain of RNApol II
DNA	Deoxyribonucleic acid
dsRBD	Double-stranded RBD
dsRNA	Double-stranded RNA
EMM	Edinburgh minimal media
EMM-N	Edinburgh minimal media without nitrogen
eRF1	Eukaryotic release factor 1
eRF3	Eukaryotic release factor 3
GFP	Green fluorescent protein
GMP	Guanosine monophosphate
GTFs	General transcription factors
GTP	Guanosine triphosphate
hnRNP	Heterogeneous nuclear RNP
IP	Immunoprecipitation
MAPK	Mitogen-activated protein kinase
MAPKK	MAPK kinase
MAPKKK	MAPKK kinase
ME	Malt extract
mRNA	Messenger RNA
miRNA	Micro RNA
mRNP	Messenger RNP
ncRNA	Non-coding RNA
NMD	Non-sense mediated mRNA decay
OD	Optical density
ORF	Open reading frame
PABP	Poly(A) binding protein
PCR	Polymerase chain reaction
PIC	Preinitiation complex
PKA	Protein kinase A
PTC	Premature translation termination codon
qPCR	Quantitative PCR
RBD	RNA binding domain
RBP	RNA binding protein
RC	Reverse complementary
RIp	RNA immunoprecipitation
RNA	Ribonucleic acid
RNApol II	RNA polymerase II
RNP	Ribonucleoprotein
RPKM	Reads per kilobase of exon model per million mapped reads for each gene

rpm	Revolution *per* minute
RRM	RNA recognition motif
rRNA	Ribosomal RNA
RT	Room temperature
RT-PCR	Reverse transcription-PCR
siRNA	Small interfering RNA
snoRNA	Small nucleolar RNA
snRNA	Small nuclear RNA
ssDNA	Single-stranded DNA
ssRNA	Single-stranded RNA
TAP	Tandem affinity purification
TBP	TATA binding protein
TF	Transcription factor
tRNA	Transfer RNA
UTR	Untranslated region
WB	Western blot
YES	Yeast extract plus supplements

ABSTRACT

Eukaryotic cells have developed a complex regulatory system in order to adapt to different environmental and cellular requirements. RNA binding proteins (RBPs) modify and specifically regulate mRNA localization, function, stability and biogenesis. Thus, changes in the RBPs can promote diseases derived of mRNA missregulation.

Using *Schizosaccharomyces pombe* as model organism we have studied the role of the RBPs Upf1 and Csx1 in posttranscriptional regulation of gene expression.

As a result we have found that Upf1 is binding a large amount of mRNAs which carry out different cellular functions. Throughout DNA microarrays experiments we have observed that Upf1 could be degrading these mRNAs. This implies a novel finding because in previous reports it has been described that Upf1 is usually degrading mRNAs that contain premature termination codons (PTCs) while our experiments reveals that Upf1 could be degrading transcripts without evident PTCs. Besides, we have demonstrated that other components of the non-sense mediated mRNA decay (NMD), such as Upf2 or Upf3, are required for Upf1-mRNA targets binding.

It has also been demonstrated that the interaction between Upf1 and Upf2, reported in other organisms is conserved in fission yeast, being the presence of Upf2 required for a proper Upf1 intracellular localization.

Previous reports have described that Upf1 is necessary for the oxidative stress response. In this work it has been proposed that the role of Upf1 in this response could be mediated by the degradation of some of its targets.

In this work it has been established the hypothesis that NMD mechanism could be taking place during transcription and translation due to the results obtained through the study of protein interactions *in vivo*. In addition it has been demonstrated that UPF1 dimerizes in mammalian cells.

Finally, it has been proved that Csx1 is playing a regulator role in the sexual differentiation response through the binding and regulation of abundance of *ste11*$^{+}$ mRNA. This finding and the previous reports establish that Csx1 is a key component of two cellular responses, being a candidate for the cross-talk between both pathways.

RESUMEN

Las células eucariotas han desarrollado un complejo sistema de regulación para adaptarse a los diferentes requerimientos celulares y ambientales. Dentro de estos sistemas de regulación se encuentran las proteínas de unión a RNA (RBPs) que modifican y regulan de manera específica la localización, función, estabilidad y biogénesis de diversos ARNs. De esta manera, cambios en las RBPs pueden provocar enfermedades derivadas de la desregulación de estos ARNs.

Utilizando como modelo la levadura de fisión *Schizosaccharomyces pombe* hemos realizado un estudio sobre el papel de las proteínas de unión a RNA Csx1 y Upf1 en la regulación post-transcripcional de la expresión génica.

Como resultado hemos hallado que la proteína Upf1 está uniendo una gran cantidad de ARNm que desempeñan diferentes funciones celulares. A través de experimentos de microarrays hemos observado que Upf1 podría estar degradando estos ARNm. La degradación de estos ARNm supone una novedad debido a que en trabajos previos se ha descrito que Upf1 degrada de manera regular los ARNm que contienen codones de terminación tempranos (PTCs), mientras que los ARNm descritos en este trabajo no contienen evidentes PTCs. Además hemos demostrado que otros componentes del sistema de degradación de ARNm NMD, como Upf2 y Upf3, son necesarios para que Upf1 lleve a cabo la unión de estos mensajeros.

Por otro lado se ha demostrado que la interacción descrita entre Upf1 y Upf2 en otros organismos está conservada en la levadura *S. pombe*, siendo la presencia de Upf2 necesaria para la correcta localización intracelular de Upf1.

En resultados previos se ha descrito que la proteína Upf1 es necesaria para la respuesta celular que se desencadena en presencia de estrés oxidativo. En este trabajo se propone que el papel de Upf1 en esta respuesta podría estar mediado por la degradación de algunas de sus dianas.

Mediante el estudio de la localización de interacciones proteicas *in vivo* que tienen lugar en el mecanismo de NMD se ha establecido la hipótesis de que este mecanismo podría tener lugar durante la transcripción y la traducción. Adicionalmente se ha propuesto una nueva función de dimerización de la proteína UPF1.

Finalmente, se ha demostrado que la proteína Csx1 está regulando la respuesta de diferenciación sexual a través de la unión y estabilización del ARNm codificante del factor de transcripción Ste11. Este hallazgo junto a los resultados publicados previamente, establecen que la proteína Csx1 sea un componente fundamental de dos respuestas celulares frente a diferentes estímulos, mediante la estabilización de los ARNm de 2 factores de transcripción, Atf1 y Ste11. Esto supone que Csx1, al igual que ocurre con la MAPK Spc1, sea un posible candidato de cross-talk entre dos rutas.

CONTENTS

INTRODUCTION

1. *SCHIZOSACCHAROMYCES POMBE*

Fission yeast *Schizosaccharomyces pombe* was isolated by P. Lindner in 1893 from East Africa millet beer. The specie's name, *pombe*, is derived from the Swahili word for beer.

According to scientific taxonomic classification, *S. pombe* is a eukaryotic organism that belongs to Fungi kingdom, Ascomycota phylum, Schizosaccharomycetales order, Schizosaccharomyces genus.

Urs Leupold isolated several *S. pombe* strains, now commonly used in the laboratory: strain 968, homothallic h^{90}; strain 975, heterothallic h^{+}; and strain 972, heterothallic h^{-} (Leupold, 1950). He developed the first approaches using fission yeast as an experimental model for studying genetics.

Fission yeast is a unicellular eukaryotic organism. These short cylindrical non-motile cells maintain their shape by growing exclusively through the cell tips and divide by medial fission to produce two daughter cells of equal size.

The genetic material of *S. pombe* is organized in three chromosomes that have been completely sequenced. Its genome contains approximately 14.1 million base pairs, with 4,970 protein-coding genes and at least 450 non-coding RNAs, making it the smallest genome of a free-living eukaryote at the time (Wood *et al.*, 2002).

S. pombe has become an important organism in studying cell cycle and the cellular responses to different stresses that provoke DNA damage and aging because of characteristics such as its easy growing, maintenance and manipulation in the laboratory and its molecular similarity to higher eukaryotic cells.

Recently it has been described, by DNA sequence analysis, that fission yeast differs phylogenetically from the budding yeast *Saccharomyces cerevisiae* as much as from *Homo sapiens*, thus several groups of genes are conserved in *S. pombe* and humans, but missing in *S. cerevisiae* (Bähler, 2004).

2. GENE EXPRESSION

Gene expression is the process by which information from a gene is used in the synthesis of a functional gene product. These products are often proteins, but in non-protein coding genes such as rRNA genes or tRNA genes, the product is a functional RNA.

This process covers different steps, including transcription and translation (Figure 1).

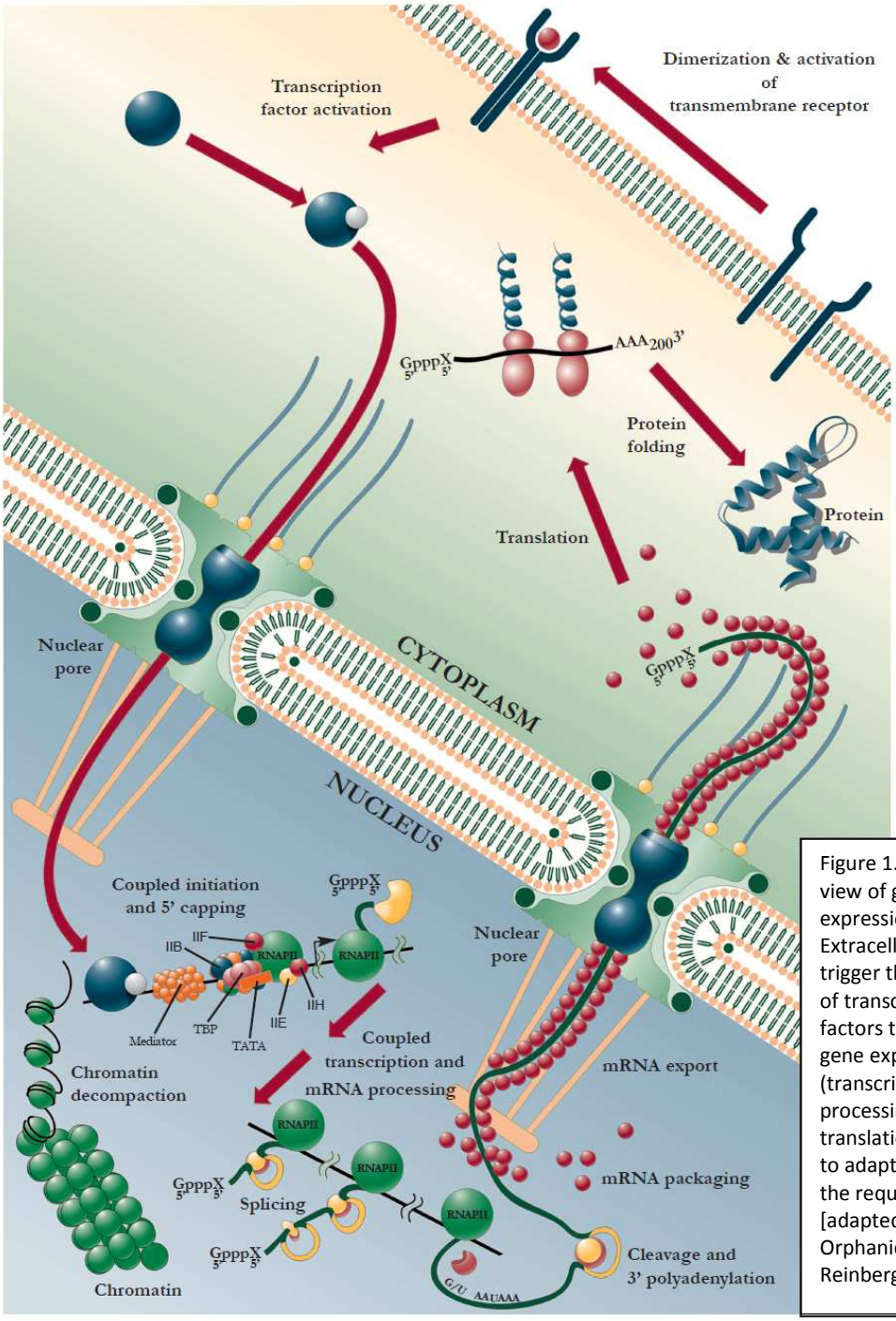

Figure 1. Schematic view of gene expression. Extracellular signals trigger the activation of transcription factors that promote gene expression (transcription, mRNA processing and translation) in order to adapt the cell to the requirements [adapted from Orphanides and Reinberg, 2002]

Prior to transcription, chromatin is relaxed, being accessible for the RNA polymerase. In eukaryotic cells there are two types of chromatin, euchromatin and heterochromatin. Transcribed genes are present in euchromatin, while heterochromatin is characterized by a high density of repeats. There are two regions in fission yeast chromosomes formed by constitutive heterochromatin: chromosome centromeres and the regions near telomeres. The assembly of heterochromatin at centromeres is required for the efficient chromosome segregation during cell cycle (Allshire *et al.*, 1995), while the presence of this chromatin structure at telomeres protects chromosomes from degradation.

Euchromatic genes localized in heterochromatin regions results in gene silencing and defects in gene silencing at centromeres can interfere with chromosome segregation.

There are different proteins involved in RNA silencing. Some of them are well characterized, like Dcr1, Ago1 or Rdp1 (Hall *et al.*, 2003; Provost *et al.*, 2002; Volpe *et al.*, 2002). These proteins are part of the RNA interference (RNAi) pathway. RNAi system controls which genes are active and their activity rate.

2.1. TRANSCRIPTION.

Transcription is the DNA-dependent synthesis of RNA. It is divided in different stages, which are coordinately regulated.

Transcription is carried out by RNA polymerases. In *S. pombe* there are three RNA polymerases: I, II and III. RNA polymerase I is involved in rRNA synthesis (Balzi *et al.*, 1985) and nucleolus formation (Hirano *et al.*, 1989), RNA polymerase III synthesizes a large variety of small RNAs, including tRNAs (Lassar *et al.*, 1983), while RNA polymerase II (RNApol II) catalyzes transcription of protein-coding genes (all mRNAs) and some non-coding RNAs (ncRNAs).

RNApol II is formed by 12 subunits, designated Rpb1-Rpb12, structurally and functionally conserved from yeast to humans (Kimura *et al.*, 2001; Sakurai *et al.*, 1999). Rpb1, Rpb2, Rpb3 and Rpb11 form the core of the enzyme with catalytic activity of RNA polymerization. Rpb1, the largest subunit of RNApol II contains the eukaryotic-specific carboxyl-terminal domain (CTD), consisting of heptapeptide repeats (consensus sequence YSPTSPS). *S. pombe* RNApol II CTD has 29 repeats (Azuma *et al.*, 1991), whereas *S. cerevisiae* and human CTDs contain 26 and 52 repeats, respectively.

Eukaryotic RNA polymerases cannot recognize the promoters of their target genes by themselves. This function is mediated by general transcription factors (GTFs). These protein factors recognize the conserved TATA box and initiator sequences present in most protein-coding genes and recruit RNApol II to the start site of transcription (Hampsey, 1998; Zawel and Reinberg, 1993). Transcription of protein-encoding genes requires assembly of a preinitiation complex (PIC) composed of template DNA, RNApol II, and five GTFs. PIC assembly is nucleated by binding the TBP (TATA binding protein) subunit of transcription factor IID (TFIID) to the TATA box, followed by the recruitment of several transcription factors (TF), TFIIB, TFIIE and TFIIH and unphosphorylated RNApol II coupled to transcription factor IIF (TFIIF). After promoter melting and transcription initiation, the CTD domain is phosphorylated, facilitating promoter clearance and progression into the

elongation phase of transcription. At the end of transcription termination, a phosphatase recycles RNApol II to its unphosphorylated form, allowing the GTFs and RNApol II to initiate another round of transcription (Mitsuzawa and Ishihama, 2004; Reinberg *et al.*, 1998).

2.1.1. mRNA PROCESSING

The mRNA processing reactions occur cotranscriptionally (Proudfoot, 2000; Proudfoot, 1989). Before a gene transcript is transported out of the nucleus, it has to go through three major processing events: capping, splicing and 3'-end formation. After these steps, the fully translatable mRNA is produced. These events include the acquisition of a cap structure at the 5' terminus, the splicing out of introns within the body of the pre-mRNA, and the generation of a 3' end, usually modified by the addition of a poly(A) tail.

2.1.1.1. CAPPING

The first pre-mRNA processing step occurs after 20-30 nucleotides have been synthesized. There is a three step reaction that adds a cap structure to the 5' end of all mRNAs. In *S. pombe* Pct1, an RNA 5' triphosphatase, hydrolyzes the triphosphate of the first nucleotide to a diphosphate. Then, Pce1, a guanylyltransferase, catalyzes the fusion of a GMP residue from GTP to the first nucleotide of the pre-mRNA by an unusual 5'-5' triphosphate linkage, forming a GpppN1- structure. The third activity is mediated by Pcm1, an RNA (guanine-7-)-methyltransferase, which adds a methyl group to the N-7 position of the guanine cap to form the fully mature cap structure, m^7GpppN1- (Saha *et al.*, 1999).

This initial cap structure is then recognized by the cap binding complex (CBC), which contains two proteins: SPAC6G10.07, which encodes the large subunit of the nuclear cap-binding complex, and SPBC13A2.01c, which encodes the small subunit of this complex. These proteins are also named after its mammalian orthologues, CBP80 and CBP20.

Once the mRNAs have been exported through the nuclear pore complex, the nuclear cap binding proteins are replaced by the cytoplasmic eukaryotic translation initiation factor 4 complex (eIF4F), which directs steady-state rounds of mRNA translation (Sonenberg, 1988).

2.1.1.2. SPLICING

Like other eukaryotes, many of *S. pombe* genes are interrupted by non-coding sequences (introns). Therefore, in order to generate a functional message from the DNA, pre-mRNA splicing must occur.

Mechanistically is possible that, during this process, one gene can increase its coding capacity to many different protein products. Pre-mRNAs can be processed combinatorially to increase the protein output variability. This process is called alternative splicing.

Splicing reactions take place inside the nucleus and can occur co- or posttranscriptionally. Afterwards, mature mRNAs will be transported to the cytoplasm in order to be translated.

The transcribed pre-mRNA itself contains some consensus *cis* elements, essential for the splicing reaction. The 5' exon-intron junction or splice site is marked by the consensus sequence GUAUGU. At the end of the intron it is present the 3' splice site, defined by CAG. Finally, about 19-50 nucleotides upstream of the 3' splice site lies the branchpoint UACUAAC (Schuler, 2008).

Chemically, splicing is based on two transesterification reactions. First, the 2' hydroxyl group of the branchpoint adenosine acts as a nucleophile to attack the 5' exon-intron junction, and trans-esterification results in a free 5' exon and a lariat-shaped molecule consisting of the intron sequences and the 3' exon. In the second step, the 3' hydroxyl group of the freed 5' exon attacks the 3' intron- exon border. The subsequent trans-esterification results in the fusion of the two exon sequences and the release of the lariat-shaped intron (Moore and Sharp, 1993).

Pre-mRNA splicing activity is associated to the spliceosome, a large highly dynamic ribonucleoprotein (RNP) complex. It consists of five small nuclear RNAs (snRNAs) called U1, U2, U4, U5 and U6 and a large amount of proteins. These snRNPs, together with many other proteins, assemble on the intron to form the spliceosome and thereby facilitate splicing (Krämer, 1996).

2.1.1.3. 3' END FORMATION

The only known protein-coding genes that do not contain a poly(A) tail in eukaryotes are the histone genes.

With this exception, all mRNAs translated into proteins contain a uniform 3' end consisting of about 200 adenosine residues. The formation of this poly(A) is mediated

by sequences present on the pre-mRNA and the polyadenylation machinery, which includes the poly(A) polymerase and two multimeric protein factors: cleavage factor I (CF I) and polyadenylation factor I (PF I).

Poly(A) binding protein (PABP1) binds the emerging poly(A) tail through its poly(A) binding domain and in turn increases the processivity of the poly(A) polymerase (Wahle and Ruegsegger, 1999).

Prior to the addition of poly(A), the pre-mRNA has to be cleaved at its 3'-end. The cleavage site in most pre-mRNAs is localized between the highly conserved AAUAAA hexamer and a downstream sequence element (DSE), which is a U- or GU-rich motif. Cleavage mainly occurs at a CA dinucleotide (Humphrey *et al.*, 1991).

2.2. TRANSLATION

After transcription and mRNA processing, translation is the third stage of protein biosynthesis, and embraces initiation, elongation and termination, being initiation and termination the most regulated steps.

Controlling gene expression by regulating translation allows cells to respond to environmental events more quickly than *de novo* transcription permits.

Translation begins with the assembly of a functional ribosome onto an mRNA. The 7-methyl guanosine cap at the 5' end of the mRNA is bound by the eukaryotic translation initiation factor 4 complex. This complex has been deeply studied in mammalian cells and it is conserved in fission yeast. The eukaryotic initiation factor 4 complex (eIF4F) includes the cap binding protein eIF-4E (*S. pombe* Tif45/Tif452), the RNA helicase eIF-4A (*S. pombe* SPAC1F5.10) and many other factors that work together with ribosomes to synthesize proteins. This complex facilitates the binding of the ribosomal small subunit to the mRNA.

After binding the mRNA, the small ribosomal subunit coupled to the initiation factor complex scans the 5' untranslated region (5'UTR) until it finds an AUG initiator codon in a favorable sequence context. Once an AUG is selected the large ribosomal subunit joins the complex and peptide synthesis begins (Hershey, 1991), and translation initiation ends.

The rate of translation initiation can be modulated by the concentration of active initiation factors or by the sequence of the 5'UTR, which establishes the intrinsic rate of initiation of translation of an mRNA, because ribosome binding is more sensitive to

secondary structures near the cap, but stable stem-loop structures anywhere in the 5'UTR can block ribosome scanning (Koromilas *et al.*, 1992; Kozak, 1989; Parkin *et al.*, 1988).

The translation initiation ratio is also modulated by 3'UTR sequences. These structures can repress or activate translation by modifying the length of the poly(A) tail, which in turn also regulates translation. Once transcribed inside the nucleus, most mRNAs are polyadenylated and then exported to the cytoplasm. Cytoplasmic enzymes promote removal and lengthening of their poly(A) tails (Sachs and Davis, 1989).

The pioneer round of mRNA translation takes place right after mRNA transcription, during translation initiation. This round involves the loading of one or more ribosomes into mRNAs. The amount of ribosomes depends on the efficiency of translation and the length of the open reading frame (Ishigaki *et al.*, 2001).

The termination of translation is the final key regulatory step in the translation of an mRNA. eRF1 (eukaryotic release factor 1) and eRF3 (eukaryotic release factor 3) are part of the functional termination complex. This genes are also known as sup45 (eRF1) and sup35 (eRF3) in fission yeast and *S.cerevisiae*. eRF1 functionally interacts with eRF3, *in vivo* and *in vitro*, to promote translation termination at all three stop codons (Stansfield *et al.*, 1995; Zhouravleva *et al.*, 1995). eRF3 is a guanosine triphosphatase that in order to develop this activity, requires both eRF1 and ribosomes (Frolova *et al.*, 1996).

3. POSTTRANSCRIPTIONAL REGULATION

Posttranscriptional regulation refers to the regulation of gene expression after mRNA has been produced.

Gene expression is susceptible to change depending on the environment request, so there should be a precise control of the mRNAs levels. Thus, some mechanisms promote mRNA synthesis and other promote mRNA degradation. Many of these mechanisms are regulated by RNA binding proteins.

3.1. RNA BINDING PROTEINS

RNA-binding proteins (RBPs) are key components in RNA metabolism. They directly interact with RNA molecules through the so-called RNA binding domains.

RBPs form dynamic interactions with protein-coding and non-protein-coding RNAs in functional units called ribonucleoprotein complexes (RNP). This interaction between RBPs and RNAs within RNP complexes remains stable and helps regulation.

Half-life, cellular localization, processing and rate at which a specific mRNA is translated are defined by the dynamic association of these RBPs with RNA.

Depending on the localization of the RNP complexes we can classify them into hnRNP (heterogeneous nuclear ribonucleoprotein) and mRNP (messenger ribonucleoprotein). The first group, hnRNP, is localized in the nucleus and it is formed by pre-mRNA and nuclear ribonucleoproteins. In contrast, mRNPs (mRNAs and cytoplasmic RBPs) are localized in the cytoplasm, but we can find also shuttling hnRNPs which are exported with the mature mRNA to the cytoplasm (Dreyfuss *et al.*, 2002).

hnRNP proteins participate in different nuclear events, such as transcriptional regulation, telomere-length maintenance, immunoglobulin gene recombination, splicing, pre-ribosomal-RNA processing, 3- end processing and nucleo-cytoplasmic transport of mRNA (Bomsztyk *et al.*, 2004).

This binding described previously is protein and mRNA specific, only a few mRNP proteins are consistently associated with most cytoplasmic mRNAs, like the poly(A) binding protein 1 (PABP1) (Burd *et al.*, 1991). It has also been described that mRNAs which encode proteins with similar function can be bound by the same RBP (Keene, 2007).

3.1.1. RBPs DOMAINS AND PROPERTIES

RBPs bind RNAs through RNA binding domains (RBD). Some well-characterized RNA-binding domains include the following (Chen and Varani, 2005; Lunde *et al.*, 2007):

- RNA-recognition motif (RRM, also known as RNA-binding domain, RBD or the RNP motif). This is the best characterized and most common RNA-binding domain of those already described.

  The RRM comprises 80-90 amino acids that form a four-stranded anti-parallel β-sheet and two helices, generating a αβ (βαββαβ) profile.

  Most characterized RRMs have been related to posttranscriptional gene expression processes.

  β-sheet surface is usually the responsible of RNA recognition through three conserved residues: an arginine or lysine and two aromatic residues. These three amino acids are localized in the two highly conserved motifs, RNP motif-1 (RNP1) and RNP2 (Wang and Tanaka Hall, 2001). By stacking, electrostatics interactions and hydrogen bonds these amino acids interact with about four nucleotides of single stranded RNA (ssRNA). Thus it is necessary to have more than one RRM *per* RBP to make the interaction between RBP and RNA more specific.

- K-homology domain (KH domain). KH domain binds to ssRNA (Lewis *et al.*, 2000) but also to single-stranded DNA (ssDNA) (Braddock *et al.*, 2002). The domain is formed by 70 amino acids with a functionally important sequence of (I/L/V)IGXXGXX(I/L/V) located approximately in the centre of the domain.

All KH domains form a three stranded β-sheet packed against three α-helices. Two KH domains subfamilies have been described, depending on the β-sheet and α-helices layout: type 1 contains a βααββα motif while in type 2 we can find a αββααβ variant.

Non-aromatic residues of KH domains recognize about 4 nucleotides of ssRNA and establish hydrophobic interactions between these residues and the bases of the RNA.

- DEAD/DEAH-box. This domain is present in RNAs helicases. It has been described that this family is required for different aspects of RNA metabolism as pre-mRNA splicing, ribosome biogenesis, nucleo-cytoplasmic transport, translation or RNA decay. Several consensus motifs have been described through the alignment of protein sequences of the DEAD-box family (Schmid and Linder, 1992; Tanner and Linder, 2001).

- PAZ and PIWI domains. These domains have been described in RBPs related to micro RNA (miRNA) and small interfering RNA (siRNA) metabolism. One of the best characterized is Argonaute (Ago1) that contains one PAZ domain and one PIWI domain in its structure.

- Double-stranded RBD. The dsRBD is a small αβ domain of 70-90 amino acids that is found in bacteria and eukaryotes. It interacts with double stranded RNA (dsRNA) (Ryter and Schultz, 1998).

- S1 domain. S1 domains have been found in several exonucleases. The domain is formed by 70 amino acids organized in a 5-stranded antiparalell β-barrel combined with 3 helix residues *per* turn. S1 domains interact with RNA by stacking interactions between bases and aromatic residues and hydrogen bonding to the bases.

- Zinc fingers. These are classical DNA-binding proteins but they can also bind RNA (Lu *et al.*, 2003). They are classified depending on the combination of cysteine (C) and histidine (H) residues (CCHH, CCCH or CCHC) of its structure.

3.1.2. FUCTIONS OF RBPs

- Alternative splicing.

It has been described that RBPs develop different functions in the regulation of the alternative splicing process (Matlin *et al.*, 2005).

In fission yeast there are some RBPs that can serve as example of this regulation through RNA interaction. Two of them are Cwf29 and Sap49, both containing RRMs. Both RBPs are components of the U2 snRNP and while Sap49 is a splicing factor (VanHoy and Wise, 1996), Cwf29 is involved in spliceosome assembly itself (Aslett and Wood, 2006).

- RNA modification

RNA editing carries out the conversion of adenosine (A) to inosine (I). This posttranscriptional modification is catalyzed by the adenosine deaminase-RNA specific (ADAR) protein (Bass, 1997). These proteins have been extensively studied in *Drosophila melanogaster* and *Homo sapiens*.

Although RNA editing occurs mainly in non-coding regions, a few genes have been identified that are subject to editing in their coding sequences (Nishikura, 2006). Some of them are present in nervous system encoding ion channels, G-protein coupled receptors and the glutamate and serotonin receptors.

- Polyadenylation

As it has been described before, polyadenylation of mRNA has a strong effect on its nuclear transport, translation efficiency and stability, and all of these processes depend on specific RBPs. As mentioned before PABP1 is a key component in the regulation of translation initiation.

- mRNA export

Usually, after pre-mRNA processing is complete the translatable mRNA is exported from the nucleus to the cytoplasm. To ensure that only fully processed mRNAs are exported, cell requires a monitoring mechanism.

There is a three step process involving different RBPs: the generation of an mRNA-carrier complex in the nucleus, the translocation of the complex through the nuclear pore complex, and the mRNA release in the cytoplasm with subsequent recycling of the carrier.

Fission yeast Mlo3 contains one RRM domain and is required for normal mRNA export process. It can bind Rae1 through Uap56 or Dss1, being Rae1 an essential nucleoporin in this process (Thakurta *et al.*, 2005).

- mRNA localization

Localization of transcripts to a specific region of the cell is critical for gene expression. RBPs play a major role in mRNA localization, and this process has been particularly well studied in budding yeast. As an example, during cell division in *S. cerevisiae*, *ASH1* mRNA is localized and translated in the distal tip of anaphase cells by its association with myosin (Myo4) and actin, resulting in accumulation of Ash1p in daughter cell nuclei. This interaction depends on other two proteins, She2 and She3. She2 binds directly the *cis* elements located partly in the coding region and in the 3'UTR of the *ASH1* mRNA and She3 protein. She3 has been defined as an adaptor between She2-*ASH1* mRNA and Myo4 (Gonsalvez *et al.*, 2004). The localized expression of the Ash1 protein is necessary for the suppression of mating type switching in the daughter cell.

- Translation

As mentioned above, translational regulation provides a rapid mechanism to control gene expression. Numerous regulatory proteins target the initiation step, often in a way that couples translation to mRNA localization. For instance, mammalian ZBP1 is regulating β-actin mRNA localization and blocking translational initiation of this mRNA (Huttelmaier *et al.*, 2005).

- mRNA turnover

Translation is tightly coupled to mRNA turnover and mRNA stability regulation.

Many RBPs have been described as mRNA stabilizers under certain circumstances. That is one of the roles described for the RBP Csx1 in *S. pombe*. The interaction between Csx1 and $atf1^{+}$ mRNA under hydrogen peroxide treatment and the noticeable decrease of $atf1^{+}$ mRNA levels in *csx1*Δ strains under the same conditions suggest that Csx1 stabilizes $atf1^{+}$ mRNA under oxidative stress conditions (Rodriguez-Gabriel *et al.*, 2003).

- Multi-functional proteins

Many RBPs, for example the RBPs included in hnRNP, bind to multiple sites on numerous RNAs to function in diverse process.

The mammalian hnRNPA1 protein can bind to exonic splicing silencer sequences and regulate alternative splicing (Hou *et al.*, 2002). Additionally, hnRNPA1 has been related to telomerase activity (Zhang *et al.*, 2006).

3.1.3. RBPs IN GENETIC DISEASE

RBPs can be subjected to posttranslational modifications. By this way these proteins can serve as sensors or adaptors, being the linker between extracellular signals and intracellular pathways.

There are numerous diseases related with aberrant RBP function: associated with RBP loss of function mechanism or associated with RNA gain of function.

Due to the high prevalence of alternative splicing that takes place in the brain, the principal clinical manifestation of RBP defects are neurodegenerative disorders. Muscular atrophies and cancer have also been related to RBPs defects (Kim *et al.*, 2009; Musunuru, 2003)].

Inactivated RBPs show a loss of function. This inactivation can be produced by genetic changes or autoimmune antibodies. If microsatellite expansion repeats are transcribed into mRNAs, an RNA gain of function can be observed. This RNA gain of function may result toxic due to the interaction of these transcripts with RBPs, interfering with their normal function (Wang and Cooper, 2007).

There are different examples of diseases with RBP loss of function mechanism, such as fragile X syndrome, paraneoplastic neurologic syndromes or spinal muscular atrophy.

On the other hand we find myotonic dystrophy, fragile X tremor ataxia syndrome or oculopharyngeal muscular dystrophy as RNA gain of function diseases.

RBP functions have been related to proliferation and cell growth. Being cancer an alteration of cellular proliferation due to changes in the activity of tumor-supressors and oncogenes, loss of RBP function might be involved in cancer. For instance, it has been found in sarcomas a significant amount of RBPs belonging to the RRM-domains-containing TET family (Riggi *et al.*, 2007), while in other types of human tumors an eIF4E and SF2/ASF up-regulation has been described (Karni *et al.*, 2007; Wendel *et al.*, 2007).

3.2. mRNA METABOLISM

mRNA metabolism includes mRNA formation, mRNA elongation and the deadenylation and subsequent degradation of mRNA.

As mentioned above 5' cap and 3' poly(A) tail are necessary for transcript stability and loss of either is sufficient to stimulate decay.

There is a huge number of proteins involved in the regulation of mRNA metabolism, including repression and activation of mRNA transcription initiation and specially mRNA decay. One example, conserved in all eukaryotic organisms, is the CCR4-NOT complex. The CCR4-NOT protein complex has a clear role in the degradation of mRNA being part of the cytoplasmic deadenylase complex (Chen *et al.*, 2002; Tucker *et al.*, 2001; Tucker *et al.*, 2002). These factors can also function at the other end of mRNA metabolism in repressing the initiation of transcription through TFIID contacts (Lemaire and Collart, 2000).

mRNA turnover is classically thought to be initiated by deadenylation but recently it has been described another two parallel decay pathways in fission yeast (Rissland and Norbury, 2009). The first one establishes a deadenylation independent deccaping and the second one is the uridylation, as another way to stimulate deccaping and consequently mRNA degradation.

3.2.1. NON-SENSE MEDIATED DECAY (NMD)

NMD is an mRNA surveillance mechanism, carefully studied in budding yeast and mammalian cells.

The main proteins involved in this pathway are conserved in fission yeast, but little is known about NMD in this organism.

NMD has been described as a mechanism that degrades mRNAs containing premature translation termination codons (PTCs), preventing the formation of truncated proteins (Culbertson and Leeds, 2003).

In mammalian cells these mRNAs containing PTCs can be a consequence of routine mistakes in gene expression, including errors in transcription initiation or pre-mRNA splicing, and ineffective DNA rearrangements of immunoglobulin and T-cell receptor genes. As result there are mRNAs that have reading frames upstream of the usual reading frame, frameshift mutations that generate nonsense codons, or nonsense mutations (Nicholson *et al.*, 2010). NMD also downregulates a number of physiological transcripts, including some selenoprotein mRNAs, mRNAs with long 3' UTRs or mRNAs of transposons, retroviruses and pseudogenes (Rehwinkel *et al.*, 2006).

The main and most conserved component of this mechanism is UPF1 (Up-Frameshift 1). This protein was first identified in yeast and *C. elegans*. UPF1 is an ATP-dependent

RNA helicase, and it has been shown that binds UPF2, other component of NMD mechanism through its N-terminus cysteine and histidine-rich (CH) domains (Clerici *et al.*, 2009; Serin *et al.*, 2001). The third component that forms the core of the NMD machinery is UPF3 (Serin *et al.*, 2001). In the human genome two UPF3 genes have been described encoding UPF3A and UPF3B proteins but in the rest of the organisms it has been described just one UPF3 protein. The major difference between both isoforms is that UPF3B is more effective triggering NMD than UPF3A.

Besides the UPF core there is another group of proteins called SMGs. SMG1 is a proteins kinase that phosphorylates UPF1. Once UPF1 is phosphorylated, it interacts with SMG5, SMG6 and SMG7. These proteins are necessary for UPF1 dephosphorylation by phosphatase PP2A (Chiu *et al.*, 2003; Ohnishi *et al.*, 2003).

UPF1 also binds the eukaryotic translation release factors eRF1 and eRF3, and together with SMG1 form the SURF complex (Kashima *et al.*, 2006).

In yeast, NMD occurs mainly once eIF4E has been bound to mRNAs. By contrast, in mammalian cells NMD has been suggested to occur during the pioneer round of translation, before the cap-binding complex (CBC) would be replaced by the translation initiation complex. Supporting this hypothesis, it has been shown that UPF1 interacts with CBP80, a component of the CBC, and CBP80 is necessary, at least in mammalian cells, for NMD (Hosoda *et al.*, 2005).

Degradation of NMD targets can be carried out by usual mRNA degradation mechanisms. This mechanism comprises a deadenylation reaction, deccaping and exonucleolytic reaction. Deadenylation is catalysed first by PAN2/PAN3 complex and once the poly(A) tail is shortened to around 110 bases by the CCR4/CAF1 complex (Ccr4p/Caf1p in yeast). Concomitant to CCR4/CAF1 complex activity DCP1/DCP2 removes the 7-methyl guanosine cap structure. These two reactions leave mRNA accessible and promote a rapid degradation 5'-3' by the exonuclease XRN1 and 3'-5' by the exosome. This is the most common way to degrade mRNAs and PTCs containing transcripts but it is not the only one. It has been described alternative degradation mechanisms such as deadenylation independent decaping or SMG6-dependent endonucleolytic pathway (Nicholson and Muhlemann, 2010).

The most controversial point of NMD is localization. UPF1 is a cytoplasmic protein, UPF2 perinuclear and UPF3 a shuttling nuclear-cytoplasmic protein, while the rest of the NMD components are localized in the cytoplasm with the exception of CBP80 that is a nuclear protein.

In yeast it has been suggested that NMD could be taking place in processing bodies (P-bodies). PTC-containing transcripts have been found in these structures and this accumulation is reduced in *upf1*Δ strains and even in *upf2*Δ or *upf3*Δ strains. Upf1 is also accumulated in P-bodies when the degradation machinery is absent, i.e in *dcp1*Δ, *dcp2*Δ or *xrn1*Δ strains (Sheth and Parker, 2006).

By contrast in mammalian cells there are different theories about where does NMD occurs. It can be inside the nucleus, in the nuclear envelope coupled to mRNA export, or in the cytoplasm, but there is no evidence about P-bodies localization of NMD components.

4. OXIDATIVE STRESS RESPONSE

Eukaryotic cells are susceptible to undergo different environmental stresses such as changes in osmolarity, exposition to reactive oxygen species or ultraviolet light, heat shock and nutritional deficiency (Shiozaki and Russell, 1995a, 1996). Cells have to survive under these conditions so they have developed different mechanisms to adapt to the new conditions.

One of the best characterized mechanisms is the one mediated by mitogen activated protein kinases (MAPKs). These MAPKs are protein kinases that can phosphorylate different substrates and are susceptible to be phosphorylated and activated. In fission yeast, the MAPK pathway that generates a cell adaptation under oxidative stress conditions, comprises two MAPK kinase kinases (MAPKKK), Win1 and Wik1/Wis4/Wak1, a MAPK kinase, Wis1 and a MAPK, Spc1/Sty1/Phh1 (Kato *et al.*, 1996; Millar *et al.*, 1995; Shiozaki and Russell, 1995a).

In response to oxidative stress, histidine kinases Mak1/Phk3, Mak2/Phk1 and Mak3/Phk2 act as sensors and activate the pathway, phosphorylating Mpr1/Spy1 which in turn transfers its phosphate to Mcs4 (Nguyen *et al.*, 2000). Mcs4 is the regulator element that activates the MAPK module, phosphorylating Wis4 MAPKKK (Shiozaki *et al.*, 1997) (Figure 2).

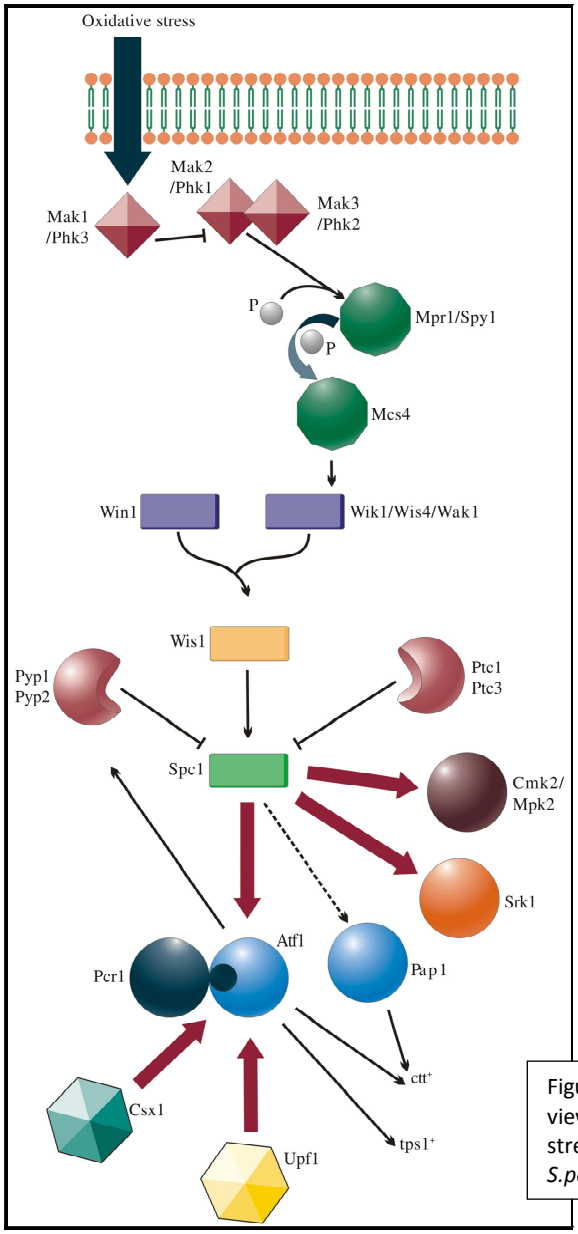

Figure 2. Schematic view of the oxidative stress response in *S.pombe*.

Constitutive activation of the pathway is lethal and there is a regulatory system that prevents MAPKs activation in the absence of stress. There are two tyrosine phosphatases, Pyp1 and Pyp2, and two serin-threonin phosphatases, Ptc1 and Ptc3, involved in this regulatory system. All of them negatively regulate Spc1 activity by its dephosphorylation (Millar *et al.*, 1995; Shiozaki and Russell, 1995b).

Under oxidative stress conditions, the main transcription factor that is activated is Atf1. Atf1 binds DNA consensus sequence ATF/CRE (TGACGTCA) that promotes the expression of many genes involved in the oxidative stress response, as *tps1*$^{+}$ or *ctt1*$^{+}$ (Wang *et al.*, 2005), but also other genes involved in osmotic stress response (*gdp1*$^{+}$, *sod2*$^{+}$), meiosis (*ste11*$^{+}$) (Takeda *et al.*, 1995) or negative regulation of the stress pathway (*pyp2*$^{+}$) (Shiozaki and Russell, 1996; Wilkinson *et al.*, 1996).

Atf1 forms a heterodimer with Pcr1 and this interaction stabilizes both proteins. Atf1 stabilization is also favoured by its phosphorylation by Spc1 (Lawrence *et al.*, 2007).

There is another transcription factor activated under oxidative stress conditions, Pap1. Activation of Atf1 or Pap1 depends on the dose of the oxidative stress. Thus, low levels of hydrogen peroxide that causes oxidative stress are enough to activate Pap1 to promote an adaptative mechanism while high levels of hydrogen peroxide activates Atf1 setting off a survival mechanism (Quinn *et al.*, 2002; Vivancos *et al.*, 2004).

Spc1 regulates the transcription factors described above but also many other proteins as Cmk2/Mpk2 (Sanchez-Piris *et al.*, 2002) or Srk1 (Smith *et al.*, 2002) under oxidative stress.

Csx1 is a key component in this response, being a genetic link between Spc1 and Atf1. *csx1*Δ strain shows a sensitive phenotype under oxidative stress conditions but not under other kind of stresses that activate Spc1 pathway. Csx1 is an RBP that contains 3 RNA recognition domains. Through these domains, Csx1 modulates the expression of many mRNAs involved in the oxidative stress response. It has been described that Csx1 binds *atf1*$^{+}$ mRNA under hydrogen peroxide treatment, stabilizing this mRNA, thus Csx1 controls *atf1*$^{+}$ mRNA turnover. Besides, Csx1 phosphorylation is abolished in *spc1*Δ strain (Rodriguez-Gabriel *et al.*, 2003).

Surprisingly, Upf1, the core component of NMD pathway, is also required in the oxidative stress response. As *csx1*Δ strain, *upf1*Δ strain shows a sensitive phenotype only under hydrogen peroxide treatment. Upf1 modulates *atf1*$^{+}$ mRNA half-life, but in this case it has not been demonstrated a physical interaction between Upf1 and *atf1*$^{+}$ mRNA. It has been described a large overlap between those genes controlled by Upf1 and Csx1. Moreover, the double mutant *upf1*Δ *csx1*Δ shows a similar sensitive phenotype than the single mutants, suggesting that both proteins participate in the same pathway (Rodriguez-Gabriel *et al.*, 2006).

5. SEXUAL DIFFERENTIATION

Homothallic (h^{90}) and heterothallic (h^{+}/h^{-}) strains reproduce by mitosis and are divided by medial fission under normal growing conditions, but under certain conditions cells with opposite mating type can conjugate and form diploid cells. Diploids then undergo meiosis and sporulation, producing haploid spores that germinate finishing the mating cycle.

The conditions that promote sexual differentiation are nitrogen starvation and low temperature (24°C). Once cells of different mating type detect these favorable conditions there is an exchange of mating pheromones that promotes the fusion between cells. Thus, there is a nutritional and a pheromone regulation in mating (Figure 3).

- NUTRITIONAL REGULATION:

Nutritional regulation is carried out by the cyclin AMP (cAMP) pathway, being cAMP the key component of this response. Changes in cytoplasmic cAMP concentration are responsible of either normal growth or mating.

In rich media there is an activation of this pathway by Gpa2, a heterotrimeric G protein, which in turn activates an adenylate cyclase, Cyr1. This protein converts ATP to cAMP and this cAMP is the activator of cAMP-dependent protein kinases, Sck1 and Cgs1-Pka1. At this point there is a repression of *ste11*$^{+}$, the main transcription factor involved in sexual differentiation. This pathway is repressed in nutrient deprivation, meaning an induction of *ste11*$^{+}$ (Higuchi *et al.*, 2002; Sugimoto *et al.*, 1991).

Under these conditions cells arrest cell cycle at G1 preventing polyploidy phenomena. In the absence of different mating type cells, they remain in a quiescent state, G0 and if nitrogen is added to the media they can return to a mitotic cycle (Kanoh *et al.*, 1996).

Under starvation, *ste11*$^{+}$ is induced by cAMP pathway, but also by Spc1 pathway. Spc1 is the MAPK involved in stress response but it can detect nitrogen depletion and transmits this signal through Atf1, which then activates *ste11*$^{+}$ mRNA transcription (Takeda *et al.*, 1995).

Increased *ste11*$^{+}$ expression mediated by cAMP and Spc1 is enough to promote its own transcription (Kunitomo *et al.*, 2000), and mating pheromone expression which will activate pheromone response through a MAPK cascade (Kjaerulff *et al.*, 2005).

Under nitrogen starvation other situations that direct sexual differentiation take place, such as inhibition of protein kinase Pat1. Under normal conditions Pat1 phosphorylates Ste11. Phosphorylated Ste11 is localized in the cytoplasm and cannot migrate to the nucleus where is necessary for gene expression (Kjaerulff *et al.*, 2005; Qin *et al.*, 2003). Pat1 activity has to be inhibited in order to proceed with the sexual differentiation program.

- PHEROMONE REGULATION:

Pheromone regulation is mediated by a MAPK pathway. Mating pheromones are the extracellular signal required to activate this pathway, and the expression of these pheromones is induced by Ste11. Pheromones are detected by a membrane receptor coupled to a G protein (Gpa1) and the signal is transmitted through a MAPK cascade. This MAPK module is formed by a MAPKKK, Byr2, a MAPKK, Byr1, and a MAPK, Spk1 which activates the transcription factor Ste11 (Kjaerulff *et al.*, 2005).

The Spk1 MAPK pathway is also regulated by Ras1 and Ste4 that activate MAPKKK Byr2.

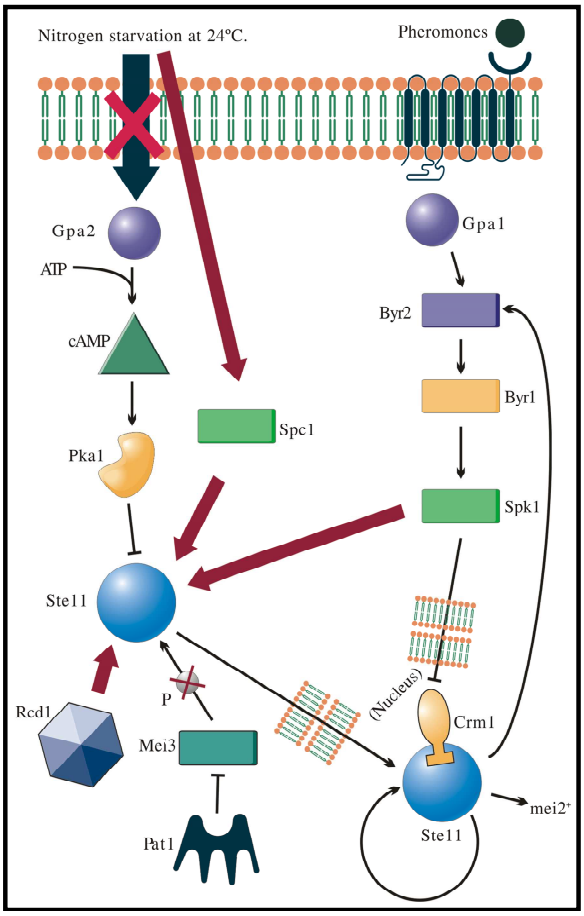

Figure 3. Schematic view of the nutritional and pheromone regulation in the sexual differentiation of *S. pombe.*

Ste11 is tightly regulated by nutritional and pheromone signaling, but there are other factors like Rcd1 or Crm1 involved in this regulation. Rcd1 is an RBP that induces *ste11*$^{+}$ expression under nitrogen starvation conditions (Okazaki *et al.*, 1998). Rcd1 belongs to the CCR4-NOT complex (Haas *et al.*, 2004). Crm1 is an exportin that extrudes Ste11 from the nucleus. Under nitrogen starvation and pheromone induction Crm1 activity is inhibited, leading to Ste11 nuclear accumulation (Qin *et al.*, 2003).

Ste11 is in turn required for sexual differentiation gene expression. One of the genes involved in sexual differentiation regulated by Ste11 is *mei2*$^{+}$. Mei2 is the most important RNA binding protein involved in meiosis (Watanabe and Yamamoto, 1994). Mei2 is inactivated by Pat1 phosphorylation. When conjugation occurs, *mei3*$^{+}$ expression is induced (Willer *et al.*, 1995). Mei3 is an inhibitor of Pat1, and this inhibition provokes Mei2 dephosphorylation and therefore entry into meiosis.

Ste11 is negatively regulated by Nrd1. Nrd1 is an RBP that repress the expression of *ste11*$^{+}$ and genes regulated by this transcription factor (Tsukahara *et al.*, 1998).

AIMS

Considering the increasing importance of studying RNA regulation, we focused our project on the study of RNA binding proteins, which regulate among many other functions, mRNA localization, half-life, stabilization and alternative splicing, using the model organism *Schizosaccharomyces pombe*.

Previous results in our laboratory described novel functions of two RBPs, Csx1 and Upf1 in the oxidative stress response. Our genetic data indicated that both proteins were functionally related. Therefore, we decided to study the functional role of Upf1 and Csx1 in *S. pombe* physiology.

Being Upf1 a protein also involved in the NMD, we focused our interest in the study of:

- Upf1 global role in posttranscriptional regulation of gene expression
- Upf1 specific role in the oxidative stress response
- The relationship between Upf1 role in posttranscriptional regulation and the NMD pathway.

Csx1 is an RBP involved in the oxidative stress response but we found that cells lacking this protein showed defects in mating. Thus, we decided to study the role of Csx1 in sexual differentiation.

MATERIALS & METHODS

1. ORGANISMS:

a) *Schizosaccharomyces pombe*

In this work *S. pombe* strains with different gene modifications have been used.

The details of the strains used in this work appear in the following table (Table1).

Table 1. List of strains used in this work.

STRAIN	GENOTYPE	REFERENCE
PR109	*h⁻ ura4-D18 leu1-32*	Paul Russell Lab
PR110	*h⁺ ura4-D18 leu1-32*	Paul Russell Lab
MR3213	*h⁻ csx1::kanMX6 ura4-D18 leu1-32*	Rodriguez-Gabriel *et al.*, 2003
MR3567	*h⁻ upf1::kanMX6 ura4-D18 leu1-32*	Rodriguez-Gabriel *et al.*, 2006
MR158	*h⁻ upf1:TAP:kanMX6 ura4-D18 leu1-32*	Laboratory collection
MR163	*h⁻ upf2::kanMX6 ura4-D18 leu1-32*	Laboratory collection
MR239	*h⁺ upf2::kanMX6 ura4-D18 leu1-32*	This work
MR252	*h⁻ rex2::kanMX6 ura4-D18 leu1-32*	Laboratory collection
MR257	*h⁻ upf1::kanMX6 rex2::kanMX6 ura4-D18 leu1-32*	Laboratory collection
MR319	*h⁹⁰ csx1:TAP:kanMX6 ura4-D18 leu1-32*	This work
PR636	*h⁹⁰ ura4-D18 leu1-32*	Paul Russell Lab
MR391	*h⁹⁰ csx1::kanMX6*	This work
JB22	*h⁻ 972*	Jürg Bähler Lab
JB420	*h⁻ upf1::kanMX6*	Jürg Bähler Lab
MR351	*h⁻ upf1:GFP:kanMX6 ura4-D18 leu1-32*	This work
MR382	*h⁻ upf2:TAP:kanMX6 ura4-D18 leu1-32*	This work
JB50	*h⁹⁰ 968*	Jürg Bähler Lab
JB489	*h⁹⁰ ste11::ura4 ura4-D18*	Jürg Bähler Lab
MR397	*h⁹⁰ csx1:TAP:kanMX6*	This work
MR400	*h⁹⁰ csx1:GFP:kanMX6*	This work
MR402	*h⁺ upf1:TAP:kanMX6 upf2::kanMX6 ura4-D18 leu1-32*	This work
MR403	*h⁻ upf1:GFP:kanMX6 upf2::kanMX6 ura4-D18 leu1-32*	This work
MR421	*h⁻/h⁺ csx1::kanMX6/csx1::kanMX6 ura4-D18/ura4-D18 leu1-32/leu1-32 ade6-M216/ade6-M210*	This work
MR428	*h⁻/h⁺ ura4-D18/ura4-D18 leu1-32/leu1-32 ade6-M216/ade6-M210*	This work
MR433	*h⁻ upf1:TAP:kanMX6 upf3::kanMX4 ura4-D18 leu1-32*	This work
MR658	*h⁻ upf1:HA:kanMX6 upf2:TAP:kanMX6 ura4-D18 leu1-32*	This work
MR626	*h⁻ upf2:VN173:kanMX6 ura4-D18 leu1-32*	This work

MR649	*h^+ upf1:VC155:kanMX6 ura4-D18 leu1-32*	This work
MR656	*h^- upf1:VC155:kanMX6 upf2:VN173:kanMX6 ura4-D18 leu1-32*	This work
V2-01-G07	*h^+ upf3::kanMX4 ura4-D18 leu1-32 ade-*	Bioneer
MR509	*h^-/h^+ pat1-14/pat1-14 ura4-D18/ura4-D18 leu1-32/leu 1-32*	Laboratory collection
MR511	*h^-/h^+ pat1-14/pat1-14 csx1::kanMX6/csx1::kanMX6 ura4-D18/ura4-D18 leu1-32/leu 1-32*	This work
MR591	*h^- upf1::kanMX6 mug105::kanMX4 ura4-D18 leu1-32*	This work
MR596	*h^- upf1::kanMX6 SPCC63.13::kanMX4 ura4-D18 leu1-32*	This work
MR595	*h^- upf1::kanMX6 SPAC11D3.09::kanMX4 ura4-D18 leu1-32*	This work
MR589	*h^- upf1::kanMX6 rad8::kanMX4 ura4-D18 leu1-32*	This work
V2-17-G02	*h^+ mug105::kanMX4 ura4-D18 leu1-32 ade-*	Bioneer
V2-11-F11	*h^+ rad8::kanMX4 ura4-D18 leu1-32 ade-*	Bioneer
V2-14-D03	*h^+ SPAC11D3.09::kanMX4 ura4-D18 leu1-32 ade-*	Bioneer
V2-27-C04	*h^+ SPCC63.13::kanMX4 ura4-D18 leu1-32 ade-*	Bioneer
MR660	*h^- upf1::kanMX6 leu1-32 otr1R(SphI)::ura4 ura4-DS/E*	This work
DG690	*h^- dcr1::kanMX6 leu1-32 otr1R(SphI)::ura4 ura4-DS/E his7-366 ade6-M210*	Martienssen Lab
ZB20	*h^- ago1::kanMX6 leu1-32 otr1R(SphI)::ura4 ura4-DS/E his7-366 ade6-M216*	Martienssen Lab
DG124	*h^- rdp1::kanMX6 leu1-32 otr1R(SphI)::ura4 ura4-DS/E his7-366 ade6-M216*	Martienssen Lab
DG21	*h^- leu1-32 otr1R(SphI)::ura4 ura4-DS/E his7-366 ade6-M216*	Martienssen Lab
MR682	*h^- upf1::kanMX6 dcr1::kanMX6 leu1-32 otr1R(SphI)::ura4 ura4-DS/E*	This work
MR680	*h^- upf1::kanMX6 ago1::kanMX6 leu1-32 otr1R(SphI)::ura4 ura4-DS/E*	This work
MR646	*h^- upf1::kanMX6 rdp1::kanMX6 leu1-32 otr1R(SphI)::ura4 ura4-DS/E*	This work
MR717	*h^{90} ura4-D18 leu1-32 + pREP1*	This work
MR718	*h^{90} ura4-D18 leu1-32 + pREP1-Ste11*	This work
MR719	*h^{90} csx1::kanMX6 ura4-D18 leu1-32 + pREP1*	This work
MR720	*h^{90} csx1::kanMX6 ura4-D18 leu1-32 + pREP1-Ste11*	This work

b) *Escherichia coli*

E. coli DH5α strain (Hanahan, 1983) was used for molecular biology techniques. Its genotype is *supE44 ΔlacU169 (ϕ80lacZΔM15) hsdR17 recA1 endA1 gyrA96 thi-1 relA1*.

c) Mammalian cells

Some of the experiments were carried out in mammalian cells, using monkey COS cell line.

2. CULTURE MEDIA

a) *S. pombe*

Culture media was prepared using de-ionized water based on Millipore system.

For solid media, Bacto™ Agar (BD) was added at 20 g/l.

Some of the media was purchased premixed from Formedium (UK).

The media was sterilized at 1 atm/121°C for 20 minutes.

- YES (Yeast Extract Supplements): 30 g/l glucose, 5 g/l yeast extract, 225 mg/l adenine, lysine hydrochloride, leucine, histidine and uracil.
- YEA (Yeast Extract Adenine minus): YES without adenine.
- EMM (Edinburgh Minimal Media): 3 g/l potassium hydrogen phthalate, 2.2 g/l disodium hydrogen phosphate, 5 g/l ammonium chloride, 20 g/l glucose, salts, vitamins and minerals (Moreno *et al.*, 1991).

  This media can be supplemented with different aminoacids/nucleotides depending on the strain request. All the aminoacids/nucleotides were added at 225 mg/l.

  Thiamine at 5 µg/ml was added to EMM for maximal repression of pREP1 plasmids expression.
- EMM-N (Edinburgh Minimal Media without Nitrogen): EMM without ammonium chloride.
- ME (Malt Extract): 30 g/l Bacto™ Malt Extract.

b) *E.coli*

E. coli was cultivated in LB (Luria- Bertani) media: 10 g/l bacto-triptone, 5 g/l yeast extract, 10 g/l sodium chloride.

For solid media, Bacto™ Agar was added at 20 g/l.

To select the cells that were transformed using ampicillin resistant plasmids, LB media was supplemented with ampicillin at 100 µg/ml.

c) Mammalian cells

Cells were grown in Dulbecco's Modified Eagle's Medium (DMEM–Gibco-BRL) supplemented with 10% Fetal Bovine Serum (FBS – Gibco-BRL).

3. GROWTH AND MANTEINANCE CONDITIONS

- Growth conditions for *S. pombe* were: 24°C for nitrogen starvation induction and thermo-sensitive alleles; 30°C-32°C for standard conditions; 39°C for heat shock experiments.

  Liquid media cultures were incubated with 180-200 rpm shaking.

  Cells were harvested either by centrifugation at 3000 xg for 2 minutes or by filtration.

- *E. coli* was cultivated at 37°C and shaking at 200 rpm.

  Bacterial cells were harvested by centrifugation at 13000 xg for 2 minutes.

- COS cells were incubated in 100 mm dishes at 37°C without shaking and 5% CO_2. To maintain cells growing they were spread out at 100 % confluence. To do that, cells were washed with serum-free DMEM to remove FBS. To strip them out, 25 % Tripsin-EDTA (Gibco-BRL) was used, and 1/10 of the cells were resuspended in DMEM supplemented with 10% FBS.

4. MOLECULAR BIOLOGY TECHNIQUES

4.1 DNA extraction

- *S. pombe* DNA extraction.

200 µl of lysis buffer (2% Triton X-100, 1% SDS, 100 mM NaCl, 10 mM Tris-HCl pH 8.0, 1 mM EDTA) were added to the yeast cell pellet. Then, 200 µl of phenol:chloroform:isoamyl alcohol (PCI; 25:24:1), pH 8.0 were added. Finally, glass beads were added and the mixture was vortexed for 2 minutes at full speed.

Extracts were centrifuged for 6 minutes at maximum speed, and aqueous layer was transferred to a new tube, that contained 200 µl of chloroform.

After vortexing for 1 minute and short centrifugation, aqueous phase was transferred to a fresh tube with 500 µl of pre-cooled ethanol. It was incubated for 1 hour at -20°C.

Afterwards it was centrifuged for 10 minutes at room temperature at 13000 xg. DNA pellet was washed once with 70% ethanol, centrifuged again at 13000 xg for 10 minutes at room temperature and finally air dried for 5 minutes at RT.

DNA was resuspended in 30 µl of TE (100 mM Tris-HCl pH 7.5, 10 mM EDTA pH 8.0) supplemented with 1 µl of RNAse A at 10 µg/ml. It was incubated at 37°C for 30 minutes, and DNA was quantified by measuring absorbance at 260 nm with Nanodrop spectrophotometer (Thermo Scientific).

- *E. coli* DNA extraction.

  - Minipreps

    E. coli cell pellets were resuspended by vortex in 150 µl of solution P1 (50 mM Tris-HCl pH 8.0, 10 mM EDTA pH 8.0, 0.0107 g RNAse A). 250 µl of solution P2 (0.8% NaOH, 1% SDS) were added, gently mixed and incubated 10 minutes at RT.

    200 µl of pre-cooled solution N3 (4 M guanidine hydrochloride, 0.5 M potassium acetate pH 4.2) were added and mixed by inversion. After 10 minutes incubation on ice, samples were centrifuged for 10 minutes at top speed and supernatant was transferred to a fresh tube. DNA was precipitated with 1 volume of isopropanol.

    After centrifugation at 13000 xg for 15 minutes, pellet was washed with 750 µl of ethanol 70% and centrifuged again at 13000 xg for 15 minutes.

    Finally, DNA was resuspended in 30-50 µl of TE supplemented with 1 µl of RNAse A at 10 µg/ml.

  - Large DNA preparations

    This protocol was designed to recover supercoiled DNA at high concentrations. This kind of DNA is the one needed for mammalian cell transfections.

    One single *E. coli* colony was selected and grown in 500 ml of LB supplemented with antibiotics (ampicillin). Cells were centrifuged at 8000 xg for 10 minutes.

    Supernatant was discarded and pellet resuspended by vortex in 36 ml of GET (9 g/l dextrose, 10 mM EDTA pH 8.0, 25 mM Tris-base pH 8.0). 4 ml of lysozime solution (10 mg/ml of lysozime dissolved in GET) were added.

    20 ml of solution 2 (0.3 N NaOH, 1% SDS) were added, and it was mixed carefully by inversion.

30 ml of potassium acetate/glacial acetic acid mixture (294.4 g/l KAc, 115 ml/l HAc) were added and after mixing by inversion, the solution was incubated for 30 minutes on ice.

Samples were centrifuged for 30 minutes at 4°C at 8500 xg.

Supernatant was transferred to a fresh tube and DNA was precipitated with 50 ml of isopropanol. It was thoroughly mixed and incubated for 30 minutes at RT. After centrifugation at 5000 xg at 20°C for 20 minutes, supernatant was discarded and pellet resuspended in 25 ml of 0.1% SSC (20X SSC: 175.32 g/l sodium chloride, 88.23 g/l sodium citrate, distilled water, pH adjusted to 7.0). The solution was incubated for 30 minutes at RT.

27.26 g of cesium chloride and 200 µl of ethidium bromide (10 mg/ml) were added to the DNA. Solution was centrifuged for 20 minutes at 20°C at 8000 xg.

Supernatant was placed into heat-sealable Beckman tubes. They were filled with 5 ml of mineral oil.

Tubes were ultracentrifuged at 45000 xg for 15 hours at 15°C.

After centrifugation we could observe a gradient, where we could distinguish supercoiled DNA, circular DNA and linear DNA. (Figure 4)

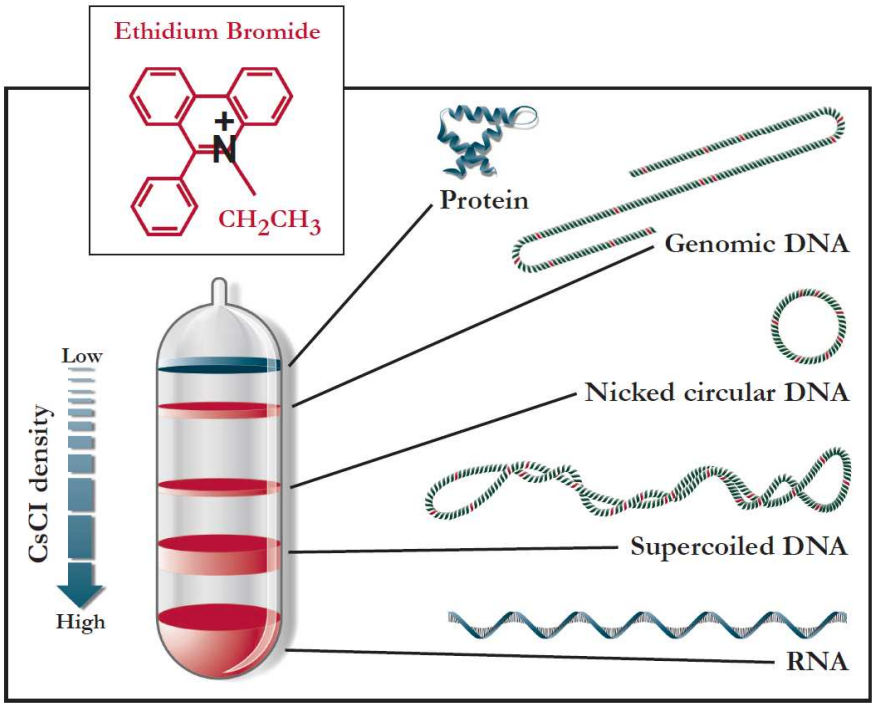

Figure 4. Schematic view of cesium chloride gradient stained with ethidium bromide. In this gradient we can distinguish different types of DNA topologies, RNA and proteins.

Using a syringe with a needle the band containing supercoiled DNA was extracted.

To remove ethidium bromide, the DNA sample was mixed with 5 ml of butanol saturated with water by vortex, and butanol phase was discarded. This step was repeated 4 times.

Finally, DNA was precipitated with 75% ethanol. It was incubated for 2 hours at -20°C. Afterwards samples were centrifuged at 15000 xg at 4°C for 30 minutes and washed with 10 ml of pre-cooled 75% ethanol. After centrifugation at 15000 xg for 15 minutes at 4°C, DNA was air dried, and resuspended in 0.5-1 ml of water.

DNA was quantified with Nanodrop spectrophotometer (Thermo Scientific).

4.2 DNA visualization

DNA fragments/molecules were separated by electrophoresis on 0.8% - 1.5% agarose gels.

Gels were prepared on 1X TAE buffer (50X TAE: 121 g Tris-base, 28.55 ml glacial acetic acid, 50 ml of 0.5 M EDTA and distilled water to 0.5 l).

To visualize DNA fragments under UV light, gels were prepared containing an intercalating agent, ethidium bromide at 5 µg/ml or 0.1% SYBR Safe (Invitrogen).

4.3 DNA TRANSFORMATION

- *S. pombe* transformation.

S. pombe gene deletion and C-terminal tagging was performed by PCR amplification followed by transformation.

The plasmid used for these experiments was pFA6a-kanMX6 and its derivatives (Bähler *et al.*, 1998). There are some variations depending on the epitope that it contains, but all of them express the kanMX6 module. Primers are described in table 2.

Table 2. Primers used for kanMX6 module amplification in this study.

PRIMER	SEQUENCE
72.Rex2del5	GATGTGTACCTCAGTTTTTAAACTTTTACTAATATAAAGATTTCATCTCAAAAT TAAAAGTCCATTCTCCAACCTCAAACGGATCCCCGGGTTAATTAA
73.Rex2del3	TACCCTTAATTTTTTTGGCATGTTTACAAGATATTGTCAATTGCTGTAAAAGTG GAATTCTTCTTTCTTGAGCAATGTTTGAATTCGAGCTCGTTTAAAC
261.Upf2_tag_5	TGGTCAGGTCTACCAAGAATCAGCAAACTGAAGAAATAATGGAACGGAAAC GTGTTAAAGAAATGGTTTTGAACTTCGAACGGATCCCCGGGTTAATTAA
262.Upf2_tag_3	AGGTTCGTCTATTCTAGTTGTAAACGAAGCAGGTAATTTACCAGCAATGGCTT AGAATTTCGGTATTTAGAGGACGAAGAGAATTCGAGCTCGTTTAAAC
Upf1_tagF	AAAGCAACGCTACCGACTTTGAAGACTTTAGAAGTCAGGTTGGTGATGATGA AAGCAAGTTCGACGAACCTACTAGGTTCCGGATCCCCGGGTTAATTAA
Upf1_tagR	ATAAAACTTGAACACCAAAAATATCAACAAATAAAAGATATGTTGGCATTCGT AATTACAAGTAAGCAAATACTTATTAAGAATTCGAGCTCGTTTAAAC
Csx1_delF	TGACTTTTGTGTCTCATTGAAACTTTGTTGTTCATTCATATTACTTACTTTCTTT TACTTTTTTTTGGATATCTATTTAACGGATCCCCGGGTTAATTAA
Csx1_delR	AATAAAAAAAAATCACGAGAGCACCCTTCAGTTCTTTAAGACATTAAACTAACT TGATCAGGAGCCCTCGAAAACTTATACGAATTCGAGCTCGTTTAAAC
Csx1_tagF	GCTTGCCTCCTCGTTCTTATTCTACATTTAATTGTACTGGTCAATACTTGCAAC CTTCTCTACGCTTGTCACGCGATTCACGGATCCCCGGGTTAATTAA

PCR amplification was set up using 500 ng of template DNA (*cassette*), 0.15 µM of each primer, 2 µl of 2.5 mM dNTPs, 2.5 µl of 10X buffer for Taq polymerase, 0.125 µl of Taq polymerase (TaKaRa) and RNAse-free water. The PCR was carried out in a gradient thermocycler (Eppendorf).

PCR product was checked by agarose gel electrophoresis.

DNA was precipitated by addition of 2.5 volumes of ethanol and 1/10 volume of 3 M sodium acetate pH 5.6.

10 ml (about 10^9 cells) of *S. pombe* cells were transformed with 1 µg of DNA by lithium acetate transformation (Okazaki *et al.*, 1990).

Cultures were plated in kanamycin-containing plates (150 mg/l). Kanamycin stability of each colony was confirmed and correct insertion of kanamycin resistance gene demonstrated using the primers described below. (Table 3)

Table 3. List of primers used in this study to check constructed strains

PRIMER	SEQUENCE
6.kantest	TGGTCGCTATACTGCTGTCG
Upf1_test	AAAACGCTTACAGACCAAACGG
Csx1_test	CATCACAAGAGAGATTTAAC
74.Rex2check3	AAAAAAGTAAGATCACCGAGG
263.Upf2_tag_check	TACCATAGTAAATTGCAAGC
267.Upf3_tagdel_check	GTATCTATCATCAGTGTATC
345.SPAC11D3.09_f_test	CGGTAGTAAGATAAGAAGCAATCGA
346.Mug105_f_test	ATCATCAACGTTGGAGGATTCAGAA
347.Rad8_f_test	CAGCTCCACCATGGATCCATAATAA
348.SPCC63.13_f_test	GATTTTTGGAAAACAGATCAAATCC
352.Ago1_R_test	TTTTCAAATTTGAATGATTTTGCTT
353.Rdp1_R_test	TTATTACCCTCATTCGAAAGCTAGC
399.Dcr1R_test	CCCATGGGGAACCTCTGAAATAT

- *E. coli* transformation.

Competent DH5α cells were used as cloning host.

Plasmids used in this work are described in the table 4.

DH5α cells (Invitrogen) were transformed by heat shock at 42°C for 45 seconds. Cells were put on ice and plated in LB plates supplemented with ampicillin (100 mg/l). Colonies were checked by miniprep, and restriction enzymes analysis.

Table 4. List of plasmids used in this work

PLASMID	DESCRIPTION	REFERENCE
pUbFC-VN173-SUMO1	Mammalian vector that contains a multi cloning site (MCS), VN173 epitope, SUMO1 sequence and ampicillin resistance gene. Vector expression is driven from human cytomegalovirus (CMV) promoter.	Gift from Dr.Kyungjin Kim
pUbFC-VC155-mBMAL1	Mammalian vector that contains a MCS, VC155 epitope, mBMAL1 sequence, ampicillin resistance gene and human CMV promoter.	Gift from Dr.Kyungjin Kim
pBiFC-VN173-pFlagVN173	Mammalian vector that contains a FLAG epitope, a MCS, VN173 epitope, ampicillin resistance gene and human CMV promoter.	Shyu *et al.*, 2006
pBiFC-VC155-pHAVC155	Mammalian vector that contains an HA epitope tag, a MCS, VC155 epitope, ampicillin resistance gene and human CMV promoter.	Shyu *et al.*, 2006
pCMV-myc-UPF1	Mammalian vector that contains a myc epitope, a MCS, UPF1 sequence, ampicillin resistance gene and human CMV promoter.	Kim *et al.*, 2005
pFlag-CBP80	Mammalian vector that contains a FLAG epitope, a MCS, CBP80 sequence, ampicillin resistance gene and human CMV promoter.	Hosoda *et al.*, 2005
pEQ863-His-eRF3	Mammalian vector that encodes 8 histidines tail, a MCS, eRF3 sequence, ampicillin resistance gene and human CMV promoter.	Janzen and Geballe, 2004
pBiFC-VN173N-UPF1	UPF1 sequence was amplified from pCMV-myc-UPF1 and cloned into XbaI-StuI site of pUbFC-VN173-SUMO1.	This work
pBiFC-VN173C-UPF1	UPF1 sequence was amplified from pCMV-myc-UPF1 and cloned into EcoRI-EcoRV site of pBiFC-VN173-pFlagVN173.	This work
pBiFC-VC155N-UPF1	UPF1 sequence was amplified from pCMV-myc-UPF1 and cloned into NotI-XhoI site of pUbFC-VC155-mBMAL1.	This work
pBiFC-VC155C-UPF1	UPF1 sequence was amplified from pCMV-myc-UPF1 and cloned into EcoRI-XhoI site of pBiFC-VC155-pHAVC155.	This work
pBiFC-VC155N-CBP80	CBP80 sequence was amplified from pFlag-CBP80 and cloned into NotI-XhoI site of pUbFC-VC155-mBMAL1.	This work

pBiFC-VC155C-CBP80	CBP80 sequence was amplified from pFlag-CBP80 and cloned into EcoRI-XhoI site of pBiFC-VC155-pHAVC155.	This work
pBiFC-VN173N-eRF3	eRF3 sequence was amplified from pEQ863-His-eRF3 and cloned into NheI-XbaI site of pUbFC-VN173-SUMO1.	This work
pBiFC-VN173C-eRF3	eRF3 sequence was amplified from pEQ863-His-eRF3 and cloned into EcoRI-BglII site of pBiFC-VN173-pFlagVN173.	This work
pREP1	High copy expression vector with thiamine-repressible *nmt1* promoter. It contains *S. pombe ars1*, *S. cerevisiae LEU2* gene and two MCS.	Maundrell, 1993
pREP1-Ste11	This plasmid contains *ste11*$^{+}$ ORF cloned into pREP1 plasmid.	gift from Dr. Juan Mata

- COS cells transfection.

Cells were transfected at 60% confluence. Mammalian cells were transfected with plasmid DNA at different concentrations to check the expression. The DNA amount ranged between 0.5-4 µg.

DNA at that different concentration was mixed with 50 µl of serum-free DMEM. This constitutes cocktail number 1.

At the same time, Lipofectamine^{TM} 2000 (Invitrogen) was mixed with 50 µl of serum-free DMEM. The ratio of the total plasmid DNA to Lipofectamine^{TM} 2000 should be 1 µg of plasmid DNA to 2-3 µl of transfection reagent. This make up cocktail number 2.

Within 5 minutes generating each cocktail, cocktail #1 and cocktail #2 were combined to generate cocktail #3. Cocktail #3 was gently mixed by inversion.

After 20 minutes incubation at room temperature, cocktail #3 was added directly to cells. It was mixed well and incubated at 37°C and 5% CO_2.

48 hours after transfection, cells were washed 3 times with 500 µl of 1X PBS (Phosphate Buffered Saline: 8 g/l NaCl, 0.2 g/l KCl, 1.48 g/l Na_2PO_4, 0.24 g/l KH_2PO_4. pH was adjusted to 7.5). Then, they were stripped out in 500 µl of 1X PBS, using a cell lifter and centrifuged at 3000 xg for 5 minutes. Supernatant was discarded, and cells were stored at -20°C.

5. GENETIC TECHNIQUES

Many of the *S. pombe* strains that were generated in this study were constructed crossing the parental strains with opposite sexual type.

Parental strains were mixed and incubated in ME plates at 24°C for 48 hours and resulting tetrads were dissected using a tetrad dissection microscope (Singer) in a YES plate that was incubated for 72 hours at 30-32°C.

Once spores have germinated, colonies were analyzed in selective plates, by PCR and/or western blotting.

When two strains, parental A (gene *A:kanMX6*) and parental B (gene *B:kanMX6*), are crossed there are 3 segregation types:

- Parental ditype (PD), two spores of the tetrad share genotype with parental A strain (*A:kanMX6*) and the other two spores share genotype with parental B strain (*B:kanMX6*).
- Non-parental ditype (NPD), none of the spores share genotype with parental strains. There are two wild type spores and two double mutant spores (*A:kanMX6 B:kanMX6*).
- Tetratype (TT), each spore is different. One shares genotype with parental A (*A:kanMX6*), a second spore shares genotype with parental B (*B:kanMX6*) and the other two spores show wild type and double mutant genotype (*A:kanMX6 B:kanMX6*).

Looking at the segregation type is easy to find out the desired mutant.

5.1 GENE INSERTION AT CENTROMERE

In *S. pombe*, it has been described that genes localized within centromeres are transcriptionally silenced because these regions are heterochromatized (Allshire *et al.*, 1994). Centromere 1 comprises inner (imr1L/imr1R) and outer (otr1L/otr1R) repeats that flank $cnt1^{+}$ (Figure 5).

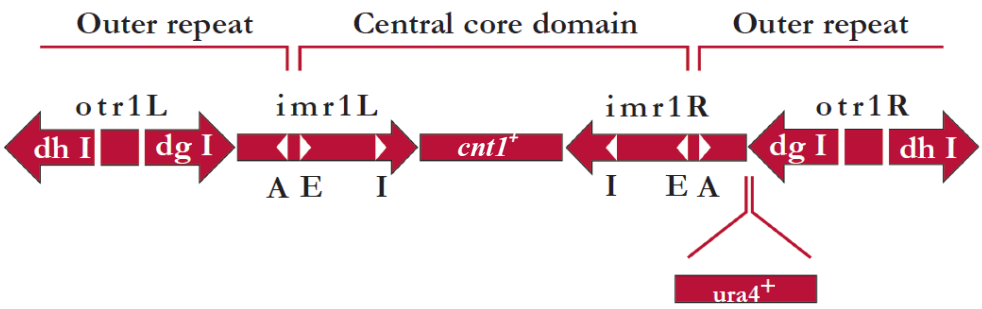

Figure 5. Schematic view of *ura4*$^{+}$ insertion at centromere 1. Fission yeast centromere 1 is formed by a central core domain, where *cnt1*$^{+}$ is localized, and outer repeats. A wild type copy of *ura4*$^{+}$ was inserted between the right inner repeat and the outer repeat.

To determine whether Upf1 is involved in heterochromatin formation, strains containing a *ura4*$^{+}$ insertion at centromere 1, otr1R(SphI):: *ura4*$^{+}$, were used (Allshire *et al*., 1994. Kind gift from Dr. Mikel Zaratiegui). Besides, these strains contain a disruption at endogenous *ura4*$^{+}$, making the centromeric version of *ura4*$^{+}$ the only intact copy of the gene. Therefore, only strains that have defects in heterochromatin formation will transcribe centromeric *ura4*$^{+}$ and will grow in minimal medium without uracil.

Strains that contain endogenous *ura4*$^{+}$ disruption and *ura4*$^{+}$ insertion at centromere were selected by PCR. In the same reaction we were able to distinguish disruption and insertion using a couple of primers (Table 5) that hybridize with *ura4*$^{+}$. To ensure that *ura4*$^{+}$ had been inserted between imr1R and otr1R regions we used another couple of primers that hybridize at ort1R and *ura4*$^{+}$ (Table 5).

Table 5. List of primers used for checking centromeric *ura4*$^{+}$ insertion and endogenous *ura4*$^{+}$ disruption.

PRIMER	SEQUENCE
395.otr1R::ura4_1	GAGGGGATGAAAAATCCCAT
396.otr1R::ura4_2	TTCGACAACAGGATTACGACC
397.otr1R::ura4_3	CATGCTCCTACAACATTACCACAA
398.p9R	CCATGCTTTTAGTGCGGTCA

6. RIP-CHIP - PURIFICATION OF PROTEIN-RNA COMPLEXES

This protocol was designed for *S. pombe* TAP-tagged proteins. To perform it, immunoprecipitation of TAP-tagged proteins was carried on Pan IgG mouse magnetic beads (Dynabeads®-Invitrogen). 100 µl of Dynabeads® were used for each experiment, and before immunoprecipitation they were coupled to anti-protein A antibody (Sigma), that recognizes and binds TAP epitope. The incubation with the antibody was performed in a rotational wheel at 4°C over night.

- PREPARATION OF EXTRACTS

Resuspend yeast cell pellets in 1 ml of pre-cooled RNAse free water and transfer to 2 ml tubes.

Centrifuge cells 1 minute at 3000 xg at 4°C.

Cells were transferred to a screw cap tube and resuspended in 500 µl of pre-cooled complete IP buffer (20 mM Tris-HCl pH 8.0, 140 mM KCl, 1.8 mM $MgCl_2$, 0.1% NP40, 1 mM PMSF and 5 µl of protease inhibitor cocktail (Sigma)). Centrifuge cells 1 minute at 3000 xg and resuspend again in 100 µl of complete IP buffer supplemented with 10% SUPERaseIN and 30 mg/ml heparin. Add 1 ml of pre-cooled glass beads and break cells in Fastprep™ FP120 (BIO101/Savant), level 6.5 for 13 seconds.

After cells were spin down, 500 µl of complete IP buffer (1% SUPERaseIN and 3 mg/ml heparin) were added and cell extracts harvested in a new tube.

Cell extracts were centrifuged at 9000 xg for 5 minutes, 4°C. Then the supernatant was placed into a new fresh tube and centrifuged again at 12000 xg for 10 minutes at 4°C.

Meanwhile, Dynabeads® were washed 3 times with IP buffer (20 mM Tris-HCl pH 8.0, 140 mM KCl, 1.8 mM $MgCl_2$, 0.1% NP40) and resuspended in 100 µl of complete IP buffer (1% SUPERaseIN and 3 mg/ml heparin). The washes were done using a magnet.

Once extracts were cleaned, 50 µl were kept as total RNA reference.

The rest of the supernatant was incubated with 100 µl of Dynabeads® previously coupled to protein A.

- IMMUNOPRECIPITATION

The immunoprecipitation was set up at 4°C in a rotational wheel for 2 hours.

After immunoprecipitation different washes were performed, using a magnet, as described:

- 4 washes with 750 µl WASH buffer (20 mM Tris-HCl pH 8, 140 mM KCl, 1.8 mM $MgCl_2$, 0.01% NP40, 10% glycerol) supplemented with 1 mM PMSF and 3 mg/ml heparin. All of them were quick washes except the third one that was performed in rotational wheel at 4°C for 15 minutes.
- 2 washes with 750 µl WASH buffer supplemented with 3 mg/ml heparin. Both at 4 °C in a rotational wheel for 15 minutes.
- 1 wash with 750 µl WASH buffer supplemented with 1% SUPERaseIN, at 4°C during 15 minutes with rotation.
- 1 wash with 500 µl WASH buffer supplemented with 1% SUPERaseIN and 1 mM DTT.

Once beads were washed, they were resuspended in 50 µl of WASH buffer (1% SUPERaseIN and 1 mM DTT)

30 units of TEV protease were added and incubated for 70 minutes at 19 °C.

Using the magnet, remaining supernatant was collected and RNA was extracted from that sample.

- RNA ISOLATION

The RNA extraction was different for total or IP RNA.

- Total extract: RNeasy mini spin columns (Qiagen) were used in this step.

  350 µl of RLT buffer and 250 µl of ethanol were added to the sample. After mixing, the sample was loaded into a column. After spin at 8000 xg samples were washed twice with 350 µl of RW1 buffer, and twice with 500 µl of RPE buffer. Then, 30 µl of RNAse-free water was added to elute the RNA and samples were centrifuged for 1 minute at top speed. This RNA was quantified using Nanodrop spectrophotometer (Thermo scientific) and distributed in 12 µl aliquots of 20 µg.

- IP extract: RNAqueous columns (Ambion) were used for this isolation.

  10 volumes of lysis buffer were added to the eluted IP RNA. After mixing, 12.5 volumes of ethanol were added loading the mixture into columns. Then columns were washed once with solution 1 (180 µl) and twice with solution 2/3 (180 µl).

  Finally, the IP RNA was eluted in RNAse-free water, pre-heated at 85°C in two steps of 7 µl each.

- cDNA LABELLING

The labels used for these experiments were Alexa Fluor 555 for total cDNA, and Alexa Fluor 647 for IP cDNA.

Labelling was performed using SuperScript™ Plus Indirect cDNA Labeling System (Invitrogen), following the manufacturer description.

After labelling, both samples (total cDNA and IP cDNA) were purified together, using the purification module included in SuperScript™ Plus Indirect cDNA Labeling System (Invitrogen). 500 µl of loading buffer were added to the mixture and everything was loaded into a column. Spin 14000 xg and add 700 µl of wash buffer. Centrifuge 2 minutes at 14000 xg.

100 µl of RNAse free-water were used to elute the labelled cDNA.

cDNA was measured by Nanodrop spectrophotometer (Thermo scientific) and then, precipitated with 3 volumes of ethanol and 1/10 volumes of sodium acetate 3 M pH 5.6.

- MICROARRAY HYBRIDIZATION

After washing cDNA with 70% ethanol, it was air dried for 10 minutes and resuspended in 40 µl of hybridization buffer (5X SSC, 6X denhardt's, 60 mM Tris-HCl pH 7.6, 0.12% sarkosyl, 48% formamide; all filter sterilised). 3 µl of polyA DNA (2 µg/µl) were added and heated at 95°C for 5 minutes. Finally, tubes were cooled and spin down and 38 µl of hybridization mix were loaded into microarrays.

Microarrays were inserted into a chamber where 2 round 25 mm filters (Whatman) soaked with 300 µl of 15X SSC were placed. This chamber was incubated at 49°C for 16 hours in a hybridization oven.

- MICROARRAY WASHING

All washes were performed in black chambers, to reduce the light effect on the microarrays.

Microarrays were placed into a chamber with solution 1 (2X SSC, 1 µM DTT) to remove the cover slip. They were transferred to another chamber with solution 1 and incubated for 5 minutes with shaking. Afterwards, they were washed twice with solution 2 (0.1X SSC, 0.1% SDS, 1 µM DTT) for 15 minutes with shaking, and then, washed quickly with solution 3 (0.1X SSC, 1 µM DTT). Microarrays were placed into another chamber with solution 3, and incubated for 5 minutes with shaking.

Microarrays then were dried by 2 minutes centrifugation at 1200 xg.

- MICROARRAY IMAGE ANALYSIS

Microarrays were scanned using GenePix 4000B scanner (Axon Instruments).

- RESULTS AND CLUSTERING

The data was analyzed with GenePix Pro 6.0 software.

7. TRANSCRIPTIONAL ANALYSIS

- RNA EXTRACTION

Pelleted cells were resuspended in 1 ml of pre-cooled DEPC water (Ambion). Resuspended cells were transferred to 2 ml tubes and spin down for 10 seconds at 5000 xg.

750 µl of TES (10 mM Tris HCl pH 7.5, 10 mM EDTA pH 8.0; 0.5% SDS) were added to each pellet, and immediately 750 µl of acidic phenol-chloroform pH 4.8 (Sigma) were added to the mixture. All samples were incubated in a 65°C heat block for 1 hour, vortexing 10 seconds every 10 minutes.

Samples were place on ice for 1 minute, vortexed 20 seconds, and centrifuged for 15 minutes at 14000 xg at 4°C.

Pre-spin 2 ml yellow phase-lock tubes (Eppendorf) for 10 seconds and add 700 µl of acidic phenol-chloroform. Add 700 µl of the water phase from samples. Mix by inversion and centrifuge for 5 minutes at 14000 xg at 4°C.

Pre-spin 2 ml phase-lock tubes and add 700 µl of chloroform:isoamyl alcohol (25:1)(Sigma). Add 700 µl of the water phase from the previous phase-lock tubes. Mix by inversion and centrifuge for 5 minutes at 14000 xg at 4°C.

Transfer 500 µl of water phase to 2 ml tubes and precipitate RNA with 3 volumes of pre-cooled ethanol 100% and 1/10 volume of 3 M sodium acetate pH 5.6 at -20°C over night.

Centrifuge 15 minutes at 14000 xg at 4°C, discard supernatant and add 500 µl of pre-cooled ethanol 70% and centrifuge 5 minutes at 14000 xg at 4°C.

Air dry 5 minutes and resuspend in 100 µl of DEPC water.

Incubate RNA 1 minute at 65°C to dissolve pellet.

The measurements were made by Nanodrop spectrophotometer (Thermo scientific). 100 µg of RNA were purified using RNeasy mini spin columns (Qiagen) as described before.

- RT- PCR

For reverse transcription, 1 µg RNA was used for the reaction, using Reverse Transcription System kit (Promega®), following manufacturer's guidelines.

Primers described in the table were used for the PCR (Table 6).

Quantitative analyses were performed using the ΔCt method.

Table 6. RT-PCR primer list

PRIMER	SEQUENCE
185.Atf1_5	AACCCCTACTGGAGCTGGAT
186.Atf1_3	GGGAACCTGGGAGAGTAAGC
187.Ste11_5_probe	ACCTAAAACCCCGAATACCG
188.Ste11_3_probe	TTAGAATTGGGCAACCAAGG
189.Act1_5_probe	AGCACCCTTGCTTGTTGACT
190.Act1_3_probe	CTCATGAATACCGGCGTTTT
415.SPAC11D3.09c_FWD	TACCCCTGAGAGTGCAGGTT
416.SPAC11D3.09c_REV	GAGTTTGATCCCATCCAAGC
417.REX2_FWD	GCGTTAATCGCTGGAAACAGT
418.REX2_REV	GATTATCTTTGGCATCTCGACAGA
419.MUG105_FWD	CGGTATTGATCGTGGATGG
420.MUG105_REV	AACCAATTTGGATTGGTGTATTG
421.RAD8_FWD	ACTTGTGCCAACCATGTTTTTA
422. RAD8_REV	GAATACGATCGATGGCCTGT
423.SPCC63.13_FWD	TGCAGTAGAAAAAGCTCGCATA
424.SPCC63.13_REV	AGGAGGTGAACTGCTTGGAA
425.SPAC3A12.06c_FWD	GTTTAAGTGACCTCATTGCGGATA
426.SPAC3A12.06c_REV	CCACCCATTGCCATTTCG
427.ACTIN_FWD	TCCTAGCTCCATGAAGGTCAA
428.ACTIN_REV	GAATGGATCCACCAATCCAG
429.SPBPB21E7.08_FWD	ACCTCACACCCACTCTCATTACC
430.SPBPB21E7.08_REV	CAGGAAGGAATTTGGAAAATGG
ura4_insertion_F	TGGGACGTGGTCTCTTGCTT
ura4_insertion_R	CCAAAGAGCCTTTGGAAGACA

8. DEEP SEQUENCING

To analyze *upf1*Δ transcriptome by high throughput sequencing of cDNA, *upf1*Δ and wild type RNA from prototrophic strains was isolated as described in the previous epigraph and cDNA was prepared using SuperScript™ Choice System for cDNA synthesis (Invitrogen).

DNA libraries were prepared following the manufacturer's instructions (Illumina). A range of fragment sizes (120–170 bp) were used for sequencing. These base pairs were attached to the FlowCell at an average concentration of 3 pM, amplified isothermally, and sequenced using Solexa reversible-terminator chemistry on the Illumina Genome Analyser. Sequence reads were mapped to the reference genome using BLAT.

The RPKM cut-offs for expressed and silent genes are based on Mortazavi et al., 2008 (Mortazavi *et al.*, 2008).

9. PROTEIN DETECTION BY WESTERN BLOTTING

- EXTRACTS

Cells were harvested as described before.

They were resuspended in 100 µl of protein lysis buffer (20 mM Tris-HCl pH 8.0, 140 mM KCl, 1.8 mM $MgCl_2$, 0.1% NP40). Lysis buffer was supplemented with 1 mM PMSF and 1 µl of protease inhibitor cocktail (Sigma).

Extracts were transferred to screw cap tubes and pre-cooled 0.40 mm diameter glass beads were added.

Cells were broken using a FastPrep™ FP120 (BIO101/Savant). The length of the pulse was 20 seconds in level 6.5.

After cells were spin down, 200 µl of lysis buffer were added to the extract.

Supernatants were centrifuged at 13000 xg for 15 minutes.

In the case of COS cells, they were lysed using passive lysis buffer (Promega®). They were incubated for 10 minutes on ice and after centrifugation at 4°C for 10 minutes, extracts were transferred to a fresh tube.

Protein concentration was determined, measuring cell extracts absorbance at λ=280 nm in a Beckman DU 640 spectrophotometer. 1/6 of absorbance represents 1 mg/ml of protein approximately.

Finally, the concentration of all the extracts was adjusted using protein lysis buffer, and the same volume of 2X DTT-SDS-PAGE loading buffer (125 mM Tris-HCl pH 6.8, 5% SDS, 25% glycerol, 3 g/l bromophenol blue, 100 mM DTT) was added.

Before loading samples in the gel, they were heated at 95°C for 5 minutes to denature the proteins.

After heating, samples could be kept at -20°C or -70°C.

- ELECTROPHORESIS

For electrophoretic protein separation from cells extracts, SDS-PAGE was used.

Acrylamide gels at 8%-10% were used in this study.

The components of the separating gel were: 375 mM Tris-HCl pH 8.8, 0.1% SDS, ddH_2O to 4 ml, 2 µl of TEMED and 0.05% PSA.

The components of the stacking gel were: 125 mM Tris-HCl pH6.8, 0.1 % SDS, ddH_2O to 2 ml, 1.5 µl of TEMED and 0.075% PSA.

The electrophoresis was performed in MiniProtean III (BioRad) chambers, and was set up with running buffer (196 mM glycine, 0.1% SDS and 50 mM Tris-HCl pH 8.3) covering the gel. 15-30 µg of protein were loaded in each well. Precision Plus Protein Dual Color standards (BioRad) was loaded as reference to determine molecular weight of proteins.

Running conditions were 1 hour at 200 V.

- PROTEIN TRANSFERENCE TO NITROCELLULOSE MEMBRANES

The proteins were electro-transferred from the gel onto a nitrocellulose membrane (Hybond, Amersham).

That process was set up with 1X transference buffer composed by 7 volumes of ddH_2O, 2 volumes of methanol and 1 volume of 10X transference buffer (58 g/l Tris-HCl, 29 g/l glycine, 3.7 g/l SDS).

Transfer was performed in Mini Trans-Blot Transfer Cell (Bio-Rad) chambers at a constant voltage (100 V) for 60 minutes.

- IMMUNODETECTION

After transfer, the membrane was incubated with 5% non-fat dry milk in TTBS (29.2 g/l NaCl, 24.2 g/l Tris-HCl pH 7.5, 500 µl/l Tween 20) over 1 hour.

Subsequently, membranes were incubated with primary antibody, previously prepared at the concentration required in 5% non-fat dry milk in TTBS. The length of the incubation will depend on the antibody but 60-90 minutes incubation at room temperature was enough for most purposes.

Membranes were washed up 3 times with TTBS for 10 minutes each one, and then were incubated with peroxidase conjugated secondary antibody, prepared at the concentration required in the same solution as primary antibody for 45-60 minutes. Membrane was washed again 3 times as described before.

For membranes development, chemioluminiscent detection system (ECL, Amersham-Biosciences) and films Hyperfilm™ MP (Amersham-Biosciences) were used. The development was carried on Kodak M35 X-OMAT developer.

The antibodies used in this work are described in the next table (Table 7).

Table7. List of antibodies used in this work.

ANTIBODY	CHARACTERISTICS	REFERENCE	USES
Anti-PAP	Peroxidase anti-peroxidase conjugated antibody	Sigma-Aldrich	WB (1:10000)
Anti-protein A	Mouse monoclonal	Sigma-Aldrich	RIp-chip, Co-immunoprecipitation
Anti-HA	Mouse monoclonal	Roche	WB (1:3000)
Anti-rabbit IgG-HRP	Donkey polyclonal	Amersham Pharmacia Biotech	WB (1:5000)
Anti-mouse IgG-HRP	Sheep polyclonal	Amersham Pharmacia Biotech	WB (1:5000)
Anti-eRF3	Rabbit polyclonal	Gift from Olivier Jean-Jean (Chauvin *et al.*, 2005)	WB (1:1000)
Anti-UPF1	Rabbit polyclonal	Maquat Lab	WB (1:1000)
Anti-CBP80	Rabbit polyclonal	Gift from Elisa Izaurralde (Izaurralde *et al.*, 1994)	WB (1:1000)
Anti-β-actin	Mouse monoclonal	Sigma-Aldrich	WB (1:3000)

Anti-calnexin	Rabbit polyclonal	Stress gene. SPA-865	WB (1:3000), Immunofluorescence (1:200)
Anti-Mab414	Mouse monoclonal	AbCam	Immunofluorescence (1:100)
Anti-manosidase II	Rabbit polyclonal	Chemicon	Immunofluorescence (1:100)
Anti-LAMP1	Rat polyclonal	Developmental Studies Hybridoma Bank	Immunofluorescence (1:50)
Anti-rat Alexa 594	Donkey polyclonal	Invitrogen	Immunofluorescence (1:500)
Anti-mouse Alexa 594	Donkey polyclonal	Invitrogen	Immunofluorescence (1:500)
Anti-rabbit Alexa 594	Donkey polyclonal	Invitrogen	Immunofluorescence (1:500)

9.1 CO-IMMUNOPRECIPITATION

To determine protein interactions, co-immunoprecipitation experiments were performed.

TAP tagged proteins were immunoprecipitated using Pan IgG mouse Dynabeads® (Invitrogen) coupled to anti-protein A (Sigma). With the exception of heparin and SUPERaseIN, RIp-chip protocol, previously described, was used for these assays.

When protein extracts were obtained, 2X DTT-SDS-PAGE loading buffer was added and western blotting was perfomed as described before.

10. FLOW CYTOMETRY

Flow cytometry was used to estimate the relative DNA content of every single cell, and define the cell cycle stage of the population.

3 ml of cells were harvested at 0.3 OD. 7 ml of ethanol were added and incubated at 4°C over 10 minutes.

Cells were spin down and resuspended in 1ml of PBS-Triton-HCl solution (1 ml PBS, 0.5% Triton-X-100, 0.1 N HCl) and incubated for 10 minutes at room temperature.

Cells were spin down and resuspended in RNAse A at 250 mg/ml. After 2-hour incubation at 37°C, 200 µl of cells were mixed with 800 µl of PBS. That mixture was gently sonicated to separate cellular aggregates.

Propidium iodide at 2.5 µg/ml was added to each sample.

Samples were ready to be analyzed by flow cytometry.

The flow cytometer used in this study was FACSCalibur (Bencton Dickinson), with 2 laser lines: blue (488 nm) and red (633 nm). The measurements were carried on using a 585/542 nm detector.

The software used to analyze the data was FlowJo.

11. MICROSCOPY

11.1 BIMOLECULAR FLUORESCENCE COMPLEMENTATION

To observe protein interaction *in vivo*, bimolecular fluorescent complementation (BiFC) technique was used. The basic principle of the BiFC assay is to fuse two nonfluorescent fragments (VN173 and VC155 epitopes) from a split fluorescent protein (VENUS) to two interaction partners. If two proteins interact with each other, the interaction brings the VN173 and VC155 fragments into close proximity to allow reconstitution of VENUS (Shyu *et al.*, 2006).

To observe protein interactions in mammalian cells, proteins were cloned into VN173 and VC155 containing plasmids described in table 4. By contrast, to see protein interaction in fission yeast cells proteins were tagged with pFA6a-VN173-kanMX6 and pFA6a-VC155-kanMX6 (Akman and MacNeill, 2009), inserting the epitopes into the genome.

11.2 *S. POMBE*

To visualize fresh *S. pombe* cultures a fluorescent inverted Axiovert200 microscope (Zeiss) was used.

11.3 MAMMALIAN CELLS

Mammalian cells were observed using a Nikon Eclipse E600FN microscope. This microscope was equipped with a mercury lamp (Nikon's Super High Pressure) and two lasers, Cobalt calypso 50 (λ= 490 nm) and Cobalt Jive 25 (λ= 561 nm).

Images were captured through a Hamamatsu camera coupled to the microscope.

For images analysis ImageJ software was used.

Immunostaining experiments were performed to visualize cell structures.

For immunofluorescence procedure, cells were incubated in 17 mm spherical cover slides pre-treated with poly-L-lysine (Sigma) and fixed with 4% para-formaldehide (PFA).

After fixation cells were permeabilized 5 times with 0.2% Triton-X-100 and washed two times with PBS.

Then cells were blocked with 1% BSA (in PBS) and primary antibody, diluted in 1% BSA, was incubated over night (antibodies details are described in table 7). Before adding secondary antibody cells were washed twice with PBS.

Secondary antibody contained a fluorescent label, so cells were incubated in the dark.

Finally cells were rinsed three times with PBS and mounted in a slide using ProLong® Gold antifade reagent (Invitrogen).

RESULTS

1. Upf1 ROLE IN POSTTRANSCRIPTIONAL REGULATION

1.1. RIp-CHIPs AND DNA MICROARRAYS

In order to determine Upf1 role in posttranscriptional regulation we performed RIp-chip experiments. With this technique we were able to distinguish what mRNAs are bound by Upf1.

RIp-chip protocol has been optimized for TAP tagged proteins so we used *upf1:TAP* strain to perform this experiment. The protocol is based on immunoprecipitation (IP) assays followed by RNA extraction. In these experiments RNA purified from total cell extract was used as reference. Total RNA and IP RNA were labeled with Alexa Fluor 555 and Alexa Fluor 647. To avoid the deviation introduced by the different affinity of each label, total and IP RNA were labeled in each replica with Alexa Fluor 555 or 647 or viceversa. After labeling, total and IP RNA were purified together and this mixture was loaded into microarrays. We made three biological replicas of this experiment where we found more than 2,000 possible Upf1 targets (Figure 6).

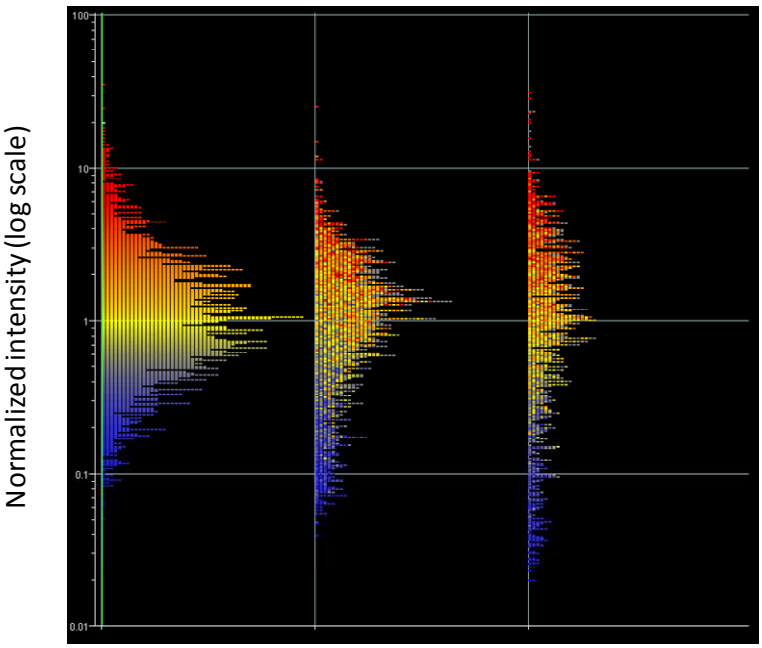

Figure 6. RIp-chip experiments. Panel a) represents the normalized intensity of all *S. pombe* ORFs in logarithmic scale. The normalized intensity indicates the enrichment level of the IP compared to the total, being the most enriched represented in red color and the most impoverished in blue. Panels b) and c) represent the normalized intensity of all *S. pombe* ORFs found in the second and third replicas, but in these cases each ORF conserve the color assigned in the first replica.

In the graphic we can observe the normalized intensity in logarithmic scale (represented in the y-axis), which indicates the enrichment level of the IP compared to the total for each *S. pombe* ORF, represented in the x-axis as small boxes. Color scale in the first replica (Figure 6a) represents the relative abundance of the mRNAs, comparing the IP to the total. Red color represents the highest enrichment of the mRNAs in the IP versus total, and

blue color represents the impoverishment of the IP compared to the total. In replica 2 and 3 (Figure 6b, 6c) each mRNA is localized depending on the expression of the data experiment, but keeping up the color of the first replica. As result of this representation we can observe a high correlation between all replicas, being the color code similar in all of them.

Upf1 has a role in mRNA degradation, suggesting that mRNAs susceptible to be degraded by Upf1 should be bound by Upf1, directly or indirectly, and overexpressed in *upf1*Δ strain. Thus, to validate Upf1-mRNA targets we performed DNA microarrays experiments in *upf1*Δ strain to monitor changes in gene expression derived of $upf1^{+}$ deletion.

For microarrays assays total RNA was extracted from wild type and *upf1*Δ strains. Wild type cDNA was labeled with Alexa Fluor 555 and cDNA obtained from cells lacking Upf1 was labeled with Alexa Fluor 647. Both cDNAs were purified together and this mixture was probed into DNA microarrays.

After data analysis we obtained the gene expression data in *upf1*Δ strain compared to wild type, where we observed that in cells lacking $upf1^{+}$ the number of overexpressed genes was higher than the number of those downregulated.

In RIp-chip experiments we have found more than 2,000 possible targets. To establish a significant cut off we decided to compare these data with the expression microarrays data.

We run a program that compares 2 lists: one list (list 1) that contains Upf1 possible targets obtained from RIp-chip experiments, sorted by their decreasing ratio IP/total; and other list (list 2), used as reference, that contains genes that in microarrays of *upf1*Δ strain appear overexpressed, sorted by the decreasing ratio *upf1*Δ/wild type. The program starts comparing the first gene of list 1 to the first gene of list 2. Then it compares the two first genes of list 1 with the two first genes of list 2 and so on. As result, the program give us the number of genes in list 1 found in list 2.

As negative control we randomized list 1. This list was also compared to list 2.

a)

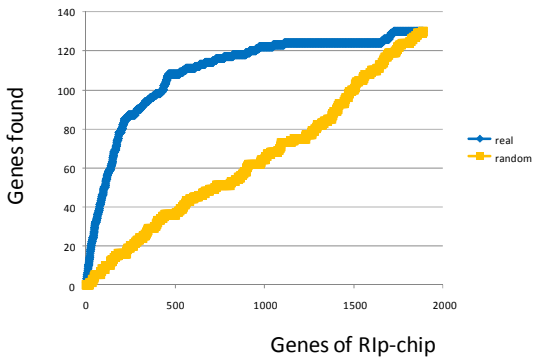

b)

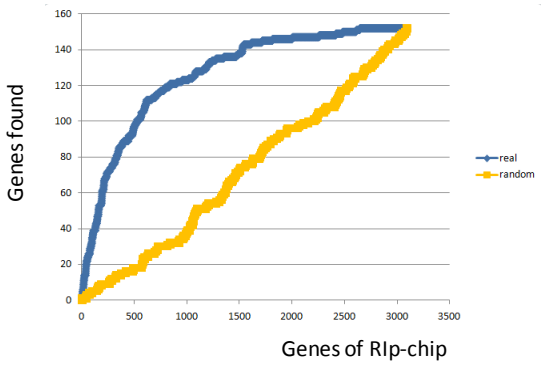

c)

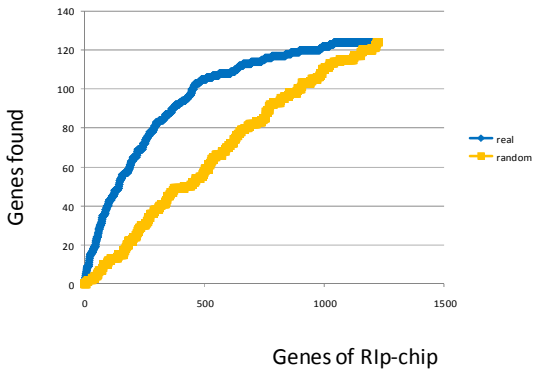

Figure 7. Comparison between Upf1 targets obtained by RIp-chip and overexpressed genes in microarrays experiments. Blue line represents a comparison between one list obtained by RIp- chip experiments which contains all *S. pombe* ORFs sorted by their ratio IP/total and other list that contains overexpressed genes in *upf1*Δ in microarrays assays, sorted by their ratio *upf1*Δ/wt. Orange line represents a comparison between the data obtained by RIp- chip but randomly ordered and the same overexpressed genes in *upf1*Δ strain sorted by their ratio *upf1*Δ/wt.
X-axis represents the number of genes described in the Rip-chip list and y-axis represents the number of genes found in microarrays lists.
Each graphic, a), b) and c), correspond to first, second and third replica respectively.

In figure 7 there are 3 graphics that correspond to each replica. In these graphics the x-axis represents the number of genes contained in list 1 and the y-axis represents the number of genes found in list 2. For instance, in the graphic of the first replica (Figure 7a) we can observe that in order to find 40 genes in the reference list, we need to compare at least 100 genes of list 1 sorted by the ratio IP/total, whilst when we order list 1 randomly we do not find 40 genes in the reference list until we have compared 500 genes.

The data showed that there was a better efficiency when we compare the list 1 sorted by the ratio IP/total instead ordered randomly, meaning that there is a correlation between the genes bound by Upf1 and the genes overexpressed in cells lacking *upf1*$^{+}$.

After 250 genes approximately, the slope of the curve is reduced, indicating a worse correlation.

According to this analysis we established the threshold in 250 genes. Therefore we compared the first 250 genes of each replica of RIp-chip and, as shows Venn diagram, there was an overlap of 59 genes (Figure 8).

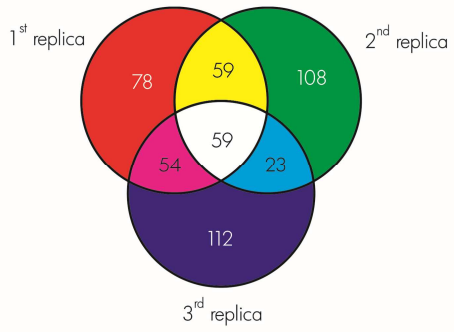

Figure 8. Venn diagram of RIp-chip replicas. To perform this diagram a threshold of 250 genes was considered in each replica, showing an overlap of 59 genes (white sector).

In order to know if there were also a correlation between mRNAs bound by Upf1 and mRNAs downregulated in *upf1*Δ strain we did a comparison between Upf1 possible targets and a reference list that contains the genes downregulated in *upf1*Δ strain compared to wild type, sorted by their decreasing ratio *upf1*Δ/wt. As graphics show, in this case there is no correlation, getting the same result when we compare the reference list to the genes of RIp-chip sorted by their ratio IP/total or ordered randomly (Figure 9).

This result indicates that Upf1 binding to its targets may lead to degradation.

a)

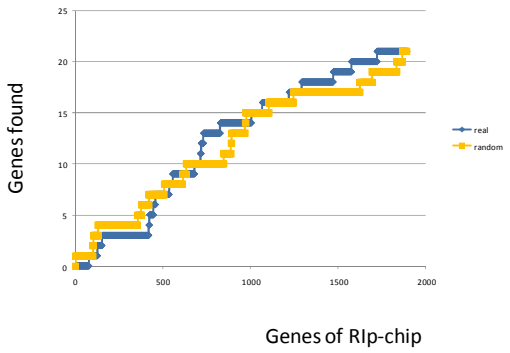

b)

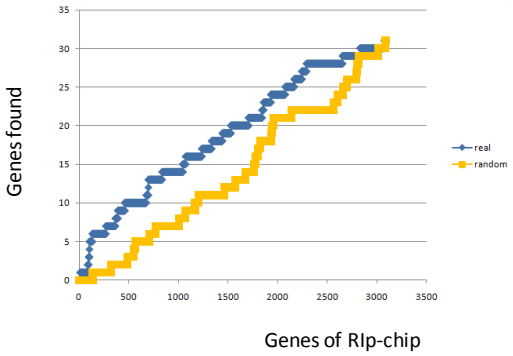

c)

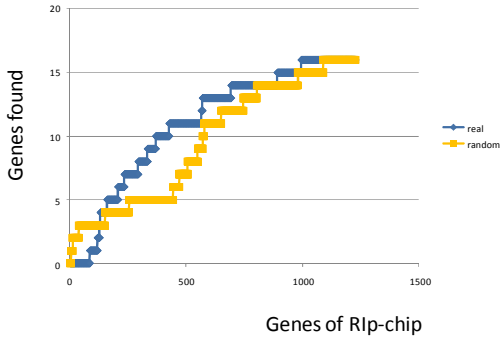

Figure 9. Comparison between Upf1 targets obtained by Rip-chip and downregulated genes in microarrays experiments. Blue line represents a comparison between one list obtained by RIp- chip experiments which contains all *S. pombe* ORFs sorted by their ratio IP/total and other list that contains downregulated genes in *upf1*Δ in microarrays assays, sorted by their ratio *upf1*Δ/wt. Orange line represents a comparison between the data obtained by RIp- chip but randomly ordered and the same downregulated genes in *upf1*Δ strain sorted by their ratio *upf1*Δ/wt.
X-axis represents the number of genes described in the Rip-chip list and y-axis represents the number of genes found in microarrays lists.
Each graphic, a), b) and c), correspond to first, second and third replica respectively.

1.2. Upf1 mRNA TARGETS

In table 8 there is a description of the genes that we have defined as putative Upf1-mRNA targets.

Table 8. List of putative Upf1 targets ordered by the enrichment level of the IP compared to the total in RIp-chip experiments.

Gene Name	Mean RIp-chip	Mean Microarray	Gene Description
spo6.RC	30.90	4.48	Spo4-Spo6 kinase complex regulatory subunit (RC)
SPAC3A12.06c	19.62	1.44	Member of the sodium or calcium exchanger protein family of membrane transporters
SPBC409.08	18.85	1.92	Spermine family transporter
SPAC11D3.13	12.65	1.76	Member of the DJ-1 or PfpI family
SPAC1039.04	11.38	1.61	Nicotinic acid plasma membrane transporter

taf3	10.11	1.64	Transcription factor TFIID complex subunit Taf3 (predicted)
SPAC3A12.19	9.83	1.73	Mitochondrial ribosomal protein subunit L27 (predicted)
fta1	9.45	1.86	CENP-L homolog Fta1
arg7	8.38	2.00	Argininosuccinate lyase
mug105	7.94	2.19	Ubiquitin-fold modifier-specific protease (predicted)
vps8	7.91	1.23	Protein with weak similarity to *S. cerevisiae* Vps8p, which is involved in vacuolar sorting
spt4	7.60	2.64	Transcription elongation factor complex subunit Spt4
syj1	7.48	1.06	Inositol-polyphosphate 5-phosphatase
SPAC823.07	7.32	1.20	GPI-phospholipase A2 activity regulator (predicted)
SPAC13C5.04.RC	7.30	1.40	Amidotransferase (predicted) (RC)
SPBC21C3.15c	7.29	1.44	Aldehyde dehydrogenase (predicted)
SPAC17A5.05c	6.91	1.57	Protein of unknown function
mok13	6.74	1.11	Alpha-1,3-glucan synthase
SPBC1773.03c	6.60	1.30	Protein containing an aminotransferase class-III domain
ckn1	6.36	1.38	ERCC-8 DNA repair homolog
mde10	6.21	1.48	Protein involved in the development of spore wall assembly
SPAC11D3.09	5.93	3.38	Agmatinase (predicted)
fap2	5.92	2.16	L-saccharopine oxidase, may be involved in L-lysine metabolism
SPAC4F10.16c	5.92	1.22	P-type ATPase (predicted)
mal1	5.83	3.01	Maltase alpha-glucosidase
SPCC63.13	5.87	1.73	DnaJ domain containing protein, part of chaperone system. Mediates interaction with heat shock proteins
mug28	5.87	1.19	RNA binding protein
bgs2	5.83	1.78	1,3-beta-glucan synthase component, required for proper spore cell wall biosynthesis
SPCC550.07	5.77	1.76	Member of the amidase family, which catalyze hydrolysis of amides
fbp1	5.73	1.82	Fructose-1,6-bisphosphatase, involved in gluconeogenesis
C11D3.11c	5.60	1.39	Zinc finger protein, truncated
mug30	5.39	2.51	Ubiquitin-protein ligase E3 (predicted)
rpb9	5.25	1.40	RNA polymerase II subunit
SPAC186.03	5.22	1.34	L-asparaginase (predicted)
rad8	5.20	1.82	Ubiquitin-protein ligase E3
SPAPB24D3.03	5.10	2.26	Agmatinase (predicted)
mok14	5.03	1.06	Alpha-1,4-glucan synthase
SPCC970.02	4.92	1.96	Mannan endo-1,6-alpha-mannosidase (predicted)
SPCC24B10.20	4.79	1.98	Protein containing a short chain dehydrogenase domain
SPBPB21E7.08	4.77	2.44	Pseudogene
SPAC22A12.08c	4.74	1.08	Member of the CDP-alcohol phosphatidyltransferase family.
SPBC11C11.11c	4.72	1.78	Mitochondrial ATP-dependent DNA helicase Irc3 (predicted)

trm12	4.57	1.30	tRNA methyltransferase Trm12 (predicted)
smb1	4.53	1.39	Sm snRNP core protein
ght1	4.49	1.00	Hexose transporter
caf5	4.28	0.79	Spermine family transmembrane transporter
rex2	4.23	2.15	RNA exonuclease (predicted)
mug67	4.23	1.50	PPPDE peptidase family (predicted)
SPAC11D3.06	4.21	2.04	Member of the MatE family transporter, which are integral membrane proteins
SPBC1347.08c	4.07	1.59	Ribonuclease H2 complex subunit (predicted)
SPBC1773.06c	3.96	1.52	Alcohol dehydrogenase (predicted)
prl28	3.95	1.29	Non-coding RNA, poly(A) bearing (predicted)
prm1	3.91	1.86	Conjugation protein Prm1 (predicted)
SPBC557.05.RC	3.91	1.16	Arrestin (RC)
ssb3	3.85	1.94	Subunit of single-stranded DNA-binding protein, required for DNA replication
SPBPB21E7.09	3.85	1.41	L-asparaginase (predicted)
msp1	3.74	1.44	Protein required for mitochondrial DNA maintenance, member of the dynamin family
skb5	3.64	1.22	Shk1 kinase binding protein 5
SPAC2F7.05c	3.09	1.63	Translation initiation factor eIF5 (predicted)

As we can observe in table 8, 56% of the genes described as putative Upf1 targets were overexpressed in *upf1*Δ strains (1.5X), being these targets involved in different cellular processes, such as transcription/translation, cell wall biosynthesis or energy metabolism. This result also indicates that Upf1 is binding many mRNAs (44%) which expression is not affected in the absence of this protein.

2. Upf1 FUNCTION IN OXIDATIVE STRESS

It has been described that Upf1 is specifically involved in the oxidative stress response but not in osmotic stress response (Rodriguez-Gabriel *et al.*, 2006).

In mammalian cells and budding yeast it has been described that Upf1 forms a complex with Upf2 to develop its function in the NMD pathway (Serin *et al.*, 2001).

We studied if these two proteins were involved in the response to any other type of stress. We performed viability assays with *upf1*Δ and *upf2*Δ strains in the presence of different types of stress. Wild type strain was used as positive growth control, and a mutant strain deficient in the MAPK Spc1, sensitive to stress, as a negative growth control.

We did serial dilutions of the strains detailed above and these dilutions were plated in different stimuli-containing plates. After 2 days, pictures were taken (Figure 10).

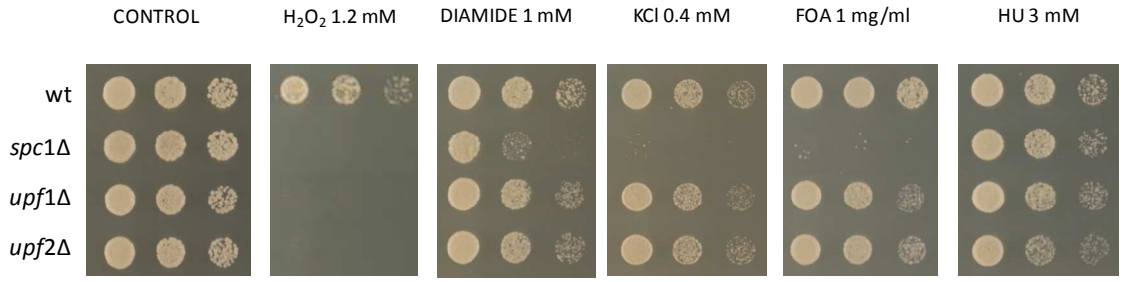

Figure 10. Survival assays in stress conditions. Serial dilutions (1/5) of the wild type, *spc1*Δ, *upf1*Δ,and *upf2*Δ strains were plated in rich media (YES) and in the presence of different stimuli: 1.2 mM hydrogen peroxide, 1 mM diamide, 0.4 mM KCl, 1 mg/ml 5' fluoroorotic acid or 3 mM hydroxyurea. Plates were incubated at 30°C for 2 days.

In figure 10 we can observe that wild type cells are able to survive under any tested condition. Cells lacking Spc1 showed a sensitive phenotype under hydrogen peroxide and potassium chloride treatment. Only in the presence of hydrogen peroxide both, *upf1*Δ and *upf2*Δ strains showed a sensitive phenotype. When cells are plated in the presence of other type of oxidative agent, like diamide, *upf1*Δ and *upf2*Δ mutants showed a wild type phenotype.

In plates containing potassium chloride, that provokes osmotic stress, under hydroxyurea chronical treatment or under 5' fluoroorotic acid exposure we did not observe any difference between wild type and *upf1*Δ or *upf2*Δ strains.

2.1. Upf1 INTERACTS WITH Upf2 *in vivo* IN FISSION YEAST

As it has been mentioned above, in budding yeast and mammals it has been described that Upf1 forms a complex with Upf2 (Serin *et al.*, 2001). In fission yeast there is no evidence about this interaction. In order to test if these two proteins bind each other *in vivo* we did TAP purification assays in vegetative growth conditions and in the presence of hydrogen peroxide (Figure 11).

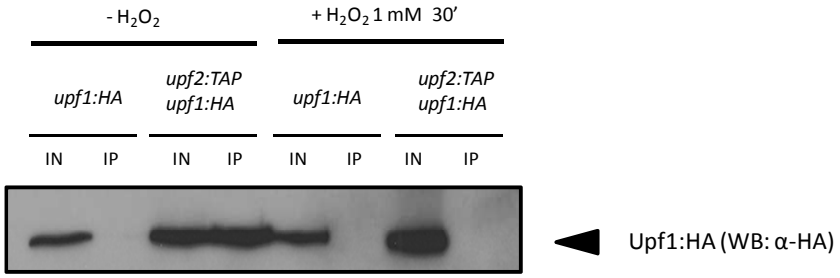

Figure 11. TAP immunoprecipitation of *upf1:HA upf2:TAP* in basal conditions and under 1 mM hydrogen peroxide treatment. *upf1:HA* strain was included as negative control of immunoprecipitation. Upf1:HA was detected using an antibody against HA epitope.

We monitored Upf1 expression by western blotting. We used *upf1:HA* strain as negative IP control and, as was expected, there was no signal in the IP extracts of this

strain. By contrast we detected a strong band in the IP extract of *upf1:HA upf2:TAP* strain in basal conditions, demonstrating that Upf2 is binding Upf1.

Performing the same experiment in the presence of hydrogen peroxide we noticed that this interaction is missing, meaning that Upf2 cannot bind Upf1 under oxidative stress conditions.

We used another technique to check Upf1-Upf2 interaction *in vivo*. Using bimolecular fluorescent complementation (BiFC) we can localize cellular protein interactions *in vivo*. This technique is based on the reconstitution of a fluorescent molecule (VENUS). This protein is split up in two non-fluorescent fragments (VN173, VC155) that are fused to the proteins of interest.

As pictures show (Figure 12) we cannot detect fluorescence neither in *upf1*:VC155 nor in *upf2*:VN173 strains, but in *upf1*:VC155 *upf2*:VN173 strain we can see small fluorescent cytoplasmic accumulations, meaning that Upf1-Upf2 interaction occurs, and it takes place in the cytoplasm.

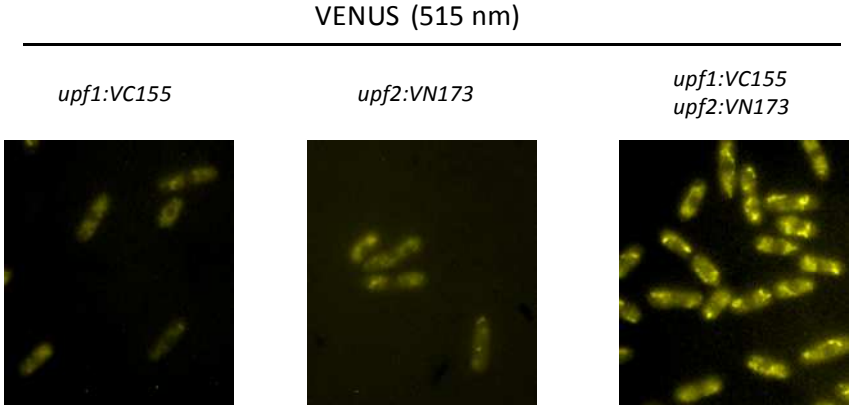

Figure 12. BiFC assays to check Upf1-Upf2 interaction *in vivo*, using *upf1:VC155 upf2:VN173* strain. *upf1:VC155* and *upf2:VN173* strains were used as negative controls. Fluorescent images were captured exciting samples at 515 nm.

2.2. NMD COMPONENTS ARE NECESSARY FOR AN EFFICIENT Upf1-mRNA BINDING

Upf1 forms a complex with Upf2 and Upf3 being this complex the core component of NMD pathway (Serin *et al.*, 2001).

In order to determine if the presence of these two proteins were required for an efficient Upf1-mRNA binding, we did immunoprecipitation assays followed by RNA extraction. By reverse transcription we generated cDNA that was used as template in qPCR to quantify the amount of mRNAs bound by Upf1 in each strain.

For this assay we selected those Upf1 targets from the 59 gene list that showed a high enrichment level in the IP compared to the total in RIp-chip experiments and overexpression in *upf1*Δ strain, with the exception of SPAC3A12.06c which expression was not altered in *upf1*Δ strain. NMD functions in the degradation of PTC-containing transcripts to avoid the formation of truncated proteins. Some of these PTC-containing transcripts are pseudogenes. According to this data full NMD complex is required for this response, meaning that when cells lack *upf2*$^{+}$ or *upf3*$^{+}$, NMD complex is not active.

The genes used for this assay are the following: *rex2*$^{+}$ that encodes an RNA exonuclease; *rad8*$^{+}$, an E3 ubiquitin protein ligase; *mug105*$^{+}$, a ubiquitin-fold modifier-specific protease; *SPAC11D3.09c*, an agmatinase; and *SPCC63.13*, a DNAJ domain protein. *SPAC3A12.06c* encodes a sodium/calcium exchanger, and as mentioned before its expression does not change in cells lacking *upf1*$^{+}$, so we included it to see if differential expression in *upf1*Δ strain was related with the binding efficiency in the presence/absence of NMD components. Finally we included the pseudogene *SPBPBP21E7.08c* as a control.

We used different backgrounds, *upf1:TAP upf2*Δ, *upf1:TAP upf3*Δ and *upf1:TAP* that will serve as control. Total RNA and IP RNA of *upf1:TAP* strain was used as reference for the data normalization.

Afterwards we compared each IP RNA to their total RNA to observe binding efficiency (Figure 13).

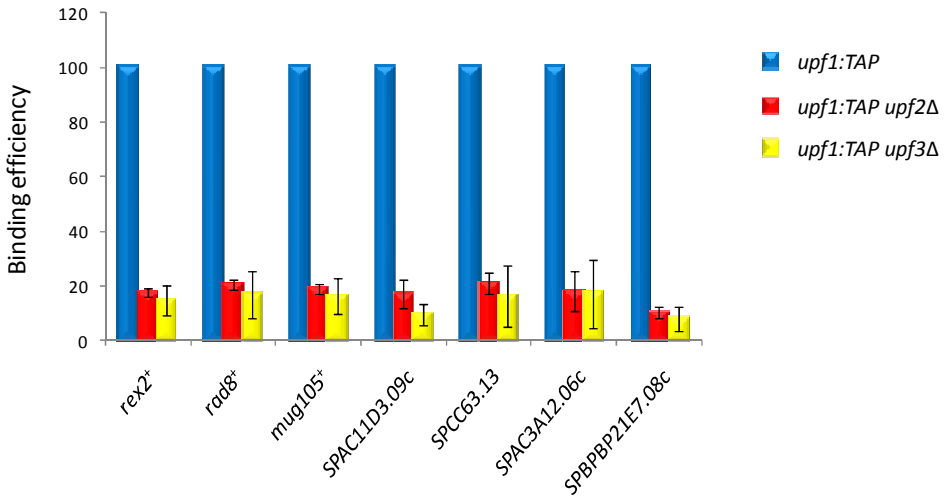

Figure 13. Upf1-mRNA targets binding efficiency in different genetic backgrounds. Total and IP data of *upf1:TAP* strain was used as reference for data normalization. Binding efficiency was calculated comparing each IP RNA to each corresponding total RNA. Blue columns represents the binding efficiency of Upf1 to *rex2*$^{+}$, *rad8*$^{+}$, *mug105*$^{+}$, *SPAC11D3.09c*, *SPCC63.13*, *SPAC3A12.06c* and *SPBPBP21E7.08c* in basal conditions. Red columns represent Upf1 binding efficiency in cells lacking Upf2 and yellow columns represent Upf1 binding efficiency in *upf1:TAP upf3*Δ strain. Bars indicate standard error.

We observed that in *upf1:TAP upf2*Δ and in *upf1:TAP upf3*Δ genetic backgrounds, the mRNA binding efficiency was about 1/5 of the *upf1:TAP* strain. All genes assayed in this experiment demonstrate that for an efficient Upf1-mRNA binding to its putative targets in fission yeast, the other components of NMD, Upf2 and Upf3, are required.

2.3. DELETION OF Upf1 TARGETS CAN RESCUE *upf1*Δ SENSITIVE PHENOTYPE UNDER OXIDATIVE STRESS CONDITIONS

We know that *upf1*Δ strains show a sensitive phenotype under oxidative stress conditions, meaning that Upf1 is playing a role in this response, but are Upf1 targets involved? To address this question we performed survival assays to characterize Upf1 targets phenotypes under oxidative stimuli.

We constructed double mutants with deletions in *upf1*$^{+}$ and the following Upf1 targets: *rex2*$^{+}$, *SPAC11D3.09c*, *rad8*$^{+}$, *SPCC63.13*, and *mug105*$^{+}$ (Figure 14).

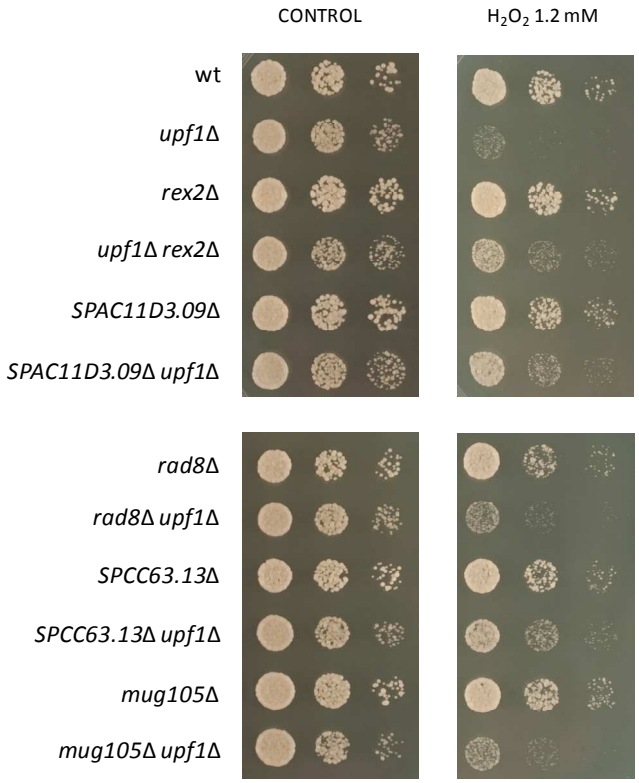

Figure 14. Survival assays in oxidative stress conditions. Serial dilutions (1/5) of wt, *upf1*Δ, *rex2*Δ, *upf1*Δ *rex2*Δ, *SPAC11D3.09*Δ, *SPAC11D3.09*Δ *upf1*Δ, *rad8*Δ, *rad8*Δ *upf1*Δ, *SPCC63.13*Δ, *SPCC63.13*Δ *upf1*Δ, *mug105*Δ, *mug105*Δ *upf1*Δ strains were plated in rich media and in the presence of 1.2 mM hydrogen peroxide. Plates were incubated at 30°C for 2 days.

After 48 hours incubation we observed that the sensitivity of three of the double *upf1*Δ mutants tested, *rex2*Δ *upf1*Δ, *SPAC11D3.09c*Δ *upf1*Δ and *SPCC63.13*Δ *upf1*Δ, was lower than the sensitivity showed by *upf1*Δ strain, while all single mutants showed a wild type phenotype under hydrogen peroxide treatment.

It has been described that in wild type cells, under oxidative stress conditions, there is an induction of the expression of transcription factor *atf1*$^{+}$ while in cells lacking Upf1 this induction is approximately one half (Rodriguez-Gabriel *et al.*, 2006).

One possible explanation of the phenotypic rescue could be that double mutants can promote an efficient induction of *atf1*$^{+}$ mRNA. This possibility was tested by qPCR, amplifying *atf1*$^{+}$ mRNA in different backgrounds in the absence and presence of hydrogen peroxide. We selected a wild type strain as positive control of *atf1*$^{+}$ induction and *upf1*Δ strain as negative control. This experiment was performed in *rex2*Δ *upf1*Δ strain where we observed a rescue of *upf1*Δ strain phenotype and in *rad8*Δ *upf1*Δ strain that did not show this phenotypic rescue.

Single mutants, *rex2*Δ and *rad8*Δ strains were also included in the assay (Figure 15).

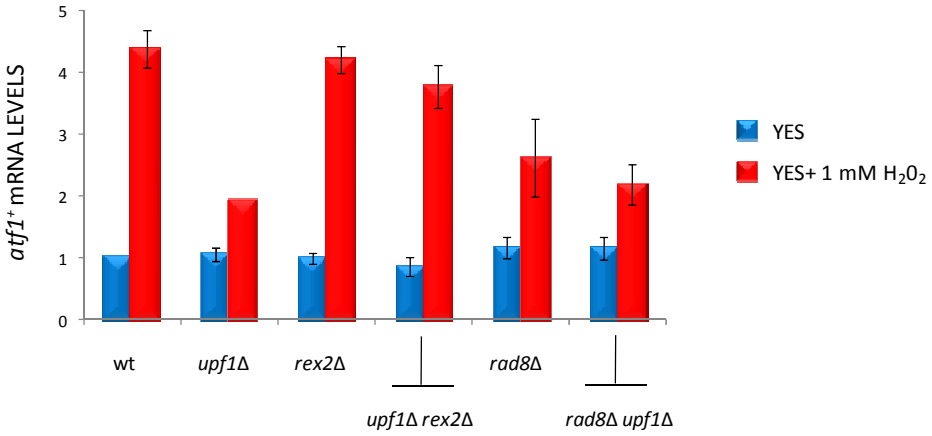

Figure 15. Quantitative real-time PCR analysis of *atf1*$^{+}$ mRNA in wt, *upf1*Δ, *rex2*Δ, *upf1*Δ *rex2*Δ, *rad8*Δ, *rad8*Δ *upf1*Δ strains in the presence and absence of 1 mM hydrogen peroxide. Bars indicate standard error.

As was expected *atf1*$^{+}$ mRNA levels in cells lacking Upf1 were reduced when compared with the levels observed in wild type cells. The double mutant *rex2*Δ *upf1*Δ showed similar induction of the transcription factor of the one observed in wild type cells, while *rad8*Δ *upf1*Δ strain only showed a slightly enhancement in the induction compared to *upf1*Δ strain.

These results indicate that some Upf1 targets, like Rex2, may exert a negative effect on oxidative stress survival mediated by their regulation of *atf1*$^{+}$ mRNA abundance.

3. Upf1 DEEP SEQUENCING

The global role of Upf1 over genome transcription can be determined by high throughput cDNA sequencing. This approach leads us to discriminate genome expression

changes at single nucleotide resolution. The sequence data reveals novel transcribed regions, obtaining the read sequences in the sense strand but also in the anti-sense strand.

To analyze the role of Upf1 in the transcriptome we performed cDNA high throughput sequencing in prototrophic wild type and *upf1*Δ strains to avoid genetic changes due to the nutritional requirements. Using the read sequences data obtained from both strains we could compare the expression of each single nucleotide and how expression was affected by the presence of Upf1(Figure 16).

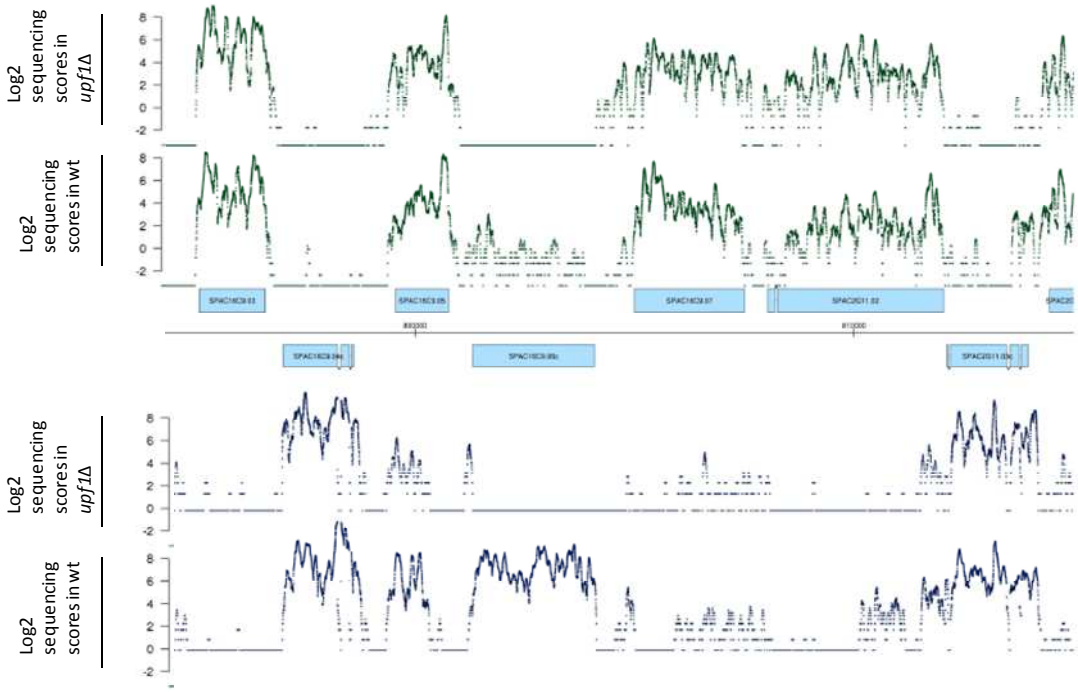

Figure 16. Genomic view of *upf1*Δ and wild type cDNA sequencing data. The upper panel shows log2 sequencing scores of anti-sense strand in *upf1*Δ and wild type strains, while the bottom panel shows log2 sequencing scores of sense strand in *upf1*Δ and wild type strains.

As example of these results we can observe, in the figure 16, the genomic view of part of the chromosome 1 of *upf1*Δ and wild type cDNA sequencing data. In this region is localized the gene that encodes Upf1, SPAC16C9.06c, and as was expected, we cannot observe *upf1*$^{+}$ expression in *upf1*Δ strain.

3.1. Upf1 AFFECTS HETEROCHROMATIN FORMATION AT CENTROMERES

The function of Upf1 at posttranscriptional level can be determined by the experiments described earlier but there are many more kinds of RNAs that may be involved in this regulation. Using high throughput cDNA sequencing we can observe changes in expression of the whole genome in different backgrounds. Thus, we can study

changes in expression in *upf1*Δ strain not only in protein coding RNAs but also in non protein coding RNAs. Using total cDNA sequencing data we can assemble the genome expression of each chromosome comparing *upf1*Δ and wild type strains (Figure 17).

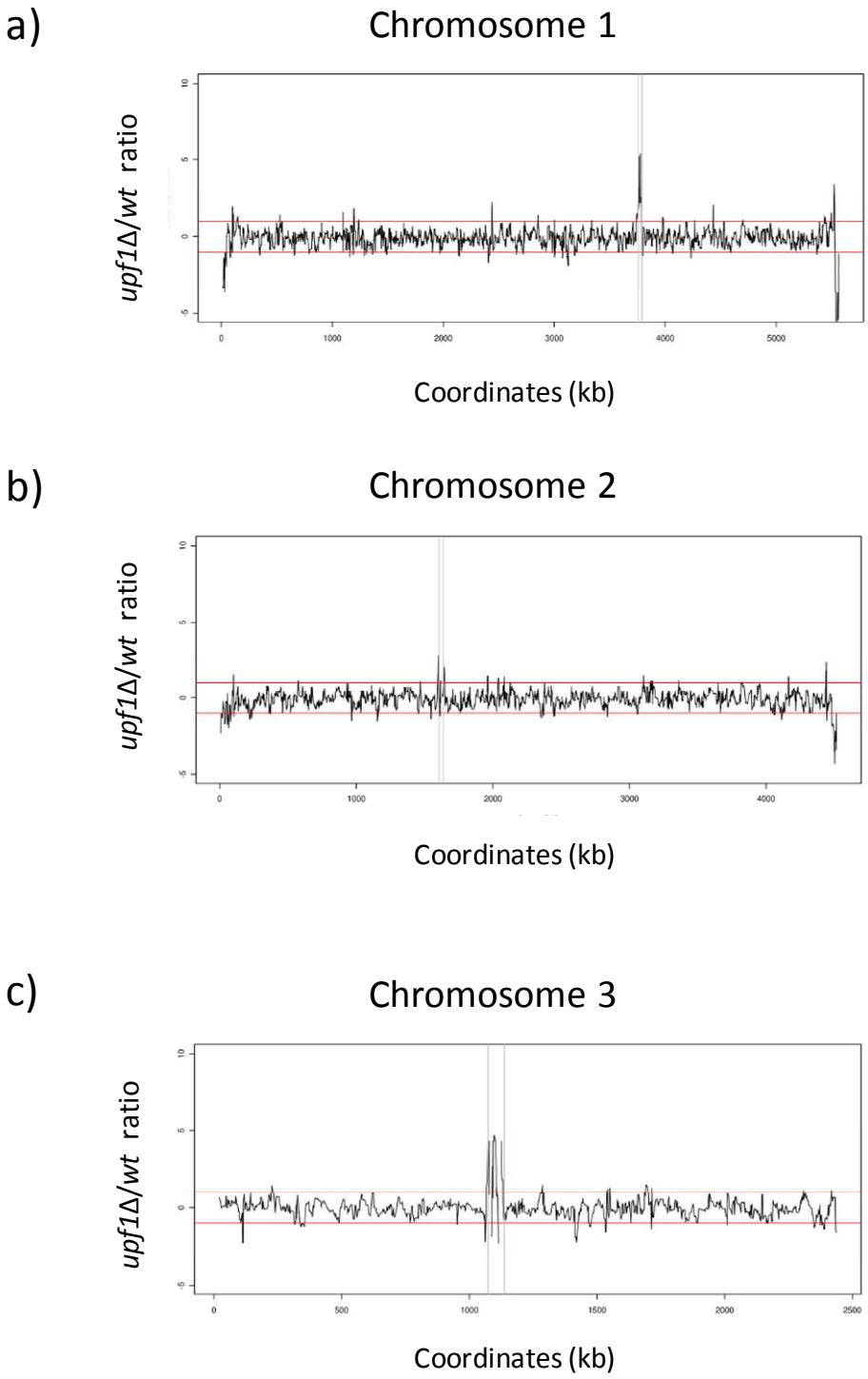

Figure 17. Each plot, a), b) and c), represents the mean ratio between *upf1*Δ and wt expression scores along genomic coordinates for each single chromosome. Red lines delimitate 1.5 overexpression/downregulation and grey lines delimitate chromosome centromeric regions.

In the figure 17 there are three panels that show the ratio of cDNA expression in *upf1*Δ strain compared to wild type represented along genomic coordinates for each chromosome.

Fission yeast chromosomes contain constitutive heterochromatin localized at centromeres and subtelomeric regions. In the figure we can observe grey lines that delimitate centromeric regions of each chromosome. These regions are overexpressed in *upf1*Δ strain. Overexpression in this region indicates that heterochromatin is not properly assembled in *upf1*Δ strain.

To confirm these results we constructed a *upf1*Δ strain which endogenous *ura4*$^{+}$ was disrupted and a wild type copy of *ura4*$^{+}$ gene was inserted at centromere. In wild type strain heterochromatin will be properly assembled at centromeres, repressing the genes located in this region. In strains with defects in heterochromatin formation, centromeric *ura4*$^{+}$ gene will be euchromatized. Under these conditions, cells will express it and therefore, will grow in the absence of uracil.

As control we used different mutants in the same background that are known to be involved in heterochromatin formation and gene silencing as *dcr1*Δ, *ago1*Δ or *rdp1*Δ (Hall *et al.*, 2003; Provost *et al.*, 2002; Volpe *et al.*, 2002). When any of these proteins is absent, cells are able to grow without uracil because they express the *ura4*$^{+}$ gene localized at centromeres.

We also constructed double mutants, *dcr1*Δ *upf1*Δ, *ago1*Δ *upf1*Δ and *rdp1*Δ *upf1*Δ.

Serial dilutions of these strains were plated in rich media and minimal media without uracil, and incubated at 30°C for three days. Afterwards pictures were taken (Figure18).

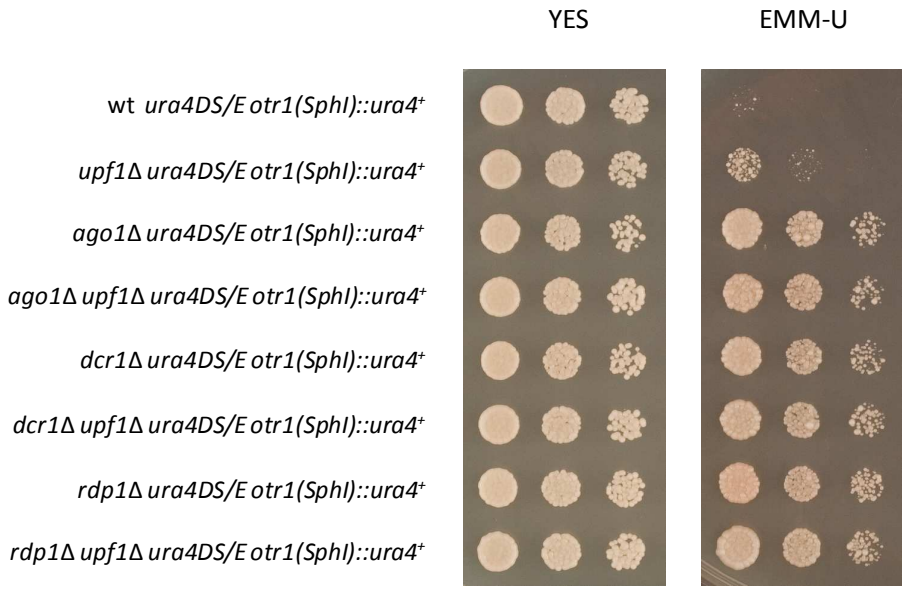

Figure 18. Growth assays in minimal media without uracil (EMM-U). Serial dilutions (1/5) of wt, *upf1*Δ, *ago1*Δ, *ago1*Δ *upf1*Δ, *dcr1*Δ, *dcr1*Δ *upf1*Δ, *rdp1*Δ, *rpd1*Δ *upf1*Δ strains, that contain endogenous *ura4*$^{+}$ disruption and a wild type *ura4*$^{+}$ inserted at centromere, were plated in rich media (YES) and EMM-U. Plates were incubated for three days at 30°C.

As we can observe in figure 18, wild type strain is not able to grow in minimal media without uracil because they cannot promote the expression of *ura4*$^{+}$ inserted at centromere. Cells lacking Upf1 can grow in this media, meaning that there is a problem in heterochromatin assembly at centromeres, although we observed more efficient growth in mutants in Ago1, Dcr1 or Rdp1. We did not observe any growth difference between single and double mutants in proteins involved in heterochromatin formation. All of them are able to survive in minimal media without uracil.

We quantified the expression of *ura4*$^{+}$ inserted at centromere to confirm that this growth was due to its expression. We extracted RNA from wild type, *upf1*Δ, *ago1*Δ and *ago1*Δ *upf1*Δ strains and analyzed *ura4*$^{+}$ expression by qPCR (Figure 19).

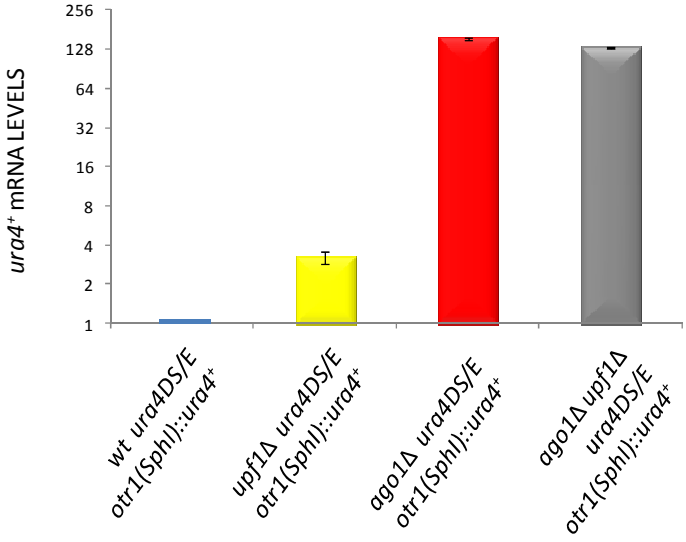

Figure 19. Quantitative PCR analysis of centromeric *ura4*$^{+}$ mRNA in wild type, *upf1*Δ, *ago1*Δ, *ago1*Δ *upf1*Δ strains that contain an endogenous *ura4*$^{+}$ disruption and wild type *ura4*$^{+}$ copy inserted at centromere. Bars indicate standard error.

We used wild type *ura4*$^{+}$ expression (1) as reference and we observed a higher expression in *upf1*Δ strain (~3X).

We also observed that *ura4*$^{+}$ expression in *upf1*Δ strain was much lower than in *ago1*Δ strain or even in *ago1*Δ *upf1*Δ.

These results indicate that Upf1 regulates heterochromatin formation and, therefore, expression of centromeric *ura4*$^{+}$ in cells lacking *upf1*$^{+}$ is enough to promote growth in minimal media without uracil.

3.2. Upf1 AFFECTS NORMAL GENOME EXPRESSION

As it was mentioned before, by cDNA sequencing we can analyze the genome expression, including untranslated regions or non-coding RNAs.

Using the data obtained by the cDNA sequencing of *upf1*Δ and wild type strains we did a comparison between both sets of data looking at differential expression of small nuclear RNAs (snRNAs), small nucleolar RNAs (snoRNAs), non-coding RNAs (ncRNAs) and pseudogenes (Figure 20).

We made a comparison using the log2 RPKM of each strain. As reference we did a comparison between our wild type and a reference wild type. Blue lines delimitate a 1.5 times overexpression/downregulation.

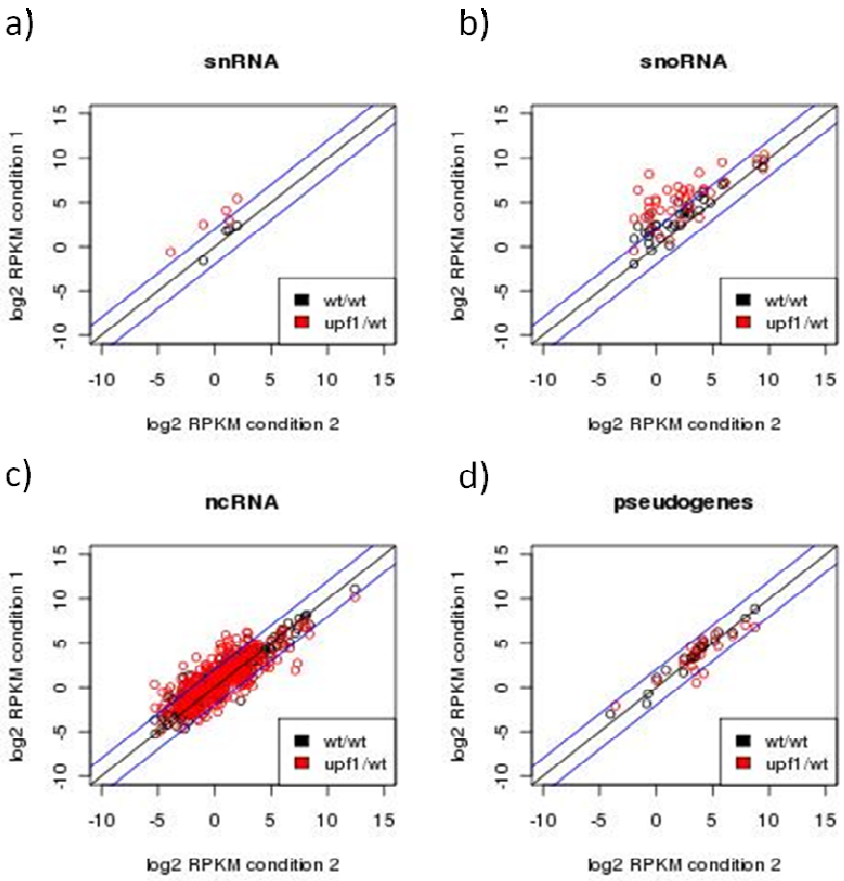

Figure 20. Scatter plots of small nuclear RNAs (snRNA)(panel a), small nucleolar RNAs (snoRNA)(panel b), non-coding RNAs (ncRNA)(panel c) and pseudogenes(panel d) expression in a comparison between log2 RPKM of our wild type and log2 RPKM of a reference wild type (black circles); and between log2 RPKM of our wild type and log2 RPKM of *upf1*Δ (red circles). Blue lines determine 1.5 overexpression/downregulation.

As we can observe in the figure 20, there is a differential expression of snRNAs and snoRNAs in *upf1*Δ strain compared to wild type. snRNAs and snoRNAs are overexpressed in cells lacking Upf1.

By contrast we cannot appreciate any significative difference in the expression of pseudogenes or non-coding RNAs.

As component of NMD, Upf1 has a role in the processing of defective spliced variants. Thus, cells lacking Upf1 should show defects in processing of spliced genes. To test this idea we selected all genes that contain introns and therefore are susceptible to suffer alternative splicing, from the cDNA sequencing data. Two numbers were defined for each intron: nTransReads, the number of reads spanning the exon-exon junction and nIntronReads, the number of reads spanning the intron-exon junctions. Splicing scores were then calculated for each introns as:

nTransReads / ((nTransReads+ nIntronReads) / 2) * 100

Introns with splicing scores bellow 80 were selected and clustered using the k-mean algorithm (Figure 21).

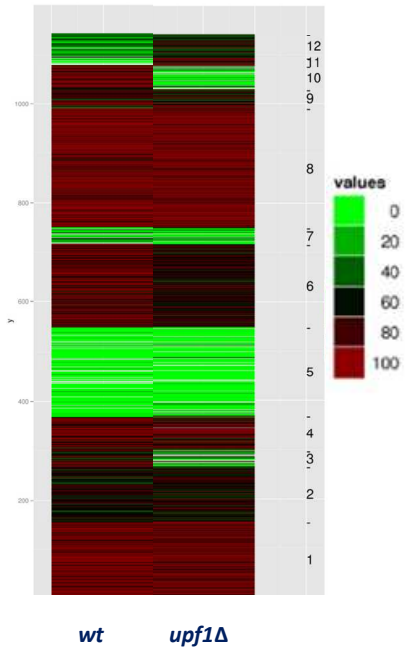

Figure 21. Analysis of splicing efficiency in *upf1*Δ strain.
Two numbers were defined for each intron:
nTransReads = the number of reads spanning the exon-exon junction.
nIntronReads = the number of reads spanning the intron-exon junctions.
Splicing scores were calculated for each introns using the following formula:
nTransReads / (nTransReads+(nIntronReads / 2)) * 100
Introns with splicing scores bellow 80 were selected and clustered using the k-mean algorithm. As result twelve clusters were obtained.

In figure 21 we can observe 12 clusters and five of them, clusters 3, 6, 10, 11 and 12 show some level of regulation specific to the *upf1*Δ background. We used the Gene Onthology database tool to carry out a study of terms enriched in these clusters. Terms such as protein binding (p=0.003), nucleus (p=0.0018) or cytoplasm (p=0.013) were enriched in these clusters. We also found the biological process related to the introns regulated by Upf1. They could be involved in cell cycle (p=0.0061) or in protein modification process (p=0.037). Some of them are early-meiotic genes (p=0.0014) or middle-meiotic genes (p=0.049) and belong to a meiosis-sporulation module (p=0.01).

4. NMD LOCALIZATION

4.1. Upf1 LOCALIZATION IN FISSION YEAST

Little is known about NMD in fission yeast. To contribute in the characterization of this mechanism in *S. pombe* we localized Upf1 *in vivo*. To perform this experiment we fused *upf1*$^{+}$ to the green fluorescent protein (GFP). As it is shown in the pictures (Figure 22), Upf1 is homogeneously distributed throughout the cytoplasm.

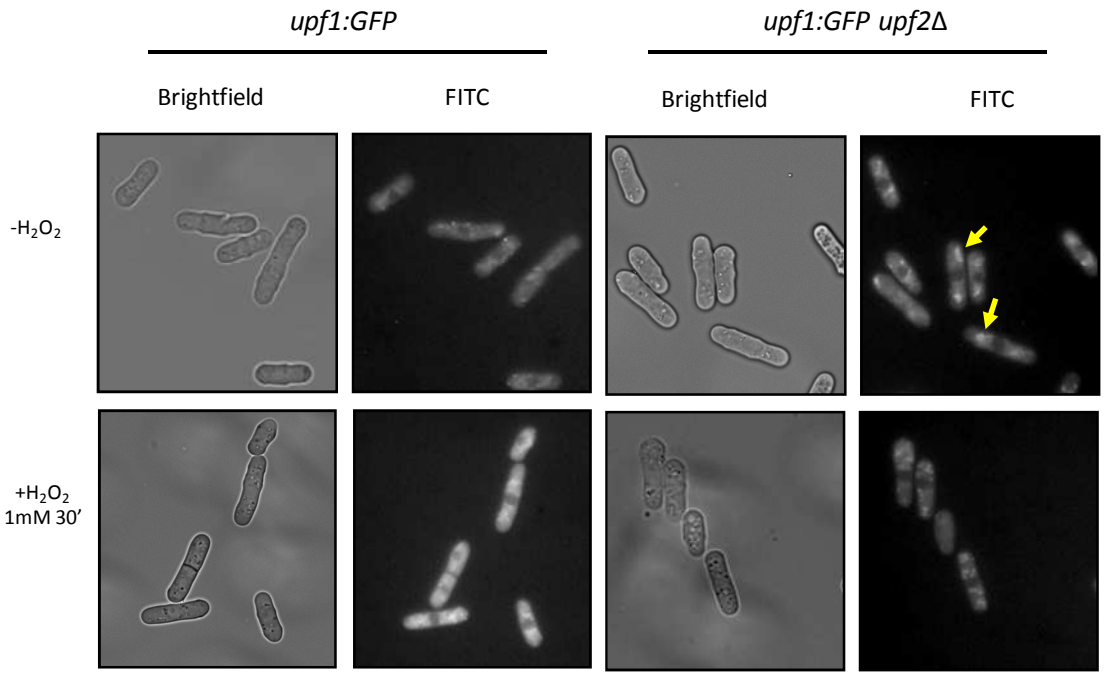

Figure 22. Fluorescence microscope images of Upf1 localization in the presence and absence of 1 mM hydrogen peroxide in *upf1:GFP* and *upf1:GFP upf2*Δ strains.

We have described that Upf1 has a role in the oxidative stress response and recently it has been described that there are RNA granules that appear as cellular stress survival mechanism (Nilsson and Sunnerhagen, 2011). Thus, one possibility was that Upf1 localization changes under these circumstances. To test this hypothesis we added hydrogen peroxide to the culture and took pictures of the cells after 30 minutes treatment. As we can observe, localization changes and Upf1-containing cytoplasmic granules appear after this treatment.

We have described that the presence of Upf2 in required for a proper Upf1-mRNA binding. We thought that Upf2 may be also required for the cytoplasmic Upf1 localization. To test this idea we constructed *upf1:GFP upf2*Δ strain. In this strain we observed that Upf1 distribution was not homogeneous, there were cytoplasmic accumulations, meaning that *upf2*$^{+}$ deletion alters Upf1 localization. Whereas *upf2*$^{+}$ deletion affects Upf1 localization in basal conditions, when we treated the cells with hydrogen peroxide we observed the same foci accumulation than in wild type cells. However, the fluorescent intensity in wild type strain under this condition was higher than in *upf2*Δ background.

4.2. UPF1 INTERACTS WITH eRF3 AND CBP80 IN MAMMALIAN CELLS

To observe interaction between NMD components *in vivo* we used bimolecular fluorescent complementation (BiFC) technique in mammalian COS cell line.

This technique is based on the reconstitution of a split fluorescent protein (VENUS) when two proteins, fused to two non-fluorescent fragments (VN173/VC155), interact.

There are two types of plasmids, one group that fuse the VN173/VC155 fragments to the amino-terminus region of the protein and other group that fuse the VN173/VC155 fragments to the carboxi-terminus region of the protein.

To visualize UPF1-eRF3 interaction we cloned eRF3 ORF into the two plasmids that contain VN173 epitope and UPF1 ORF into both VC155 containing plasmids.

Cells were transfected with different amounts of each plasmid DNA in order to select the DNA concentration producing the same amount of proteins than endogenous levels.

We followed the expression of these plasmids using antibodies against eRF3 or UPF1 by western blotting (Figure 23). For 100 mm dishes transfection we selected the following DNA amounts: 2 µg of pBiFC-VC155N-UPF1, 1 µg of pBiFC-VC155C-UPF1, 1 µg of pBiFC-VN173N-eRF3, and 0.5 µg of pBiFC-VN173C-eRF3.

a)

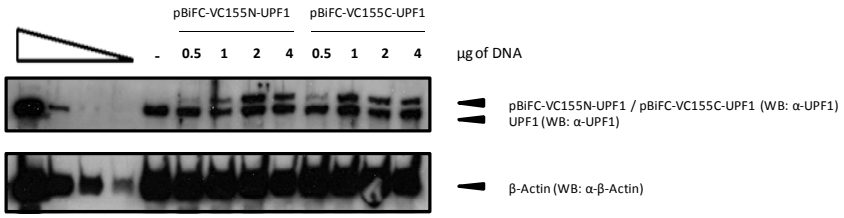

b)

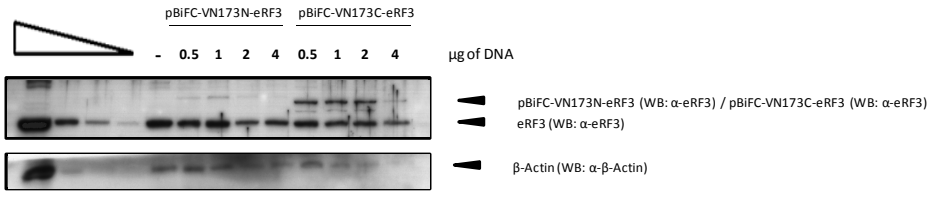

Figure 23. COS cells were transfected with 4 plasmids: pBiFC-VC155N-UPF1, pBiFC-VC155C-UPF1, pBiFC-VN173N-eRF3 and pBiFC-VN173C-eRF3. Panel a) shows western blotting (WB) using anti-UPF1, that detects the expression of pBiFC-VC155N-UPF1, pBiFC-VC155C-UPF1 and endogenous UPF1, and anti-β-Actin, that was used as control of variations in protein loading. Panel b) shows western blotting (WB) using anti-eRF3, that detects the expression of pBiFC-VN173N-eRF3, pBiFC-VN173C-eRF3 and endogenous eRF3, and anti-β-Actin, that was used as control of variations in protein loading. The leftmost four lanes, which analyzed 3-fold protein dilutions of non-transfected cells, demonstrate that the analysis is semiquantitative

Afterwards we checked the interaction between all plasmid combinations by fluorescent microscopy. We detected interaction in all combinations but the highest fluorescent intensity was detected when we combined plasmids with the epitope fused to the amino terminus part of the proteins, pBiFC-VC155N-UPF1 and pBiFC-VN173N-eRF3.

Cells were co-transfected with these plasmids and fixed after 24 hours. Nuclear envelope was delimitated by immunofluorescence, using an antibody against nuclear pore component 414. In the figure (Figure 24) we can observe that this interaction takes place in the cytoplasm. Single transfection of each plasmid was used as negative control.

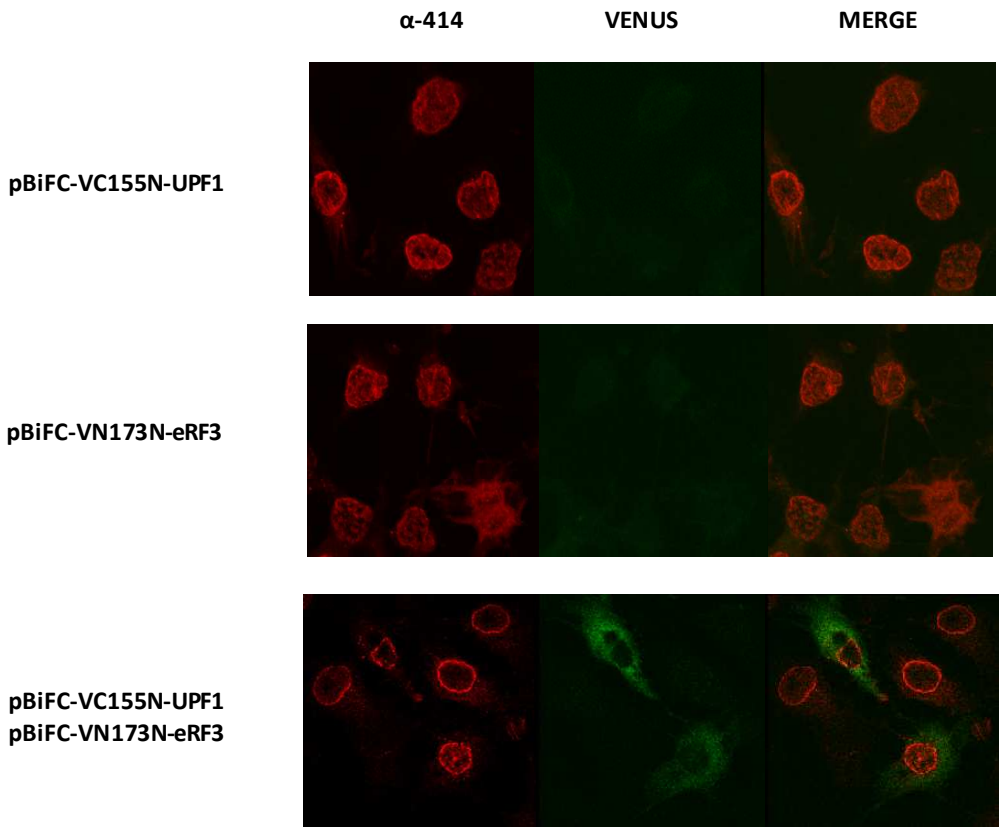

Figure 24. Fluorescence images of COS cells transfected with plasmids expressing the protein fragments indicated in each panel fused to UPF1 and eRF3. After transfection, cells were fixed and immunofluorescence assays were performed using anti-414 to determine nuclear envelope (left panel). Left and middle panel were combined into the right panel (merge).

To visualize UPF1-CBP80 interaction we cloned UPF1 ORF into VN173 containing plasmids and CBP80 ORF into VC155 plasmids.

In order to determine the amount of plasmid DNA that promotes the same expression than endogenous protein we performed transfections with different plasmid DNA concentrations.

Cells were co-transfected with all plasmid combination and interaction was visualized by fluorescent microscope. In this case we could only observe UPF1-CBP80 interaction in pBiFC-VN173N-UPF1 and pBiFC-VC155N-CBP80 co-transfection.

Looking at the western blotting results (Figure 25a, 25b) we established the following DNA amounts for 100 mm dishes transfection: 4 µg of pBiFC-VN173N-UPF1 and 2 µg of pBiFC-VC155N-CBP80.

After 48 hours, co-transfected cells were fixed with para-formaldehide. Nuclear envelope was stained using a monoclonal antibody against nuclear pore component 414. pBiFC-VN173N-UPF1 and pBiFC-VC155N-CBP80 single transfection was used as negative control. UPF1-CBP80 interaction was localized inside the nucleus (Figure 26).

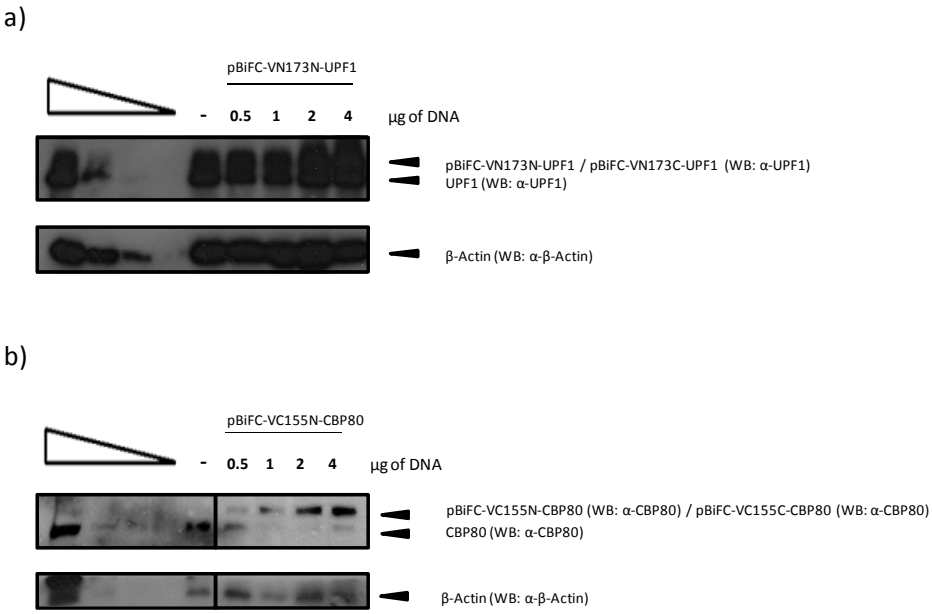

Figure 25. COS cells were transfected with 2 plasmids: pBiFC-VN173N-UPF1, pBiFC-VC155N-CBP80. Panel a) shows western blotting (WB) using anti-UPF1, that detects the expression of pBiFC-VN173N-UPF1 and endogenous UPF1, and anti-β-Actin, that was used as control of variations in protein loading. Panel b) shows western blotting (WB) using anti-CBP80, that detects the expression of pBiFC-VC155N-CBP80 and endogenous CBP80, and anti-β-Actin, that was used as control of variations in protein loading. The leftmost four lanes, which analyzed 3-fold protein dilutions of non-transfected cells, demonstrate that the analysis is semiquantitative.

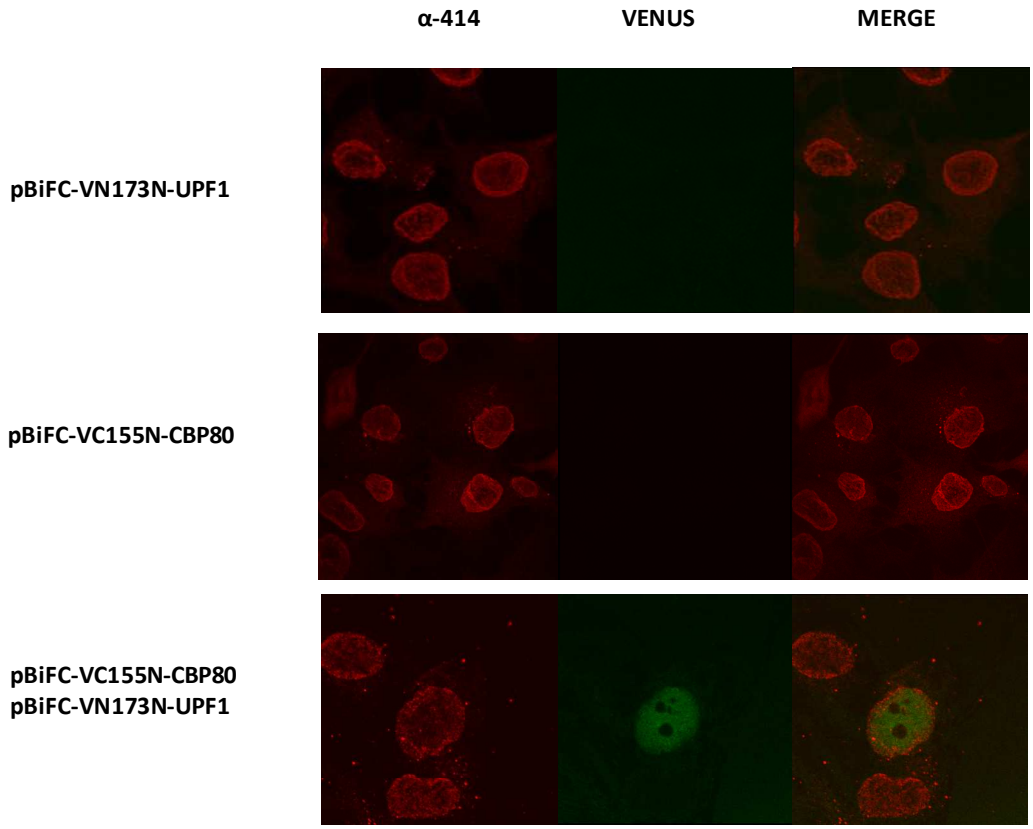

Figure 26. Fluorescence images of COS cells transfected with plasmids expressing the protein fragments indicated in each panel fused to UPF1 and CBP80. After transfection, cells were fixed and immunofluorescence assays were performed using anti-414 to determine nuclear envelope (left panel). Left and middle panel were combined into the right panel (merge).

4.3. UPF1 DIMERIZES IN MAMMALIAN CELLS

Using the transfection conditions established above, we tested the possible dimerization of UPF1 *in vivo*. We combined UPF1 containing plasmids to see if we could detect fluorescence in any plasmid combination. When cells were co-transfected with pBiFC-VN173N-UPF1 and pBiFC-VC155N-UPF1 plasmids, we observed that UPF1 dimerization was localized in small cytoplasmic granules (Figure 27). As in previous experiments single transfection of pBiFC-VN173N-UPF1 and pBiFC-VC155N-UPF1 was used as negative control and nuclear envelope was stained by immunofluorescence with a monoclonal antibody against 414.

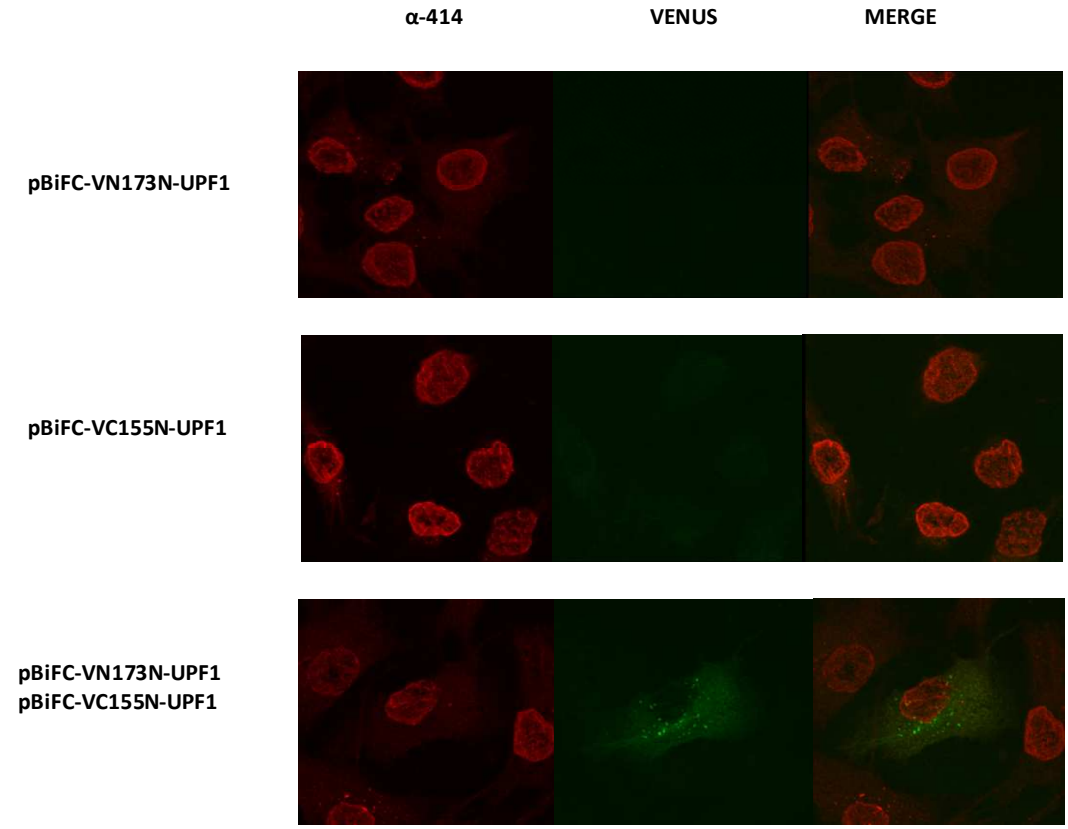

Figure 27. Fluorescence images of COS cells transfected with plasmids expressing UPF1 fused to different protein fragments indicated in each panel. After transfection, cells were fixed and immunofluorescence assays were performed using anti-414 to determine nuclear envelope (left panel). Left and middle panel were combined into the right panel (merge).

In order to discriminate the precise localization of this interaction we performed immunofluorescence assays, using different antibodies against late endosomes/lysosomes (α-LAMP1), Golgi (α-manosidase II) and endoplasmic reticulum (α-calnexin), in COS cells co-transfected with pBiFC-VN173N-UPF1 and pBiFC-VC155N-UPF1 (Figure 28).

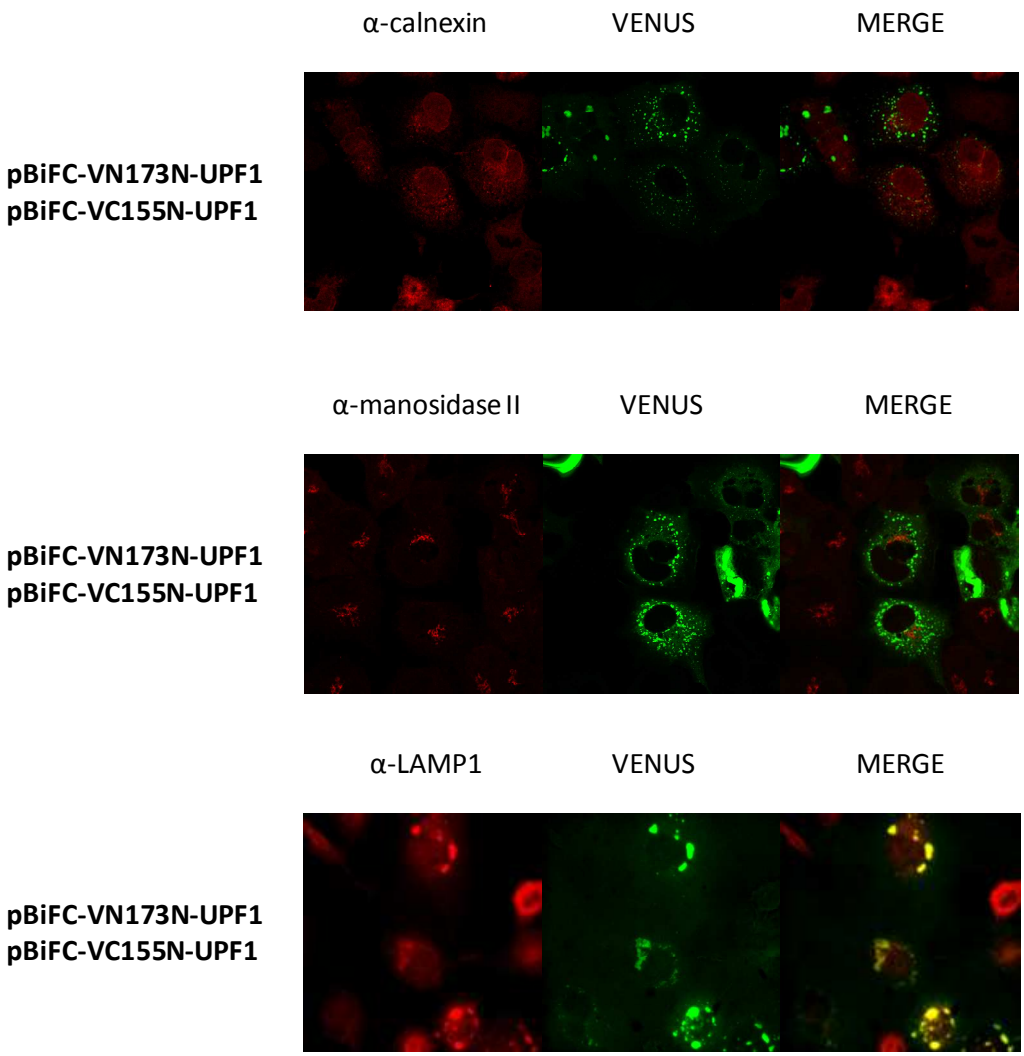

Figure 28. Fluorescence images of COS cells transfected with pBiFC-VN173N-UPF1 and pBiFC-VC155N-UPF1 plasmids. After transfection, cells were fixed and immunofluorescence assays were performed using anti-calnexin, anti-manosidase II and anti-LAPM1 to determine endoplasmic reticulum, Golgi and late endosomes/lysosomes respectively (left panel). Left and middle panel were combined into the right panel (merge).

When we looked at the merge panel (Figure 28) we cannot see co-localization between UPF1 dimerization and Golgi neither between UPF1 dimerization and endoplasmic reticulum. By contrast, when we stained cells with an antibody against late endosomes/lysosomes (α-LAMP1) we observed a clear co-localization of UPF1 dimerization, meaning that UPF1 dimerization is localized in the endolytic pathway.

5. Csx1 FUNCTION IN SEXUAL DIFFERENTIATION

Csx1 controls *pyp2*$^{+}$ mRNA expression, and *atf1*$^{+}$ mRNA levels under oxidative stress conditions and its phosphorylation depends on Spc1 activity (Rodriguez-Gabriel *et al.*, 2003).

Among many other responses, Spc1 mediates sexual differentiation. Spc1, through Atf1 phosphorylation, regulates transcription of Ste11 transcription factor (Shiozaki and Russell, 1996), the main factor responsible of sexual differentiation, and therefore strains lacking Spc1 are sterile.

During the construction of different strains containing mutations in Csx1 we realized that the mating efficiency of those crosses was much lower than wild type strain.

We hypothesized that the genetic relationship between Csx1 and Spc1/Atf1 might not be restricted to oxidative stress conditions, but also to sexual differentiation.

To analyze the ability of cells lacking Csx1 to mate, we observed sporulation in homothallic strains, *h*^{90} wild type and *h*^{90} *csx1*Δ. Both strains were plated in sporulation media (ME) and incubated at 24°C. After 48 hours pictures were taken (Figure 29).

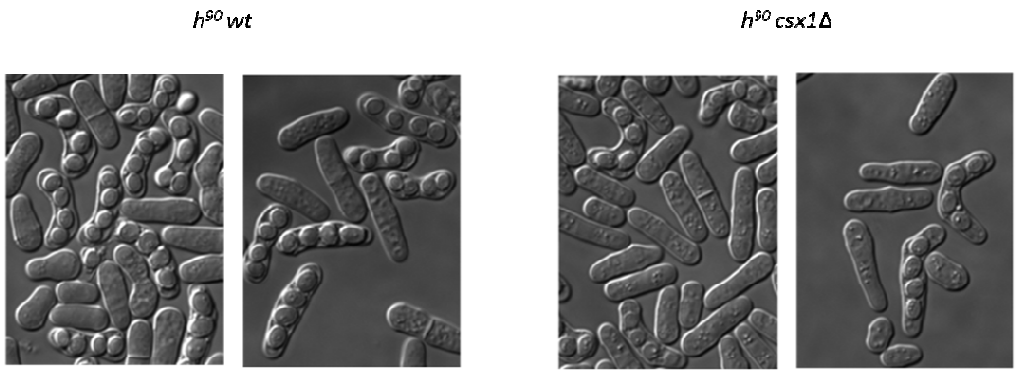

Figure 29. Morphology of homothallic wild type and *csx1*Δ strains after 48 hours in ME at 24°C. Pictures were taken using Nomarski filter.

In the pictures we did not observe any morphological difference between tetrads formed in *csx1*Δ and wild type strains. However, the number of zygotes or tetrads in cells lacking Csx1 appeared to be much lower than in wild type.

To quantify sporulation efficiency we inoculated these strains in ME media for 48 hours at 24°C. 10 µl of a cell dilution was placed into Neubauer chamber and normal cells, tetrads and zygotes were counted. To determine sporulation percentage we compared the number of tetrads and zygotes to the total number of cells (Figure 30).

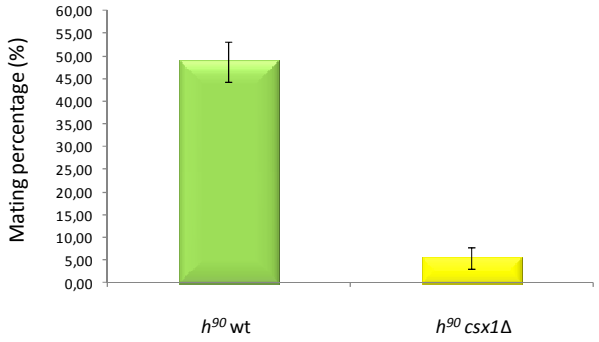

Figure 30. Mating percentage reached by homothallic wild type and *csx1*Δ strains after 48 hours in ME at 24°C. Bars indicate standard error.

As it is shown in figure 30 sporulation percentage of wild type strain is about 45-55% while in *csx1*Δ strain ranges between 4-8%.

To elucidate whether sporulation defect in *csx1*Δ strain was due to a problem in conjugation or in meiosis we performed the same experiment using diploid strains. These strains do not require conjugation for sporulation, thus they can undergo meiosis under nitrogen starvation conditions and low temperature (24°C). Using the same conditions than for haploid strains we quantified cells in h^-/h^+ $csx1^+/csx1^+$ strain, used as reference, and in h^-/h^+ *csx1*Δ/*csx1*Δ strain. In h^-/h^+ $csx1^+/csx1^+$ strain we observed (Figure 31) higher sporulation values than in homothallic haploid strains. The same effect was observed in h^-/h^+ *csx1*Δ/*csx1*Δ strain, but in this case the values were half of those reached by h^-/h^+ $csx1^+/csx1^+$ strain. This result indicates that diploid cells lacking Csx1 can undergo meiosis *per se*, but not with the same efficiency as wild type strain, demonstrating that Csx1 is required for meiosis.

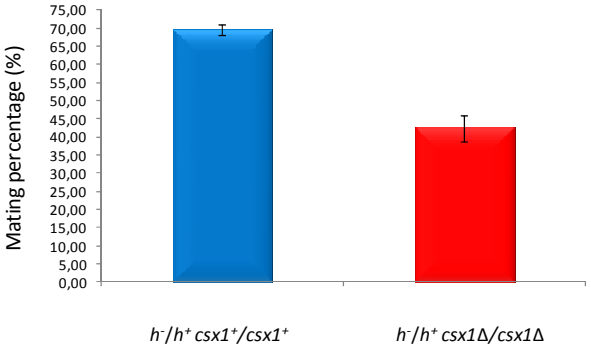

Figure 31. Mating percentage reached by diploid $csx1^+/csx1^+$ and *csx1*Δ/*csx1*Δ strains after 48 hours in ME at 24°C. Bars indicate standard error.

5.1. ROLE OF Csx1 IN G1 CELL CYCLE ARREST

When homothallic strains are subjected to nitrogen starvation conditions and low temperature (24°C) they mate and sporulate, and one of the first steps in this response is to arrest cell cycle at G1. Therefore a possible explanation of *csx1*Δ sterility could be that *csx1*Δ strains cannot arrest cell cycle at this stage. To test this possibility we performed flow cytometry assays, after induction of sexual differentiation, analyzing DNA content using propidium iodide staining. We included *ste11*Δ strain in the assay to analyze if cells

require this transcription factor cells to arrest at G1, and *spc1*Δ strain as negative control. Spc1 is required for cell cycle arrest, being this activity the main role of Spc1 in sexual differentiation (Shiozaki and Russell, 1996) (Figure 32).

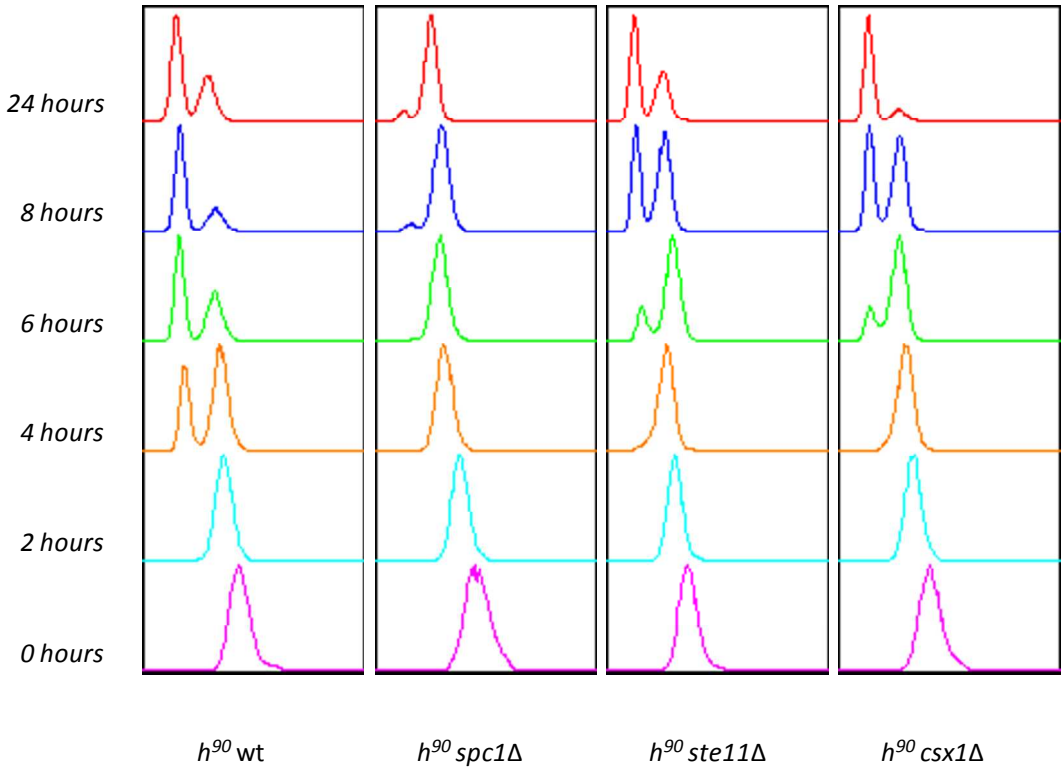

Figure 32. Flow cytometry histograms. Homothallic wild type, *spc1*Δ, *ste11*Δ, *csx1*Δ strains were incubated in EMM-N for 24 hours and samples were taken at the indicated times. DNA relative amount was estimated by the fluorescent signal amount emitted by propidium iodide.

For this experiment cells were incubated in minimal media (EMM) and mating was induced in minimal media without ammonium source at 24°C. They were harvested every two hours during a time course. Looking at wild type strain profile (Figure 32) we observed a single cell population in G2 at 0 hours and 2 hours induction. At 4 hours there are two cell populations, one in G2 and another in G1. At 8 hours G2 peak is almost completely displaced to G1. The profile showed by *csx1*Δ and *ste11*Δ strains is almost identical, both mutant strains can arrest cell cycle at G1, but the arrest in these strains is slower than in wild type strain, G1 peak appears at 8 hours induction instead of 4. In agreement with previous published works (Shiozaki and Russell, 1996) *spc1*Δ strain profile demonstrates that Spc1 is required for cell cycle arrest at G1.

5.2. EFFECT OF *cxs1Δ* IN POSTTRANSCRIPTIONAL REGULATION UNDER NITROGEN STARVATION CONDITIONS

We have confirmed that *csx1Δ* strains did not have any defect in G1 arrest under nitrogen starvation, so our next step was to determine *atf1*$^{+}$ and *ste11*$^{+}$ mRNA levels in this mutant to test if posttranscriptional response was altered. We perform qPCR to determine mRNA expression levels under nitrogen starvation at 24°C for 6 hours. We used h^{90} wild type strain as reference (Figure 33).

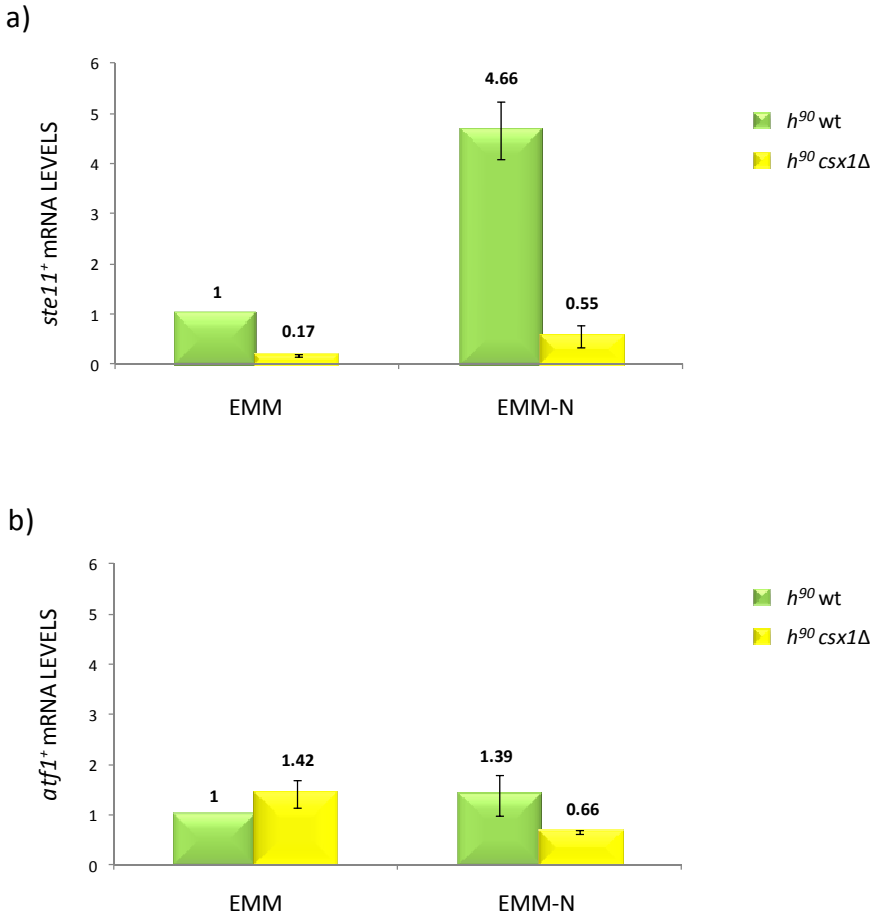

Figure 33. Quantitative real-time PCR analysis of *ste11*$^{+}$ mRNA (panel **a)**) and *atf1*$^{+}$ mRNA (panel **b)**) in homothallic wild type and *csx1Δ* strains in minimal media (EMM) and in the absence of nitrogen source (EMM-N) for 6 hours. Numbers above of the bars indicate mean values. Bars indicate standard error.

In h^{90} *csx1Δ* strain we observed (Figure 33a) that after 6 hours in the absence of nitrogen at 24°C, *ste11*$^{+}$ mRNA levels were approximately 1/10 of the levels found in wild type homothallic strain, but the most surprising finding was that the levels of *ste11*$^{+}$ in the mutant strain were also 1/10 of those found in wild type strain in basal conditions. The induction of this transcription factor under nitrogen starvation in wild type strain is 4-6

times, and the range of induction observed in the mutant strain is approximately the same but even after induction *ste11*$^{+}$ mRNA levels only reach wild type levels in basal conditions.

By contrast, when we look at the *atf1*$^{+}$ mRNA levels in both strains (Figure 33b) we found that *atf1*$^{+}$ expression was not induced. The expression data obtained in *csx1*Δ and wild type strains after 6 hours in nitrogen starvation at 24°C was similar to the data obtained in basal conditions. We could not consider any significant difference in *atf1*$^{+}$ expression when we compared mRNA levels in wild type and *csx1*Δ strains.

5.3. Csx1 BINDS *ste11*$^{+}$ mRNA

Figure 33 shows that *ste11*$^{+}$ mRNA levels are altered in *h*^{90} *csx1*Δ strain. One possible explanation could be that Csx1 would be binding *ste11*$^{+}$ mRNA and therefore stabilizing it. To test this hypothesis we did RNA-immunoprecipitation (RIp) assays using *h*^{90} *csx1:TAP* strain and *h*^{90} wild type strain as negative control of immunoprecipitation. RIp assays were followed by reverse transcription (RT) reaction to generate cDNA. This cDNA was used as template in a PCR reaction to amplify *ste11*$^{+}$ mRNA.

We performed the same experiment in minimal media (EMM) and in minimal media without nitrogen (EMM-N) at 24°C, harvesting cells at 0, 1 and 3 hours nitrogen starvation, to see if this binding was present in any condition (Figure 34).

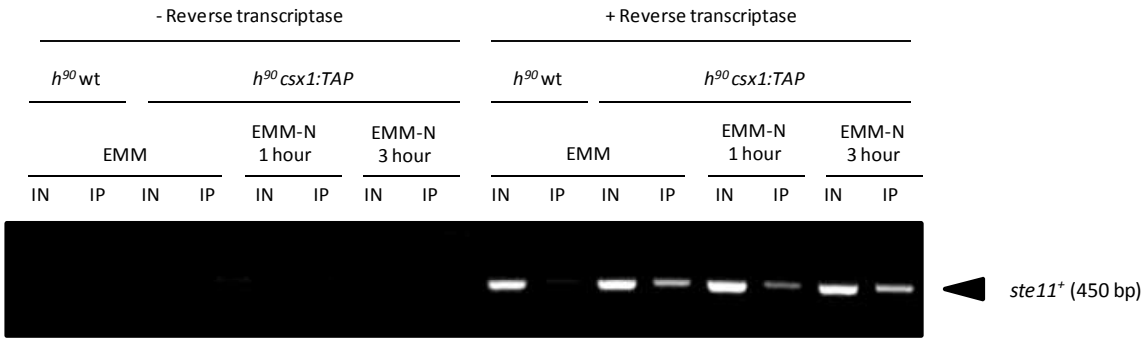

Figure 34. Binding of Csx1 to *ste11*$^{+}$ mRNA. TAP immunoprecipitation was performed with homothallic wild type and csx1:TAP strains in minimal media (EMM) and in the absence of ammonium source (EMM-N) for 1 hour and 3 hours. Afterwards RNA was isolated and cDNA was generated by reverse transcription. *ste11*$^{+}$ mRNA was amplified by PCR and monitored by agarose electrophoresis.

In the figure 34 we can observe a 1.5% agarose gel picture. As was expected in the negative control of RT reaction, where RNase free water instead enzyme was added, there was not amplification of this mRNA. This result was also observed in IP extracts of wild type cells. By contrast, we can observe *ste11*$^{+}$ amplification in the IP extracts of *h*^{90} *csx1:TAP* strain, meaning that Csx1 is binding *ste11*$^{+}$ mRNA and this binding is maintained in all conditions described before.

5.4. *Ste11* RESCUES *csx1Δ* PHENOTYPE

We have observed that strains lacking Csx1 are sterile. This disability in sexual differentiation in *csx1*Δ strain could be due to *ste11*$^{+}$ mRNA instability and cells could not appropriately respond to nitrogen starvation conditions. We transformed homothallic *csx1*Δ strain with pREP1-Ste11. This plasmid contains *ste11*$^{+}$ ORF under *nmt1* promoter, repressible by thiamine. Using this plasmid we tested if cells lacking Csx1 but overexpressing Ste11, were able to undergo conjugation and meiosis. Homothallic wild type strain was also transformed with this plasmid and used as control.

This experiment was carried out in plates containing minimal media without nitrogen in the absence of thiamine to promote sexual differentiation and plasmid expression, respectively. Homothallic wild type and csx1Δ strains were also transformed with control pREP1 plasmid (Figure 35).

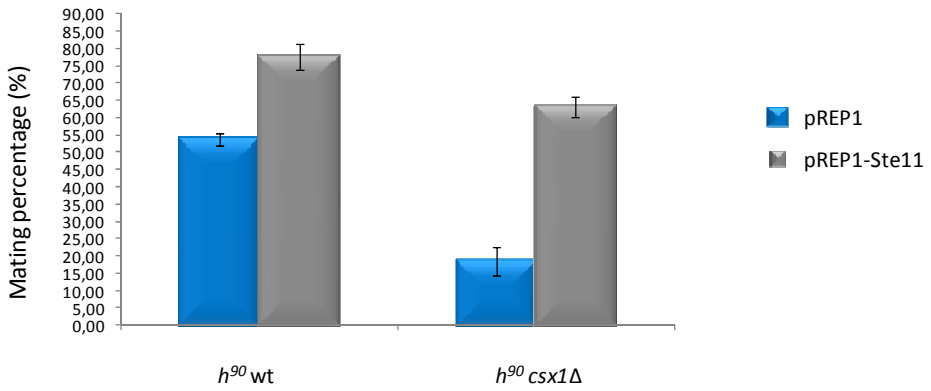

Figure 35. Quantitative analysis of *ste11*$^{+}$ mRNA expression. Homothallic wild type and *csx1*Δ strains transformed with pREP1 and pREP1-Ste11 plasmids were plated in minimal media without nitrogen and thiamine and incubated for 48 hours at 24°C. Afterwards mating percentage was calculated as described before. Bars indicate standard error.

As was expected, in *h*^{90} *wt*+pREP1 and *h*^{90} *csx1*Δ+pREP1 we observed similar mating efficiency as those described for untransformed strains in the previous epigraphs.

Overproduction of Ste11 induced an increase in mating efficiency in wild type strains (Figure 35).

In *h*^{90} *csx1*Δ+pREP1-Ste11 strain, under *nmt1*$^{+}$ promoter activation and therefore *ste11*$^{+}$ overexpression, we observed that mating percentage reached and even surpassed wild type levels.

This result indicates that the mating defect in *csx1*Δ strains is mostly due to the missregulation of Ste11.

DISCUSSION

Eukaryotic organisms suffer many changes along their lives. They have to respond to cellular proliferation cues and differentiation requirements but also to environmental stresses. For those purposes, eukaryotic cells have developed different mechanisms to detect extracellular signals and integrate them, producing specific biochemical responses.

To discriminate these signals there are different membrane receptors, being many of them specific for each response. Afterwards the signal is amplified and transmitted by a module of proteins, generally a MAPK cascade, which in turn will activate precise transcription factors that promote the expression of the necessary proteins through which cells will adapt them shelves to the requirements. This process is tightly regulated because these responses must be quick and efficient.

For many years it was thought that the main point of regulation of gene expression was performed at the level of transcription factors, but in the last decade it has emerged the figure of the RNA binding proteins (RBPs). That establishes another layer of regulation. Transcription factors promote the synthesis of different mRNAs, while RBPs can module the localization, half-life, translation, or alternative splicing of those mRNAs. Thus, RBPs are essential in the regulation of specific responses playing a fundamental role in posttranscriptional regulation.

So far there was a unified theory of gene expression, where DNA was transcribed to mRNA and mRNA traduced to proteins, but during the last 20 years, especially during the last decade, the role of RNA is becoming more and more important. Several studies in different organisms indicate that the transcribed portions of genomes are larger and more complex than expected. This complexity is explained not only by coding sequences but also by regulatory sequences in untranslated regions, non-coding RNAs, alternative start and polyadenylation sites, and the regulation of intron splicing.

We have used *S. pombe* as model organism to study the role of two RNA binding proteins, Csx1 and Upf1, in posttranscriptional regulation. These two proteins are involved in stress response mechanisms, connecting external stimuli with posttranscriptional regulation.

ROLE OF Upf1 IN POSTTRANSCRIPTIONAL REGULATION

Upf1 is a protein highly conserved in all eukaryotic organisms. It contains a DEAD-box domain with ATP-dependent helicase activity, through which it can bind mRNAs. The major function of Upf1 is to be the core component of the non-sense mediate mRNA decay (NMD). This mRNA surveillance mechanism degrades transcripts containing premature termination

codons (PTCs) avoiding the formation of truncated proteins. The importance of this pathway lies on the fact that defects on NMD can promote the formation of those truncated proteins causing genetic diseases.

It is difficult to explain the conservation of Upf1 in eukaryotic cells, assuming that this is the only role. In order to know additional roles of Upf1 in posttranscriptional regulation in eukaryotic cells, we performed RIp-chip experiments in fission yeast. Throughout these assays we can identify Upf1 cellular targets. Knowing which mRNAs are bound by Upf1 we can determine new Upf1 functions.

Upf1 could be binding these mRNAs either to stabilize or to degrade them. To address this issue we performed DNA microarrays in *upf1*Δ strain. If Upf1 is degrading mRNAs, these mRNAs should be overexpressed in *upf1*Δ strain. By contrast if the function of Upf1 is to stabilize these mRNAs, the result in the microarrays experiments will be the opposite.

In figure 8 and 9 we have confirmed a high correlation between genes bound by Upf1 and those genes overexpressed in *upf1*Δ strain, meaning that probably Upf1 is binding most of these mRNAs to induce their degradation.

Establishing a significant cut off and comparing the data of each replica we detailed a list of putative Upf1 mRNA targets. Looking at table 8 we can observe that Upf1 is binding many different mRNAs, involved in diverse cellular functions. As it has been described in other organisms (Culbertson and Leeds, 2003), we expected that *S. pombe* Upf1 would be binding mRNAs that contain PTCs as pseudogenes or intron containing mRNAs, that could insert PTCs by alternative splicing, but surprisingly we have found that Upf1 is binding and degrading intron-less mRNAs and mRNAs without evident PTCs. These results suggest a new dimension in degradation mediated by Upf1, because Upf1 would be degrading not only PTC-containing transcripts but also other mRNAs to maintain their transcript levels. The function of some of these mRNAs suggests a direct relationship between Upf1 and transcription regulation, while others link Upf1 to cellular functions like metabolism regulation, cell wall biosynthesis, or meiosis.

In other organisms NMD mechanism requires the formation of a complex between Upf1 and Upf2/Upf3, being this complex required to degrade PTC-containing transcripts, but little is known about this complex in fission yeast. Using two different techniques, BiFC and co-immunoprecipitation, we have demonstrated that Upf1 interacts with Upf2 *in vivo*, and this interaction takes place in the cytoplasm. Therefore, the complex formed by Upf1 and Upf2 in mammals is conserved in fission yeast.

Our next objective was to study in fission yeast if this complex was necessary for an efficient Upf1-mRNA binding. As occurs in other organisms, Upf1 binds several mRNAs that are susceptible to be degraded by NMD pathway and the presence of Upf2 and Upf3 is indispensable for this mRNA degradation.

We have proved that when the NMD lacks Upf2 or Upf3, Upf1 is not able to bind its targets with the same efficiency than when the three components are present in the cell.

A novel finding of this study is that components of NMD are essential for the Upf1-mRNA binding, not only for mRNAs expected to be susceptible of NMD degradation (PTC-containing mRNAs) but also for all mRNAs bound by Upf1, even those without PTCs.

ROLE OF Upf1 IN OXIDATIVE STRESS RESPONSE

It has been reported that Upf1 is involved in the oxidative stress response (Rodriguez-Gabriel *et al.*, 2006). Upf1 is modifying *atf1*$^{+}$ mRNA half-life, but surprisingly stabilizing it.

Our first interest was to investigate if Upf2 has any role in the oxidative stress response. We have demonstrated that cells lacking Upf2 show the same sensitive phenotype under hydrogen peroxide treatment than *upf1*Δ strain, meaning that both proteins are required for this response. We have also observed that the interaction described between Upf1 and Upf2 under standard growth conditions in co-immunoprecipitation assays is missing under oxidative stress conditions. Therefore, we conclude that under hydrogen peroxide treatment the NMD pathway is working independently on Upf1-Upf2 interaction or NMD does not work at all. We favor the first hypothesis because previous reports have demonstrated that Upf1 is binding more amounts of PTCs-containing transcripts under hydrogen peroxide treatment and is still able to degrade them (Rodriguez-Gabriel *et al.*, 2006).

Upf1 induces the degradation of many mRNAs and the expression of those mRNAs is therefore induced in cells lacking Upf1. The overexpression of these genes could promote an excess of protein production that can be detrimental for the cells because they can be interfering with essential cellular functions. Strains lacking Upf1 are viable, meaning that the mRNA overexpression produced is not dramatically affecting normal growth, but *upf1*Δ strain shows a reduced viability under hydrogen peroxide treatment. Could this unknown protein excess be responsible of this sensitivity phenotype? Our working hypothesis was that if Upf1 negatively regulated genes detrimental to cell growth under oxidative stress conditions, deletion of Upf1 would lead to overproduction of those gene products and reduced viability. To investigate this possibility we constructed different double deletion mutants in Upf1 and its

putative targets and performed survival assays. The results showed that when cells lack Upf1 and some of its targets, cells are less sensitive to oxidative stress conditions. With these data we have proved that the role of Upf1 in the oxidative stress response might be mediated by some of its targets. Upf1 is regulating the mRNA abundance of some genes which overexpression is damaging the cells under oxidative stress circumstances but not in basal conditions.

Another related question that we wanted to answer was how Upf1 was stabilizing *atf1*$^{+}$mRNA instead of degrading it. We established the following hypothesis: Upf1 is not stabilizing directly *atf1*$^{+}$. We thought that some of the putative targets of Upf1 were responsible of the different mRNA levels of *atf1*$^{+}$ under hydrogen peroxide treatment in *upf1*Δ strain. Upf1 is degrading several mRNAs and these mRNAs could be in turn degrading *atf1*$^{+}$ mRNA. When cells lack Upf1, its targets are overexpressed and therefore they increasingly degrade *atf1*$^{+}$, explaining why in *upf1*Δ strain *atf1*$^{+}$ mRNA levels are so low. By contrast, in *upf1*$^{+}$ strain, Upf1 is degrading its targets, and they cannot negatively regulate *atf1*$^{+}$, thus, in wild type strain there is a proper induction of *atf1*$^{+}$ mRNA in oxidative stress conditions.

To confirm this hypothesis we performed qPCR to quantify the levels of *atf1*$^{+}$ transcription factor under hydrogen peroxide treatment in different strains. Cells able to rescue *upf1*Δ sensitive phenotype under oxidative conditions showed similar amounts of *atf1*$^{+}$ mRNA to wild type strain (Figure 15). By contrast, we observed that cells that cannot rescue *upf1*Δ sensitive phenotype showed similar *atf1*$^{+}$ mRNA levels than the ones found in cells lacking Upf1.

Using these data we have proposed a double negative regulation mechanism that could explain the role of Upf1 in the oxidative stress response. We have demonstrated that some of Upf1 targets are involved in this response. In one hand, Upf1 is binding *rad8*$^{+}$ and *mug105*$^{+}$, both proteins are related to protein ubiquitination. These mRNAs are overexpressed in cells lacking Upf1, but double mutants cannot rescue *upf1*Δ sensitive phenotype. On the other hand, Upf1 is binding other transcripts as *rex2*$^{+}$, *SPAC11D3.09*, *SPCC63.13* that encodes an RNA exonuclease, an agmatinase, and a DNAJ domain protein. These proteins have been related with different cellular processes by bioinformatics sequencing alignments. All of them are overexpressed in *upf1*Δ strain, but in this case, double mutants in these proteins and Upf1 can rescue *upf1*Δ sensitive phenotype.

The difference between these two groups of genes lies on the levels of *atf1*$^{+}$ mRNA. When cells lack genes of the first group *atf1*$^{+}$ mRNA levels reached are similar to the levels

displayed by *upf1*Δ strain. By contrast, the induction of *atf1*$^{+}$ in *rex2*Δ *upf1*Δ strain is similar to the induction observed in wild type strain.

The double negative regulation can explain the involvement of Upf1 targets in the oxidative response and also why Upf1 is stabilizing *atf1*$^{+}$ mRNA.

Upf1 LOCALIZATION

During the study of the role of Upf1 in the oxidative stress response, we performed localization assays. As result, we observed that Upf1 is distributed throughout the cytoplasm. In cells treated with hydrogen peroxide, Upf1 localization changes and we observed small cytoplasmic granules.

Recently it has been described that cellular stresses can promote the formation of RNA granules (Nilsson and Sunnerhagen). In this study there is a localization description of different proteins, like Csx1 or Pabp, under different treatments. For instance, under osmotic stress these proteins co-localize in cytoplasmic granules. These granules are formed by proteins and poly(A)$^{+}$ RNAs.

In *S. cerevisiae* it has been described that transcripts containing PTCs are localized in P-bodies and this accumulation is reduced in strains lacking Upf1 (Sheth and Parker, 2006).

P-bodies and stress RNA granules are substantially different. Their functions are different: stress granules are formed as a consequence of cellular stress and could be responsible of an mRNA storage (Hoyle *et al.*, 2007), while P-bodies accumulate proteins involved in mRNA decay. The mRNAs localized in P-bodies can exit and re-initiate translation (Brengues *et al.*, 2005). The granules formed by Upf1 under hydrogen peroxide treatment could be P-bodies, containing the RNAs susceptible to be degraded by NMD, but these granules are not formed in basal conditions, only in the presence of hydrogen peroxide, suggesting that could be stress granules.

When cells lack Upf2, Upf1 is accumulated in cytoplasmic structures, meaning that Upf2 is required for a proper Upf1 localization in basal conditions. As we have mentioned before, the presence of Upf2 and Upf3 is essential for an efficient binding between Upf1 and its putative targets. One possibility is that in cells lacking Upf2, Upf1 is retained in these cytoplasmic structures. This situation could avoid a normal Upf1 function, abolishing the interaction between Upf1 and its targets.

By contrast, in the presence of hydrogen peroxide, Upf1 follows the same localization pattern in wild type cells and *upf2*Δ cells. This suggests that Upf2 is not required for a specific Upf1 localization in oxidative stress conditions, but it is essential for a proper Upf1 localization and function in basal conditions.

As mentioned before, in budding yeast it has been described that NMD components are localized in P-bodies, but these cellular structures have not been found in mammals. Many theories about NMD localization in mammals have been proposed to try to explain where this pathway takes place. In mammalian cells, NMD has been deeply studied and many protein interactions involved in this mechanism have been described.

Some of the interactions described are between UPF1 and eRF3 and between UPF1 and CBP80. CBP80 is a component of the cap binding complex and its function is developed during transcription. By contrast, the eukaryotic release factor 3 (eRF3) is involved in translation. UPF1 is binding both proteins during NMD, but CBP80 is localized inside the nucleus while eRF3 is located in the cytoplasm.

We did an approximation to try to answer how UPF1, a cytoplasmic protein, could be binding both proteins localized in two different places. Using the bimolecular fluorescence complementation technique we localized both interactions in mammalian cells. We proved that UPF1 interacts with both proteins *in vivo*. CBP80 interacts with UPF1 inside the nucleus, while eRF3 interacts with UPF1 along the cytoplasm.

The interaction between the cap binding protein CBP80 and UPF1 suggest that, in mammalian cells, UPF1 detects PTC-containing transcripts right when they are being transcribed and not once they have been exported out of the nucleus. On the other hand we have found that UPF1 interacts with eRF3 in the cytoplasm, suggesting that UPF1 is binding transcripts during translation to avoid the formation of truncated proteins. Therefore, UPF1 could be a shuttling protein between nucleus and cytoplasm.

So far, transcription, mRNA processing and translation have been described as independent processes of gene expression, but in the last decade it has been established that transcription is coupled to mRNA processing and even translation. This theory has been supported by new findings of interactions between RNApol II and many proteins involved in capping or splicing and translation (Proudfoot, 2000; Proudfoot, 1989).

The NMD is a mechanism that degrades PTC-containing transcripts and has always been related to the pioneer round of translation. If the interactions between UPF1 and

CBP80/eRF3 observed in mammalian cells are functional during NMD it could mean that this mechanism would be involved both in transcription and translation.

Using the plasmids constructed to monitor interactions detailed before, we tested the possibility of UPF1 dimerization. This observation could establish a new UPF1 function, because it is known that UPF1 interacts with many proteins, but never has been described a UPF1 dimerization.

During this study we have confirmed that UPF1 dimerizes *in vivo* and this dimerization follows a particular pattern in mammalian cells, being observed small cytoplasmic granules when this interaction occurs.

In order to localize UPF1 dimerization in these cells we performed immunoflourescence assays with different cellular markers. As result we co-localize this interaction with antibodies against LAMP1. LAMP1 is a lysosomal-associated membrane protein. The localization of UPF1 dimerization with lysosomal markers indicates that this interaction has a relationship with the endolytic pathway.

These data suggest that UPF1 dimerization could be required for NMD and the PTC-containing transcripts may be degraded by the endolytic pathway. Other possibility could be that an excess of UPF1 protein will be coupled in dimers and degraded by lysosomes.

Upf1 AFFECTS NORMAL GENOME EXPRESSION

Using high throughput cDNA sequencing we studied the role of Upf1 in the whole genome expression. This technique led us to study not only the expression of coding transcripts but also the regulatory sequences of untranslated regions and non-coding transcripts. This technique allowed us to have a global vision of Upf1 role in transcriptome at single nucleotide resolution.

One of the most interesting findings of this study is that Upf1 is involved in heterochromatin formation. We compared the transcripts expression in *upf1*Δ and wild type strains and the mean ratio between *upf1*Δ expression scores and wild type expression was represented along genomic coordinates for each single chromosome (Figure 16). This result indicated that centromeric expression seemed to be induced or derepressed in cells lacking Upf1.

Heterochromatin in fission yeast is assembled in centromeric and subtelomeric regions. This means that genes localized in these regions are not transcribed. When we

observed an induction of centromeric expression in *upf1*Δ strain we hypothesized that Upf1 could be involved in heterochromatin formation. In cells lacking Upf1 there would not be a proper heterochromatin assembly at centromeres, promoting the transcription of genes localized there.

Heterochromatin formation is regulated by proteins involved in RNAi and gene silencing such as Dcr1, Ago1 or Rdp1. When these proteins are not present in the cell, there is not heterochromatin formation at centromeres producing the transcription of genes localized in this region.

To check these results we constructed different mutants in a strain that contains wild type copy of *ura4*$^{+}$ inserted at centromere. In wild type strain centromeric *ura4*$^{+}$ expression is repressed, and cells are auxotrophs for uracil. Using as control *dcr1*Δ, *ago1*Δ and *rdp1*Δ strains we confirmed that in *upf1*Δ strain there was not a proper heterochromatin assembly at centromere, observing growth in minimal media without uracil in cells that express *ura4*$^{+}$ only at centromere. The growth observed in *upf1*Δ strain was intermediate between the one observed in wild type and *dcr1*Δ, *ago1*Δ, *rdp1*Δ strains.

To assert that the growth observed was due to the centromeric *ura4*$^{+}$ expression we quantified its expression by qPCR. As result we demonstrated that in *upf1*Δ strain there was 3 times more expression of *ura4*$^{+}$ gene compared to wild type strain. As we expected the centromeric *ura4*$^{+}$ expression was much higher in *ago1*Δ strain and in double mutant *upf1*Δ *ago1*Δ.

These results propose that Upf1 could be collaborating in the regulation of heterochromatin formation in fission yeast. As we have described previously, Upf1 is binding many mRNAs, so one possibility could be that the involvement of Upf1 in heterochromatin assembly would be indirect as occurs in the oxidative response.

Using the cDNA sequencing data we have studied the differential expression of many types of transcripts in *upf1*Δ strain compared to wild type. As result we have described that Upf1 is required for a normal expression of snRNAs and snoRNAs. snRNAs are involved in the spliceosome formation. This structure is assembled during mRNA processing, specifically during splicing reactions. snoRNAs guide modifications of tRNAs, rRNAs and snRNAs.

It has been described an interplay between the RNA silencing pathway and snoRNAs-mediate RNA processing. In fission yeast snoRNAs and sno-derived RNAs (sdRNA) are associated to Ago1, and sdRNA biogenesis is regulated by components of the RNAi pathway as

Dcr1 (Buhler *et al.*, 2008; Taft *et al.*, 2009). Looking at the previous results, snoRNAs overexpression could explain the defects in heterochromatin formation in *upf1*Δ strain.

Finally, using cDNA sequencing data we analyzed the splicing efficiency in cells lacking Upf1. This protein is the core component of NMD and this pathway degrades transcripts that can insert PTCs by alternative splicing.

As we expected we found significant differences in splicing efficiency in *upf1*Δ strain compared to *wild type* strain. Five of twelve clusters showed different levels of intron-containing transcripts due to the absence of Upf1. The genes grouped in these clusters revealed that Upf1 is regulating splicing of meiotic genes, genes involved in cell cycle or in protein modification processes.

Upf1 is involved by this way in other cellular processes different to the ones described before.

Csx1 IS INVOLVED IN SEXUAL DIFFERENTIATION

Csx1 is an RBP that contains 3 RRM. Csx1 has been described being involved in the oxidative stress response, regulating the expression of the transcription factor $atf1^{+}$ (Rodriguez-Gabriel *et al.*, 2003).

To construct strains by crossing, two strains with opposite mating type have to be plated in sporulation media (ME) and incubated at 24°C. This media contains reduced ammonium source and when cells detect these conditions they arrest their cell cycle at G1 and start the sexual differentiation. When we tried to construct strains containing *csx1*Δ mutations we observed that the mating efficiency of these crosses was much lower than the efficiency observed in other control strains.

We performed different experiments to quantify the sporulation percentage of homothallic *csx1*Δ strain. As pictures and quantitative analysis showed, h^{90} *csx1*Δ strain is almost sterile. Thus, this strain could have defects in conjugation, meiosis or both.

To discriminate between conjugation and meiosis defects we quantified sporulation using diploid strains. Diploid strains can undergo meiosis under nitrogen starvation at 24°C. In h^{-}/h^{+} *csx1*Δ/ *csx1*Δ strain we observed an enhancement of sporulation compared to h^{90} *csx1*Δ strain but still the levels were half of those found in $csx1^{+}/csx1^{+}$ strain. This result indicates that strains lacking Csx1 show defects in conjugation and meiosis.

To develop sexual differentiation is required an arrest of cell cycle at G1. One possible explanation of *csx1*Δ strain sterility could be that these cells were not able to arrest cell cycle

at G1. By flow cytometry we confirmed that h^{90} *csx1*Δ strain did not show any defect in cell cycle, arresting at G1 after 8 hours in nitrogen starvation, showing a similar behavior than wild type strain. This experiment was also performed using an h^{90} *ste11*Δ strain. Contrary to the previous published data by Kjaerulff, S. and colleagues (Kjaerulff *et al.*, 2005) we found that cells lacking Ste11 are able to arrest cell cycle at G1 stage and these cells exhibit a similar pattern than the one showed by cells lacking Csx1. The differences between both results can be due to that these cells are not synchronized, meaning that cells could show a delay in the cell cycle arrest at G1 not being detected after 7 hours in nitrogen starvation as they described in their report. To rule out this possibility we harvested cells incubated in the absence of nitrogen after 24 hours, and we actually confirmed that we could not observe cell cycle arrest during the first 6 hours in nitrogen starvation.

Sexual differentiation is regulated by different pathways, including the MAPK Spc1 that activates Atf1, which in turn activates Ste11 transcription factor. All pathways activate in last term Ste11, being this protein essential for the sexual development.

We have demonstrated that *csx1*Δ strain shows defects in sporulation and these defects are not due to a defect in cell cycle. Csx1 is an RBP that could be modulating RNAs involved this response.

To test if Csx1 was involved in the posttranscriptional regulation of sexual differentiation we quantified the mRNA levels of $atf1^{+}$ and $ste11^{+}$ under nitrogen starvation. We observed that in strain lacking Csx1, $ste11^{+}$ mRNA levels were almost undetectable, not only under nitrogen starvation but also in regular minimal media. This effect was not observed when we quantified $atf1^{+}$ mRNA expression, meaning that low levels of $ste11^{+}$ found in *csx1*Δ were not due to a defect in $atf1^{+}$ expression.

RBPs are classified depending on their RNA binding domains. Through these domains RBPs can bind RNAs to stabilize or degrade them, affecting their mRNA half-life.

We performed RNA immunoprecipitation assays to test if Csx1 was binding $ste11^{+}$ mRNA. Through these assays we confirmed that Csx1 is binding $ste11^{+}$ mRNA as in minimal media as in mating inducing conditions. If Csx1 is stabilizing the mRNA encoding this transcription factor through its binding, it would explain why in *csx1*Δ strain we can hardly detect expression of $ste11^{+}$.

We have demonstrated that Csx1 is essential for sexual differentiation and the sporulation defects showed by *csx1*Δ strain could be explained by a reduced $ste11^{+}$ expression

in this strain. Performing *ste11*$^{+}$ overexpression experiments we confirmed that cells lacking Csx1 recover mating ability when Ste11 levels are restored.

These results propose Csx1 as a novel regulator of sexual differentiation. As occurs with the MAPK Spc1, Csx1 is involved in two different pathways, the oxidative stress response and sexual differentiation. The cross-talk defined between both pathways through Spc1 could be extended to Csx1.

Csx1 is an RPB that is stabilizing different RNAs. It is binding *atf1*$^{+}$ mRNA under oxidative stress conditions but not in basal conditions, and *ste11*$^{+}$ in minimal media and nitrogen starvation. The signals that allow Csx1 to distinguish the different stimuli and therefore bind each mRNA remain unknown, but it is an interestingly research field.

CONCLUSIONS

- *S. pombe* Upf1 is involved in different cellular processes through the binding and degradation of several mRNAs. Upf1 requires the presence of Upf2 and Upf3 to develop this function.

- As occurs in other organisms, fission yeast Upf1 interacts with Upf2. This interaction is missing under oxidative stress conditions.

- In fission yeast, Upf1 role in the oxidative stress response is mediated by its cellular targets which modified expression levels of the main transcription factor involved in this response, Atf1.

- Upf1 forms stress granules under hydrogen peroxide treatment. In cells lacking Upf2 we observe the same foci formation.

- Upf1 is involved in heterochromatin assembly at centromeres. This function can be mediated through the regulation of snoRNAs and snRNAs expression.

- Upf1 participates in the splicing regulation of several genes, mainly those ones involved in meiosis.

- Mammalian UPF1 interacts with eRF3 *in vivo*. This interaction takes place in the cytoplasm. By contrast, the interaction between UPF1 and CBP80 occurs inside the nucleus. In addition, it has been demonstrated that UPF1 dimerizes *in vivo*. UPF1 dimers have been localized in the endolytic pathway.

- In S. pombe, the RBP Csx1 is involved in the sexual differentiation response through the binding and the regulation of the abundance of $ste11^{+}$ mRNA.

- ✓ La proteína Upf1 está involucrada en diferentes procesos celulares a través de la unión y degradación de diversos ARNm en la levadura de fisión *S. pombe*. Para llevar a cabo esta función necesita la presencia de Upf2 y Upf3.

- ✓ En *S. pombe*, al igual que ocurre en otros organismos, Upf1 interacciona con la proteína Upf2. Dicha interacción desaparece en condiciones de estrés oxidativo.

- ✓ En la levadura de fisión, el papel desarrollado por la proteína Upf1 en la respuesta celular frente a estrés oxidativo está regulada a través de sus dianas celulares que modifican los niveles del principal factor de transcripción de esta respuesta, Atf1.

- ✓ Upf1 forma gránulos de estrés bajo tratamiento de peróxido de hidrógeno en *S. pombe*. Esta formación de gránulos se mantiene en cepas carentes en la proteína Upf2.

- ✓ Upf1 está involucrada en la formación de heterocromatina en los centrómeros. Esta función puede estar mediada a través de la regulación de la expresión de snRNAs y snoRNAs.

- ✓ Upf1 está implicada en el procesamiento de intrones de genes principalmente relacionados con meiosis.

- ✓ En mamíferos, UPF1 interacciona *in vivo* con la proteína eRF3 en el citoplasma. También interacciona con la proteína CBP80 aunque esta interacción tiene lugar en el interior del núcleo. Adicionalmente se ha demostrado que UPF1 dimeriza *in vivo* y que esta formación de dímeros se localiza en la ruta endolítica.

- ✓ En la levadura *S. pombe* la proteína de unión a ARN, Csx1, está involucrada en la respuesta de diferenciación sexual a través de la unión y regulación de la abundancia del ARNm *ste11*$^{+}$.

BIBLIOGRAPHY

Akman, G., and MacNeill, S.A. (2009) MCM-GINS and MCM-MCM interactions *in vivo* visualised by bimolecular fluorescence complementation in fission yeast. *BMC Cell Biol* **10**: 12.

Allshire, R.C., Javerzat, J.P., Redhead, N.J., and Cranston, G. (1994) Position effect variegation at fission yeast centromeres. *Cell* **76**: 157-169.

Allshire, R.C., Nimmo, E.R., Ekwall, K., Javerzat, J.P., and Cranston, G. (1995) Mutations derepressing silent centromeric domains in fission yeast disrupt chromosome segregation. *Genes Dev* **9**: 218-233.

Aslett, M., and Wood, V. (2006) Gene Ontology annotation status of the fission yeast genome: preliminary coverage approaches 100%. *Yeast* **23**: 913-919.

Azuma, Y., Yamagishi, M., Ueshima, R., and Ishihama, A. (1991) Cloning and sequence determination of the *Schizosaccharomyces pombe rpb1* gene encoding the largest subunit of RNA polymerase II. *Nucleic Acids Res* **19**: 461-468.

Bähler, J., Wu, J.Q., Longtine, M.S., Shah, N.G., McKenzie, A., 3rd, Steever, A.B., Wach, A., Philippsen, P., and Pringle, J.R. (1998) Heterologous modules for efficient and versatile PCR-based gene targeting in *Schizosaccharomyces pombe*. *Yeast* **14**: 943-951.

Bähler, J.W., V. (2004) The genome and beyond. In *The Molecular Biology of Schizosaccharomyces pombe*. Egel, R. (ed). Heidelberg: Springer.

Balzi, E., Di Pietro, A., Goffeau, A., van Heerikhuizen, H., and Klootwijk, J. (1985) The RNA polymerase I initiation site and the external transcribed spacer of the fission yeast *Schizosaccharomyces pombe* ribosomal RNA genes. *Gene* **39**: 165-172.

Bass, B.L. (1997) RNA editing and hypermutation by adenosine deamination. *Trends Biochem Sci* **22**: 157-162.

Bomsztyk, K., Denisenko, O., and Ostrowski, J. (2004) hnRNP K: one protein multiple processes. *Bioessays* **26**: 629-638.

Braddock, D.T., Louis, J.M., Baber, J.L., Levens, D., and Clore, G.M. (2002) Structure and dynamics of KH domains from FBP bound to single-stranded DNA. *Nature* **415**: 1051-1056.

Brengues, M., Teixeira, D., and Parker, R. (2005) Movement of eukaryotic mRNAs between polysomes and cytoplasmic processing bodies. *Science* **310**: 486-489.

Buhler, M., Spies, N., Bartel, D.P., and Moazed, D. (2008) TRAMP-mediated RNA surveillance prevents spurious entry of RNAs into the *Schizosaccharomyces pombe* siRNA pathway. *Nat Struct Mol Biol* **15**: 1015-1023.

Burd, C.G., Matunis, E.L., and Dreyfuss, G. (1991) The multiple RNA-binding domains of the mRNA poly(A)-binding protein have different RNA-binding activities. *Mol Cell Biol* **11**: 3419-3424.

Chauvin, C., Salhi, S., Le Goff, C., Viranaicken, W., Diop, D., and Jean-Jean, O. (2005) Involvement of human release factors eRF3a and eRF3b in translation termination and regulation of the termination complex formation. *Mol Cell Biol* **25**: 5801-5811.

Chen, J., Chiang, Y.C., and Denis, C.L. (2002) CCR4, a 3'-5' poly(A) RNA and ssDNA exonuclease, is the catalytic component of the cytoplasmic deadenylase. *EMBO J* **21**: 1414-1426.

Chen, Y., and Varani, G. (2005) Protein families and RNA recognition. *FEBS J* **272**: 2088-2097.

Chiu, S.Y., Serin, G., Ohara, O., and Maquat, L.E. (2003) Characterization of human Smg5/7a: a protein with similarities to *Caenorhabditis elegans* SMG5 and SMG7 that functions in the dephosphorylation of Upf1. *RNA* **9**: 77-87.

Clerici, M., Mourao, A., Gutsche, I., Gehring, N.H., Hentze, M.W., Kulozik, A., Kadlec, J., Sattler, M., and Cusack, S. (2009) Unusual bipartite mode of interaction between the nonsense-mediated decay factors, UPF1 and UPF2. *EMBO J* **28**: 2293-2306.

Culbertson, M.R., and Leeds, P.F. (2003) Looking at mRNA decay pathways through the window of molecular evolution. *Curr Opin Genet Dev* **13**: 207-214.

Dreyfuss, G., Kim, V.N., and Kataoka, N. (2002) Messenger-RNA-binding proteins and the messages they carry. *Nat Rev Mol Cell Biol* **3**: 195-205.

Frolova, L., Le Goff, X., Zhouravleva, G., Davydova, E., Philippe, M., and Kisselev, L. (1996) Eukaryotic polypeptide chain release factor eRF3 is an eRF1- and ribosome-dependent guanosine triphosphatase. *RNA* **2**: 334-341.

Gonsalvez, G.B., Little, J.L., and Long, R.M. (2004) ASH1 mRNA anchoring requires reorganization of the Myo4p-She3p-She2p transport complex. *J Biol Chem* **279**: 46286-46294.

Haas, M., Siegert, M., Schurmann, A., Sodeik, B., and Wolfes, H. (2004) c-Myb protein interacts with Rcd-1, a component of the CCR4 transcription mediator complex. *Biochemistry* **43**: 8152-8159.

Hall, I.M., Noma, K., and Grewal, S.I. (2003) RNA interference machinery regulates chromosome dynamics during mitosis and meiosis in fission yeast. *PNAS* **100**: 193-198.

Hampsey, M. (1998) Molecular genetics of the RNA polymerase II general transcriptional machinery. *Microbiol Mol Biol Rev* **62**: 465-503.

Hanahan, D. (1983) Studies on transformation of *Escherichia coli* with plasmids. *J Mol Biol* **166**: 557-580.

Hershey, J.W. (1991) Translational control in mammalian cells. *Annu Rev Biochem* **60**: 717-755.

Higuchi, T., Watanabe, Y., and Yamamoto, M. (2002) Protein kinase A regulates sexual development and gluconeogenesis through phosphorylation of the Zn finger transcriptional activator Rst2p in fission yeast. *Mol Cell Biol* **22**: 1-11.

Hirano, T., Konoha, G., Toda, T., and Yanagida, M. (1989) Essential roles of the RNA polymerase I largest subunit and DNA topoisomerases in the formation of fission yeast nucleolus. *J Cell Biol* **108**: 243-253.

Hosoda, N., Kim, Y.K., Lejeune, F., and Maquat, L.E. (2005) CBP80 promotes interaction of Upf1 with Upf2 during nonsense-mediated mRNA decay in mammalian cells. *Nat Struct Mol Biol* **12**: 893-901.

Hou, V.C., Lersch, R., Gee, S.L., Ponthier, J.L., Lo, A.J., Wu, M., Turck, C.W., Koury, M., Krainer, A.R., Mayeda, A., and Conboy, J.G. (2002) Decrease in hnRNP A/B expression during erythropoiesis mediates a pre-mRNA splicing switch. *EMBO J* **21**: 6195-6204.

Hoyle, N.P., Castelli, L.M., Campbell, S.G., Holmes, L.E., and Ashe, M.P. (2007) Stress-dependent relocalization of translationally primed mRNPs to cytoplasmic granules that are kinetically and spatially distinct from P-bodies. *J Cell Biol* **179**: 65-74.

Humphrey, T., Sadhale, P., Platt, T., and Proudfoot, N. (1991) Homologous mRNA 3' end formation in fission and budding yeast. *EMBO J* **10**: 3503-3511.

Huttelmaier, S., Zenklusen, D., Lederer, M., Dictenberg, J., Lorenz, M., Meng, X., Bassell, G.J., Condeelis, J., and Singer, R.H. (2005) Spatial regulation of beta-actin translation by Src-dependent phosphorylation of ZBP1. *Nature* **438**: 512-515.

Ishigaki, Y., Li, X., Serin, G., and Maquat, L.E. (2001) Evidence for a pioneer round of mRNA translation: mRNAs subject to nonsense-mediated decay in mammalian cells are bound by CBP80 and CBP20. *Cell* **106**: 607-617.

Izaurralde, E., Lewis, J., McGuigan, C., Jankowska, M., Darzynkiewicz, E., and Mattaj, I.W. (1994) A nuclear cap binding protein complex involved in pre-mRNA splicing. *Cell* **78**: 657-668.

Janzen, D.M., and Geballe, A.P. (2004) The effect of eukaryotic release factor depletion on translation termination in human cell lines. *Nucleic Acids Res* **32**: 4491-4502.

Kanoh, J., Watanabe, Y., Ohsugi, M., Iino, Y., and Yamamoto, M. (1996) *Schizosaccharomyces pombe gad7*$^{+}$ encodes a phosphoprotein with a bZIP domain, which is required for proper G1 arrest and gene expression under nitrogen starvation. *Genes Cells* **1**: 391-408.

Karni, R., de Stanchina, E., Lowe, S.W., Sinha, R., Mu, D., and Krainer, A.R. (2007) The gene encoding the splicing factor SF2/ASF is a proto-oncogene. *Nat Struct Mol Biol* **14**: 185-193.

Kashima, I., Yamashita, A., Izumi, N., Kataoka, N., Morishita, R., Hoshino, S., Ohno, M., Dreyfuss, G., and Ohno, S. (2006) Binding of a novel SMG-1-Upf1-eRF1-eRF3 complex (SURF) to the exon junction complex triggers Upf1 phosphorylation and nonsense-mediated mRNA decay. *Genes Dev* **20**: 355-367.

Kato, T., Jr., Okazaki, K., Murakami, H., Stettler, S., Fantes, P.A., and Okayama, H. (1996) Stress signal, mediated by a Hog1-like MAP kinase, controls sexual development in fission yeast. *FEBS Lett* **378**: 207-212.

Keene, J.D. (2007) RNA regulons: coordination of post-transcriptional events. *Nat Rev Genet* **8**: 533-543.

Kim, M.Y., Hur, J., and Jeong, S. (2009) Emerging roles of RNA and RNA-binding protein network in cancer cells. *BMB Rep* **42**: 125-130.

Kim, Y.K., Furic, L., Desgroseillers, L., and Maquat, L.E. (2005) Mammalian Staufen1 recruits Upf1 to specific mRNA 3'UTRs so as to elicit mRNA decay. *Cell* **120**: 195-208.

Kimura, M., Sakurai, H., and Ishihama, A. (2001) Intracellular contents and assembly states of all 12 subunits of the RNA polymerase II in the fission yeast *Schizosaccharomyces pombe*. *Eur J Biochem* **268**: 612-619.

Kjaerulff, S., Lautrup-Larsen, I., Truelsen, S., Pedersen, M., and Nielsen, O. (2005) Constitutive activation of the fission yeast pheromone-responsive pathway induces ectopic meiosis and reveals *ste11* as a mitogen-activated protein kinase target. *Mol Cell Biol* **25**: 2045-2059.

Koromilas, A.E., Lazaris-Karatzas, A., and Sonenberg, N. (1992) mRNAs containing extensive secondary structure in their 5' non-coding region translate efficiently in cells overexpressing initiation factor eIF-4E. *EMBO J* **11**: 4153-4158.

Kozak, M. (1989) Circumstances and mechanisms of inhibition of translation by secondary structure in eucaryotic mRNAs. *Mol Cell Biol* **9**: 5134-5142.

Krämer, A. (1996) The structure and function of proteins involved in mammalian pre-mRNA splicing. *Annu Rev Biochem* **65**: 367-409.

Kunitomo, H., Higuchi, T., Iino, Y., and Yamamoto, M. (2000) A zinc-finger protein, Rst2p, regulates transcription of the fission yeast *ste11*$^{+}$ gene, which encodes a pivotal transcription factor for sexual development. *Mol Biol Cell* **11**: 3205-3217.

Lassar, A.B., Martin, P.L., and Roeder, R.G. (1983) Transcription of class III genes: formation of preinitiation complexes. *Science* **222**: 740-748.

Lawrence, C.L., Maekawa, H., Worthington, J.L., Reiter, W., Wilkinson, C.R., and Jones, N. (2007) Regulation of *Schizosaccharomyces pombe* Atf1 protein levels by Sty1-mediated phosphorylation and heterodimerization with Pcr1. *J Biol Chem* **282**: 5160-5170.

Lemaire, M., and Collart, M.A. (2000) The TATA-binding protein-associated factor yTafII19p functionally interacts with components of the global transcriptional regulator Ccr4-Not complex and physically interacts with the Not5 subunit. *J Biol Chem* **275**: 26925-26934.

Leupold, U. (1950) Die Vererbung von Homothallie und Heterothallie bei *Schizosaccharomyces pombe*. *CR Trav Lab Carlsberg Ser Physiol* **24**: 381-480.

Lewis, H.A., Musunuru, K., Jensen, K.B., Edo, C., Chen, H., Darnell, R.B., and Burley, S.K. (2000) Sequence-specific RNA binding by a Nova KH domain: implications for paraneoplastic disease and the fragile X syndrome. *Cell* **100**: 323-332.

Lu, D., Searles, M.A., and Klug, A. (2003) Crystal structure of a zinc-finger-RNA complex reveals two modes of molecular recognition. *Nature* **426**: 96-100.

Lunde, B.M., Moore, C., and Varani, G. (2007) RNA-binding proteins: modular design for efficient function. *Nat Rev Mol Cell Biol* **8**: 479-490.

Matlin, A.J., Clark, F., and Smith, C.W. (2005) Understanding alternative splicing: towards a cellular code. *Nat Rev Mol Cell Biol* **6**: 386-398.

Maundrell, K. (1993) Thiamine-repressible expression vectors pREP and pRIP for fission yeast. *Gene* **123**: 127-130.

Millar, J.B., Buck, V., and Wilkinson, M.G. (1995) Pyp1 and Pyp2 PTPases dephosphorylate an osmosensing MAP kinase controlling cell size at division in fission yeast. *Genes Dev* **9**: 2117-2130.

Mitsuzawa, H., and Ishihama, A. (2004) RNA polymerase II transcription apparatus in *Schizosaccharomyces pombe*. *Curr Genet* **44**: 287-294.

Moore, M.J., and Sharp, P.A. (1993) Evidence for two active sites in the spliceosome provided by stereochemistry of pre-mRNA splicing. *Nature* **365**: 364-368.

Moreno, S., Klar, A., and Nurse, P. (1991) Molecular genetic analysis of fission yeast *Schizosaccharomyces pombe*. *Methods Enzymol* **194**: 795-823.

Mortazavi, A., Williams, B.A., McCue, K., Schaeffer, L., and Wold, B. (2008) Mapping and quantifying mammalian transcriptomes by RNA-Seq. *Nat Methods* **5**: 621-628.

Musunuru, K. (2003) Cell-specific RNA-binding proteins in human disease. *Trends Cardiovasc Med* **13**: 188-195.

Nguyen, A.N., Lee, A., Place, W., and Shiozaki, K. (2000) Multistep phosphorelay proteins transmit oxidative stress signals to the fission yeast stress-activated protein kinase. *Mol Biol Cell* **11**: 1169-1181.

Nicholson, P., and Muhlemann, O. (2010) Cutting the nonsense: the degradation of PTC-containing mRNAs. *Biochem Soc Trans* **38**: 1615-1620.

Nicholson, P., Yepiskoposyan, H., Metze, S., Zamudio Orozco, R., Kleinschmidt, N., and Muhlemann, O. (2010) Nonsense-mediated mRNA decay in human cells: mechanistic insights, functions beyond quality control and the double-life of NMD factors. *Cell Mol Life Sci* **67**: 677-700.

Nilsson, D., and Sunnerhagen, P. (2011) Cellular stress induces cytoplasmic RNA granules in fission yeast. *RNA* **17**: 120-133.

Nishikura, K. (2006) Editor meets silencer: crosstalk between RNA editing and RNA interference. *Nat Rev Mol Cell Biol* **7**: 919-931.

Ohnishi, T., Yamashita, A., Kashima, I., Schell, T., Anders, K.R., Grimson, A., Hachiya, T., Hentze, M.W., Anderson, P., and Ohno, S. (2003) Phosphorylation of hUPF1 induces formation of mRNA surveillance complexes containing hSMG-5 and hSMG-7. *Mol Cell* **12**: 1187-1200.

Okazaki, K., Okazaki, N., Kume, K., Jinno, S., Tanaka, K., and Okayama, H. (1990) High-frequency transformation method and library transducing vectors for cloning mammalian cDNAs by trans-complementation of *Schizosaccharomyces pombe*. *Nucleic Acids Res* **18**: 6485-6489.

Okazaki, N., Okazaki, K., Watanabe, Y., Kato-Hayashi, M., Yamamoto, M., and Okayama, H. (1998) Novel factor highly conserved among eukaryotes controls sexual development in fission yeast. *Mol Cell Biol* **18**: 887-895.

Orphanides, G., and Reinberg, D. (2002) A unified theory of gene expression. *Cell* **108**: 439-451.

Parkin, N.T., Cohen, E.A., Darveau, A., Rosen, C., Haseltine, W., and Sonenberg, N. (1988) Mutational analysis of the 5' non-coding region of human immunodeficiency virus type 1: effects of secondary structure on translation. *EMBO J* **7**: 2831-2837.

Proudfoot, N. (2000) Connecting transcription to messenger RNA processing. *Trends Biochem Sci* **25**: 290-293.

Proudfoot, N.J. (1989) How RNA polymerase II terminates transcription in higher eukaryotes. *Trends Biochem Sci* **14**: 105-110.

Provost, P., Silverstein, R.A., Dishart, D., Walfridsson, J., Djupedal, I., Kniola, B., Wright, A., Samuelsson, B., Radmark, O., and Ekwall, K. (2002) Dicer is required for chromosome segregation and gene silencing in fission yeast cells. *PNAS* **99**: 16648-16653.

Qin, J., Kang, W., Leung, B., and McLeod, M. (2003) Ste11p, a high-mobility-group box DNA-binding protein, undergoes pheromone- and nutrient-regulated nuclear-cytoplasmic shuttling. *Mol Cell Biol* **23**: 3253-3264.

Quinn, J., Findlay, V.J., Dawson, K., Millar, J.B., Jones, N., Morgan, B.A., and Toone, W.M. (2002) Distinct regulatory proteins control the graded transcriptional response to increasing H_2O_2 levels in fission yeast *Schizosaccharomyces pombe*. *Mol Biol Cell* **13**: 805-816.

Rehwinkel, J., Raes, J., and Izaurralde, E. (2006) Nonsense-mediated mRNA decay: Target genes and functional diversification of effectors. *Trends Biochem Sci* **31**: 639-646.

Reinberg, D., Orphanides, G., Ebright, R., Akoulitchev, S., Carcamo, J., Cho, H., Cortes, P., Drapkin, R., Flores, O., Ha, I., Inostroza, J.A., Kim, S., Kim, T.K., Kumar, P., Lagrange, T., LeRoy, G., Lu, H., Ma, D.M., Maldonado, E., Merino, A., Mermelstein, F., Olave, I., Sheldon, M., Shiekhattar, R., Zawel, L., and et al. (1998) The RNA polymerase II general transcription factors: past, present, and future. *Cold Spring Harb Symp Quant Biol* **63**: 83-103.

Riggi, N., Cironi, L., Suva, M.L., and Stamenkovic, I. (2007) Sarcomas: genetics, signalling, and cellular origins. Part 1: The fellowship of TET. *J Pathol* **213**: 4-20.

Rissland, O.S., and Norbury, C.J. (2009) Decapping is preceded by 3' uridylation in a novel pathway of bulk mRNA turnover. *Nat Struct Mol Biol* **16**: 616-623.

Rodriguez-Gabriel, M.A., Burns, G., McDonald, W.H., Martin, V., Yates, J.R., 3rd, Bahler, J., and Russell, P. (2003) RNA-binding protein Csx1 mediates global control of gene expression in response to oxidative stress. *EMBO J* **22**: 6256-6266.

Rodriguez-Gabriel, M.A., Watt, S., Bahler, J., and Russell, P. (2006) Upf1, an RNA helicase required for nonsense-mediated mRNA decay, modulates the transcriptional response to oxidative stress in fission yeast. *Mol Cell Biol* **26**: 6347-6356.

Ryter, J.M., and Schultz, S.C. (1998) Molecular basis of double-stranded RNA-protein interactions: structure of a dsRNA-binding domain complexed with dsRNA. *EMBO J* **17**: 7505-7513.

Sachs, A.B., and Davis, R.W. (1989) The poly(A) binding protein is required for poly(A) shortening and 60S ribosomal subunit-dependent translation initiation. *Cell* **58**: 857-867.

Saha, N., Schwer, B., and Shuman, S. (1999) Characterization of human, *Schizosaccharomyces pombe*, and *Candida albicans* mRNA cap methyltransferases and complete replacement of the yeast capping apparatus by mammalian enzymes. *J Biol Chem* **274**: 16553-16562.

Sakurai, H., Mitsuzawa, H., Kimura, M., and Ishihama, A. (1999) The Rpb4 subunit of fission yeast *Schizosaccharomyces pombe* RNA polymerase II is essential for cell viability and similar in structure to the corresponding subunits of higher eukaryotes. *Mol Cell Biol* **19**: 7511-7518.

Sanchez-Piris, M., Posas, F., Alemany, V., Winge, I., Hidalgo, E., Bachs, O., and Aligue, R. (2002) The serine/threonine kinase Cmk2 is required for oxidative stress response in fission yeast. *J Biol Chem* **277**: 17722-17727.

Schmid, S.R., and Linder, P. (1992) D-E-A-D protein family of putative RNA helicases. *Mol Microbiol* **6**: 283-291.

Schuler, M.A. (2008) Splice sites requirements and switches in plants. In *Nuclear pre-mRNA processing in plants*. Reddy, A.S.N.G., M.V (ed).

Serin, G., Gersappe, A., Black, J.D., Aronoff, R., and Maquat, L.E. (2001) Identification and characterization of human orthologues to *Saccharomyces cerevisiae* Upf2 protein and Upf3 protein (*Caenorhabditis elegans* SMG-4). *Mol Cell Biol* **21**: 209-223.

Sheth, U., and Parker, R. (2006) Targeting of aberrant mRNAs to cytoplasmic processing bodies. *Cell* **125**: 1095-1109.

Shiozaki, K., and Russell, P. (1995a) Cell-cycle control linked to extracellular environment by MAP kinase pathway in fission yeast. *Nature* **378**: 739-743.

Shiozaki, K., and Russell, P. (1995b) Counteractive roles of protein phosphatase 2C (PP2C) and a MAP kinase kinase homolog in the osmoregulation of fission yeast. *EMBO J* **14**: 492-502.

Shiozaki, K., and Russell, P. (1996) Conjugation, meiosis, and the osmotic stress response are regulated by Spc1 kinase through Atf1 transcription factor in fission yeast. *Genes Dev* **10**: 2276-2288.

Shiozaki, K., Shiozaki, M., and Russell, P. (1997) Mcs4 mitotic catastrophe suppressor regulates the fission yeast cell cycle through the Wik1-Wis1-Spc1 kinase cascade. *Mol Biol Cell* **8**: 409-419.

Shyu, Y.J., Liu, H., Deng, X., and Hu, C.D. (2006) Identification of new fluorescent protein fragments for bimolecular fluorescence complementation analysis under physiological conditions. *Biotechniques* **40**: 61-66.

Smith, D.A., Toone, W.M., Chen, D., Bahler, J., Jones, N., Morgan, B.A., and Quinn, J. (2002) The Srk1 protein kinase is a target for the Sty1 stress-activated MAPK in fission yeast. *J Biol Chem* **277**: 33411-33421.

Sonenberg, N. (1988) Cap-binding proteins of eukaryotic messenger RNA: functions in initiation and control of translation. *Prog Nucleic Acid Res Mol Biol* **35**: 173-207.

Stansfield, I., Jones, K.M., Kushnirov, V.V., Dagkesamanskaya, A.R., Poznyakovski, A.I., Paushkin, S.V., Nierras, C.R., Cox, B.S., Ter-Avanesyan, M.D., and Tuite, M.F. (1995) The products of the SUP45 (eRF1) and SUP35 genes interact to mediate translation termination in *Saccharomyces cerevisiae*. *EMBO J* **14**: 4365-4373.

Sugimoto, A., Iino, Y., Maeda, T., Watanabe, Y., and Yamamoto, M. (1991) *Schizosaccharomyces pombe ste11*$^{+}$ encodes a transcription factor with an HMG motif that is a critical regulator of sexual development. *Genes Dev* **5**: 1990-1999.

Taft, R.J., Glazov, E.A., Lassmann, T., Hayashizaki, Y., Carninci, P., and Mattick, J.S. (2009) Small RNAs derived from snoRNAs. *RNA* **15**: 1233-1240.

Takeda, T., Toda, T., Kominami, K., Kohnosu, A., Yanagida, M., and Jones, N. (1995) *Schizosaccharomyces pombe atf1*$^{+}$ encodes a transcription factor required for sexual development and entry into stationary phase. *EMBO J* **14**: 6193-6208.

Tanner, N.K., and Linder, P. (2001) DExD/H box RNA helicases: from generic motors to specific dissociation functions. *Mol Cell* **8**: 251-262.

Thakurta, A.G., Gopal, G., Yoon, J.H., Kozak, L., and Dhar, R. (2005) Homolog of BRCA2-interacting Dss1p and Uap56p link Mlo3p and Rae1p for mRNA export in fission yeast. *EMBO J* **24**: 2512-2523.

Tsukahara, K., Yamamoto, H., and Okayama, H. (1998) An RNA binding protein negatively controlling differentiation in fission yeast. *Mol Cell Biol* **18**: 4488-4498.

Tucker, M., Valencia-Sanchez, M.A., Staples, R.R., Chen, J., Denis, C.L., and Parker, R. (2001) The transcription factor associated Ccr4 and Caf1 proteins are components of the major cytoplasmic mRNA deadenylase in *Saccharomyces cerevisiae*. *Cell* **104**: 377-386.

Tucker, M., Staples, R.R., Valencia-Sanchez, M.A., Muhlrad, D., and Parker, R. (2002) Ccr4p is the catalytic subunit of a Ccr4p/Pop2p/Notp mRNA deadenylase complex in *Saccharomyces cerevisiae*. *EMBO J* **21**: 1427-1436.

VanHoy, R.W., and Wise, J.A. (1996) Molecular analysis of a novel *Schizosaccharomyces pombe* gene containing two RNP consensus-sequence RNA-binding domains. *Curr Genet* **29**: 307-315.

Vivancos, A.P., Castillo, E.A., Jones, N., Ayte, J., and Hidalgo, E. (2004) Activation of the redox sensor Pap1 by hydrogen peroxide requires modulation of the intracellular oxidant concentration. *Mol Microbiol* **52**: 1427-1435.

Volpe, T.A., Kidner, C., Hall, I.M., Teng, G., Grewal, S.I., and Martienssen, R.A. (2002) Regulation of heterochromatic silencing and histone H3 lysine-9 methylation by RNAi. *Science* **297**: 1833-1837.

Wahle, E., and Ruegsegger, U. (1999) 3'-End processing of pre-mRNA in eukaryotes. *FEMS Microbiol Rev* **23**: 277-295.

Wang, G.S., and Cooper, T.A. (2007) Splicing in disease: disruption of the splicing code and the decoding machinery. *Nat Rev Genet* **8**: 749-761.

Wang, L.Y., Shimada, K., Morishita, M., and Shiozaki, K. (2005) Response of fission yeast to toxic cations involves cooperative action of the stress-activated protein kinase Spc1/Sty1 and the Hal4 protein kinase. *Mol Cell Biol* **25**: 3945-3955.

Wang, X., and Tanaka Hall, T.M. (2001) Structural basis for recognition of AU-rich element RNA by the HuD protein. *Nat Struct Biol* **8**: 141-145.

Watanabe, Y., and Yamamoto, M. (1994) *S. pombe mei2*$^{+}$ encodes an RNA-binding protein essential for premeiotic DNA synthesis and meiosis I, which cooperates with a novel RNA species meiRNA. *Cell* **78**: 487-498.

Wendel, H.G., Silva, R.L., Malina, A., Mills, J.R., Zhu, H., Ueda, T., Watanabe-Fukunaga, R., Fukunaga, R., Teruya-Feldstein, J., Pelletier, J., and Lowe, S.W. (2007) Dissecting eIF4E action in tumorigenesis. *Genes Dev* **21**: 3232-3237.

Wilkinson, M.G., Samuels, M., Takeda, T., Toone, W.M., Shieh, J.C., Toda, T., Millar, J.B., and Jones, N. (1996) The Atf1 transcription factor is a target for the Sty1 stress-activated MAP kinase pathway in fission yeast. *Genes Dev* **10**: 2289-2301.

Willer, M., Hoffmann, L., Styrkarsdottir, U., Egel, R., Davey, J., and Nielsen, O. (1995) Two-step activation of meiosis by the mat1 locus in *Schizosaccharomyces pombe*. *Mol Cell Biol* **15**: 4964-4970.

Wood, V., Gwilliam, R., Rajandream, M.A., Lyne, M., Lyne, R., Stewart, A., Sgouros, J., Peat, N., Hayles, J., Baker, S., Basham, D., Bowman, S., Brooks, K., Brown, D., Brown, S., Chillingworth, T., Churcher, C., Collins, M., Connor, R., Cronin, A., Davis, P., Feltwell, T., Fraser, A., Gentles, S., Goble, A., Hamlin, N., Harris, D., Hidalgo, J., Hodgson, G., *et al*. (2002) The genome sequence of *Schizosaccharomyces pombe*. *Nature* **415**: 871-880.

Zawel, L., and Reinberg, D. (1993) Initiation of transcription by RNA polymerase II: a multi-step process. *Prog Nucleic Acid Res Mol Biol* **44**: 67-108.

Zhang, Q.S., Manche, L., Xu, R.M., and Krainer, A.R. (2006) hnRNP A1 associates with telomere ends and stimulates telomerase activity. *RNA* **12**: 1116-1128.

Zhouravleva, G., Frolova, L., Le Goff, X., Le Guellec, R., Inge-Vechtomov, S., Kisselev, L., and Philippe, M. (1995) Termination of translation in eukaryotes is governed by two interacting polypeptide chain release factors, eRF1 and eRF3. *EMBO J* **14**: 4065-4072.